Distribution Agreement

In presenting this thesis or dissertation as a partial fulfillment of the requirements for an advanced degree from Emory University, I hereby grant to Emory University and its agents the non-exclusive license to archive, make accessible, and display my thesis or dissertation in whole or in part in all forms of media, now or hereafter known, including display on the world wide web. I understand that I may select some access restrictions as part of the online submission of this thesis or dissertation. I retain all ownership rights to the copyright of the thesis or dissertation. I also retain the right to use in future works (such as articles or books) all or part of this thesis or dissertation.

Signature:

_____ _____

Anne Hotard Lopez-Ona Date

The Role of Enhanced Glycoprotein Activity in Respiratory Syncytial Virus Pathogenesis

By

Anne Hotard Lopez-Ona
Doctor of Philosophy

Graduate Division of Biological and Biomedical Science
Microbiology and Molecular Genetics

_____

Martin L. Moore, Ph.D.
Advisor

_____

Gregory Melikian, Ph.D.
Committee Member

_____

Richard K. Plemper, Ph.D.
Committee Member

_____

Paul Rota, Ph.D.
Committee Member

_____

David Steinhauer
Committee Member

Accepted:

_____

Lisa A. Tedesco, Ph.D.
Dean of the James T. Laney School of Graduate Studies

_____

Date

The Role of Enhanced Glycoprotein Activity in Respiratory Syncytial Virus Pathogenesis

By

Anne Hotard Lopez-Ona
B.S., Louisiana State University, 2009

Advisor: Martin L. Moore, Ph.D.

An abstract of
A dissertation submitted to the Faculty of the
James T. Laney School of Graduate Studies of Emory University
in partial fulfillment of the requirements for the degree of
Doctor of Philosophy
In
Graduate Division in Biological and Biomedical Sciences
Microbiology and Molecular Genetics
2014

Abstract

The Role of Enhanced Glycoprotein Activity in Respiratory Syncytial Virus Pathogenesis

By
Anne Hotard Lopez-Ona

Respiratory syncytial virus (RSV) is the most important cause of lower respiratory tract infections in infants worldwide. To date, there is no vaccine for RSV, prophylaxis is limited to high risk infants or those with chronic heart or lung disease, and treatment is limited to symptom management. Severe RSV infections in infants are characterized by mucus secretion, epithelial cell sloughing, and immune cell infiltration in the lungs. Different RSV strains exhibit differential pathogenesis in the mouse model of RSV-induced disease, with chimeric strain A2-line19F presenting human-like disease in this model. We developed an improved recombination-mediated mutagenesis reverse genetics system based on RSV strain A2-line19F to generate mutants in both the attachment (G) and fusion (F) glycoproteins. We identified residues critical for the fusion activity of the line 19 F protein, and hypothesized that a virus with these residues mutated would have reduced pathogenesis in the mouse model compared to the parental A2-line19F. While we demonstrated a correlation between fusion activity and early viral load in the mouse, we were unable to discern a correlation between fusion activity or viral load and mucus induction, an important parameter of RSV pathogenesis. We described an additional mutant of line 19 F which enhanced the fusion activity of the protein. The virus expressing this F protein augmented pathogenesis in mice, highlighted by early weight loss, severe lung pathology, and high viral loads.

RSV strains in the BA clade contain a 60 nucleotide duplication in the G gene. We hypothesized that this duplication would boost the function of the G protein. We generated recombinant viruses expressing a consensus BA G protein with and without the duplication, and found that the duplicated region enhances virus binding to cells by a glycosaminoglycan dependent mechanism. Additionally, we discovered that the virus with the duplication exhibited higher viral loads in mice than the virus without the duplicated region. Based on these results, we concluded that the duplication gives RSV BA strains an advantage in virus infectivity and possibly in transmission. Taken together, we identified mutations in both major glycoproteins of RSV which enhanced protein activity and viral pathogenesis.

The Role of Enhanced Glycoprotein Activity in Respiratory Syncytial Virus Pathogenesis

By

Anne Hotard Lopez-Ona
B.S., Louisiana State University, 2009

Advisor: Martin L. Moore, Ph.D.

A dissertation submitted to the Faculty of the
James T. Laney School of Graduate Studies of Emory University
in partial fulfillment of the requirements for the degree of
Doctor of Philosophy
In
Graduate Division of Biological and Biomedical Sciences
Microbiology and Molecular Genetics
2014

Acknowledgements

I would like to acknowledge my advisor, Martin Moore, for putting faith in me as a rotation student and helping me become the scientist I am today. I appreciate the trust and respect he has shown me and thank him for sticking with me. I would also like to say thank you to the many members of the Moore lab over the years, who have either helped me with my own project, or let me help them with theirs and trusted me as a teacher. Together, you have been my family away from home and helped me reach my goals.

I would also like to say a special thank you to all the members of my family, especially my husband Brian, and my father Daniel. These two men have been my support staff throughout this time in my life, and were always willing to listen when I needed help. Everyone in my family helped me keep going when I did not think I could finish this, so a little bit of my Ph.D. belongs to all of you as well.

Table of Contents

Figures and Tables

Chapter 2

Chapter 3

Chapter 4

Chapter 5

Chapter 1

Introduction – An Overview of Respiratory Syncytial Virus

Respiratory syncytial virus epidemiology and disease

Respiratory syncytial virus (RSV) was initially isolated from chimpanzees and characterized as chimpanzee coryza agent (1). A pair of indistinguishable viruses were later isolated from infants, and together the three were termed “respiratory syncytial virus” (2, 3). Since these initial isolation and characterization events, RSV has been recognized as the most important viral lower respiratory pathogen for infants, resulting in up to 199,000 annual deaths of children under 5 years old worldwide (4). While most of these deaths occur in developing countries, in the United States, there are 3 times more infants hospitalized for RSV than influenza each year (5), signifying the widespread burden of this disease.

Symptoms of RSV infections range from runny nose and cough to wheezing, pneumonia, and severe bronchiolitis (5). The most severe cases of RSV are caused when disease is no longer limited to the upper respiratory tract, but spreads to the lower respiratory tract of the individual. In these severe cases, small airways in the lungs can become blocked by plugs of mucus, inflammatory cells, and necrotic tissue, as described in autopsies of fatal RSV cases (6, 7). To date there are no approved vaccines for preventing RSV, and prophylaxis with a monoclonal antibody (Synagis) is limited to babies born prematurely, with pre-existing lung complications, or with chronic heart disease (8, 9). Therapeutic treatment is largely limited to symptom management as there are no licensed drugs directly targeting the virus.

Seasonal outbreaks of RSV occur annually, beginning in mid to late fall and ending in spring. Factors affecting the seasonality of RSV are not completely understood, but humidity, temperature, and socioeconomic factors, such as childhood nutrition, are

thought to be important (10-12). There are two antigenic subgroups of RSV, A and B, which were originally classified based on reactivity to monoclonal antibodies (13). More recently, new isolates are classified as A or B strains based on phylogenetic analysis of the second hypervariable region in the attachment glycoprotein gene (14). Both A and B subgroups are further subdivided into clades, and as recently as 2012, new genotypes representing additional clades continued to emerge (15). Strains from each subgroup can and do co-circulate in a given year, and strains from either subgroup may predominate from year to year (14).

Respiratory syncytial virus genome organization

RSV is a negative sense, non-segmented RNA virus in the *Paramyxoviridae* family, genus *Pneumovirus*. The 15.2 kilobase (kb) genome is comprised of ten genes that encode for eleven viral proteins. At the 3´ end of the genome is a region of untranslated RNA called the leader sequence. The leader contains binding sites and signals for the virally encoded RNA-dependent RNA polymerase (RdRP) to initiate either transcription or replication. When replication begins, the polymerase creates a full-length positive-sense genome, commonly referred to as the antigenome. The antigenome is then used as a template by the polymerase to generate a new, negative-sense genome, with initiation occurring at a promoter in the untranslated trailer RNA at the 5´ end of the genome (reviewed in ref (16)).

The RdRP can only begin scanning for transcriptional start signals if it first binds the leader RNA. Each RSV gene is flanked by a gene start (Gs) and gene end (Ge) sequence. Transcription initiation occurs at each Gs, and terminates in the subsequent Ge.

After the nascent transcript is polyadenylated and released, the RdRP is free to scan for the next Gs to initiate transcription of the next gene. This process is somewhat inefficient, such that the RdRP molecule falls off the RNA template before beginning transcription at a subsequent Gs. It is this reason that causes transcription of RSV genes, like other paramyxoviruses, to occur in a gradient fashion, with the leader proximal genes transcribed most frequently and the trailer proximal genes transcribed least frequently (reviewed in ref (16)).

The gene order of the RSV genes is 3´-NS1-NS2-N-P-M-SH-G-F-M2-L-5´. The two non-structural (NS) genes encode proteins NS-1 and NS-2, which function to antagonize the immune response to RSV in a number of ways, including STAT-1 and STAT-2 degradation (17, 18). Deletion of NS-1 or NS-2, singly or in combination, has been used as a strategy to generate live attenuated vaccine candidates (19-21). More recently, modulation of NS-1 and NS-2 levels by codon usage deoptimization was shown to be both attenuating and immunogenic (22). The RSV nucleoprotein (N), binds the genomic and antigenomic RNA molecules during infection to prevent degradation, and the N-RNA structure takes the form of a left-hand helix (23). The phosphoprotein (P), is a small phosphorylated protein necessary for efficient RNA replication and transcription (24). P binds N, L, and M2-1, and is indispensable for a functional RdRP complex (25-28). The RSV matrix (M) protein was shown to form oligomers that may be critical to assembly of viral particles (29), and recent reports suggest that M oligomers provide shape to the RSV virion (30, 31).

RSV encodes three glycoproteins – the small hydrophobic (SH), attachment (G), and fusion (F) proteins. While the function of the SH protein is still not well understood,

it has been posited to function as a pore forming ion channel (32), and the SH protein of another *Pneumovirus*, human metapneumovirus, was recently shown to possess viroporin-like qualities (33). Deletion of SH is tolerated by RSV both *in vitro* and *in vivo* (34). In contrast to SH, the G and F proteins are the major RSV surface glycoproteins and the main targets of neutralizing antibodies to RSV (35). The attachment and fusion glycoproteins will be discussed in greater detail below.

The only RSV gene which encodes two proteins is the M2 gene, encoding both M2-1 and M2-2. M2-1 interacts with both P and RNA (36), likely in its role as a processivity factor for the RdRP, and was also recently described to be located adjacent to M in viral particles (30). M2-2 is a determinant in the switch from transcription to replication, and viruses with M2-2 deleted have been tested as vaccine candidates (37, 38). The Gs sequence of the RSV polymerase (L) gene overlaps with the Ge sequence of the M2 gene, but when this orientation was mutated to be a classic Ge-intergenic-Gs sequence, transcription of L still occurred (39). While the L protein requires N, P, and M2-1 as cofactors for virus replication and gene expression (28), individual mutations in L can drastically alter the transcriptional profile of the virus (40). Additionally, a number of temperature-sensitive RSV-attenuating mutations in L have been described and characterized as potential vaccine candidates (41).

Respiratory syncytial virus attachment and fusion glycoproteins

The G protein is a type II transmembrane protein with an amino terminal transmembrane domain and an ectodomain comprised of two highly variable mucin-like domains and a central conserved region. A secreted form of G is produced by translation

initiation at an internal methionine (position 48) and subsequent cleavage of the signal and anchor domains (42). G was described as the RSV attachment glycoprotein in 1987 (43), and has since been shown to bind to heparan sulfate (44, 45), the fractalkine receptor (CX3CR1) (46), surfactant protein A (SP-A) (47), Annexin II (48), DC-SIGN, and L-SIGN (49) on host cells. Interestingly, although G was shown to bind the above molecules, it is dispensable for viral replication *in vivo*, suggesting that is not the only protein responsible for virus attachment to cells (50). The ectodomain of G is heavily glycosylated, with the majority of moieties being O-linked carbohydrates (51). The attached sugars are poorly immunogenic, and may be a mechanism by which RSV evades the host immune response, as vaccine candidates including small peptides of only the central conserved, unglycosylated region afforded complete protection to challenge in mice (52-54).

Based on reactivity to monoclonal antibodies, RSV strains are classified as either subgroup A or subgroup B (13, 55). Within each subgroup, viruses are further subdivided into clades based on phylogenetic analysis of the C-terminal third of the G gene (reviewed in (56)). Over the last decade, a major shift occurred in the subgroup B strains when a 60 nucleotide duplication was discovered in the G gene (57-59). Isolation of strains belonging to the previously existing subgroup B clades is less evident since the duplication was introduced, but isolates without the duplication are beginning to re-emerge (60, 61). A recently described clade of subgroup A strains contains a similar duplication, albeit longer (72 nucleotides) (15, 61). The emergence of RSV strains of both genotypes containing duplications in the same region of G suggests that G is flexible in its ability to accept mutations, and suggests that the duplication is advantageous for the

virus. The hypothesis of the duplication providing a selective advantage for RSV will be discussed further in Chapter 4.

The F protein of RSV, like the fusion protein of other paramyxoviruses, is a type I transmembrane protein as well as a type I viral fusion protein (62). RSV F is comprised of two disulfide bond-linked subunits (F_1 and F_2) which are generated during F processing through cleavage of the premature F_0 by the host cell protease furin (63, 64). This cleavage event allows the fusion peptide of RSV F, located at the amino terminus of the F_1 subunit, to be free for its eventual insertion into an opposing membrane during the fusion process. Contrary to the standard model, a recent study suggested that F mediates virus-cell fusion after endocytosis, and that the second furin cleavage event does not occur until the virion is located in an endosome (65). The structures of the pre- and post-fusion RSV F were recently described (66-68). As indicated by the differences in the structures, F undergoes major refolding during the fusion process, with the irreversible event culminating in formation of an extremely stable post-fusion protein containing a six-helix bundle. Unlike the G protein, F is indispensable for virus replication, as an RSV with the F gene deleted could only be rescued by expressing in *trans* either a heterologous glycoprotein with fusion function, or the F protein itself (69, 70).

Like the G protein, RSV F is a major target for neutralizing antibodies. To date, four major antigenic sites have been described on the pre-fusion RSV F protein (68). Although G is accepted as the major attachment protein for RSV, the F protein was also shown to bind host proteins, with nucleolin being the most recent receptor candidate described (71). While F proteins of different strains can have differential fusion activity,

the role that fusion activity plays in pathogenesis of RSV is not completely understood. This topic will be further discussed in Chapter 3.

The respiratory syncytial virus mouse model and strain variation

In 1979, Prince et al. published a study in which they infected twenty inbred mouse strains with RSV to determine the relative susceptibility of each strain to the virus (72). Five years later, a second study determined that in the case of BALB/c mice, older mice were more susceptible to RSV infection than younger mice, as determined by viral load in the lungs (73). In both studies, BALB/c mice were only semi-permissive to RSV infection, and neither group observed outward signs of illness in the infected mice. Yet another study described that high titer inoculation of BALB/c mice with the A2 strain of RSV caused weight loss, fur ruffling, and infiltration of immune cells into lungs of infected mice (74). Since these experiments were carried out, BALB/c mice have become one of the most popular models of RSV infection, with A2 and Long strains the most commonly studied.

While A2 and Long strains of RSV are widely used to study RSV pathogenesis in BALB/c mice, they do not provide the best model of RSV disease. Pathogenesis of RSV in BALB/c mice is strain dependent (75, 76), and some virus strains are capable of replicating human disease in mice better than the A2 or Long strains. An important example of this variation is the line 19 strain. Originally isolated at the University of Michigan, line 19 was shown to exhibit enhanced disease in BALB/c mice compared to A2 (75). In a comparative study, line 19 infection resulted in increased airway hyper-reactivity, greater airway mucus induction, and greater interleukin-13 (IL-13) induction

relative to infection with A2 (75). When a chimeric virus was generated in the genetic background of A2 but harboring the fusion protein of line 19, similar phenotypes were observed, suggesting a role for the fusion protein in the enhanced pathogenesis of the line 19 strain relative to the A2 strain (77).

Studies initiated globally for the past three decades have attempted to determine a link between RSV strains and disease severity in infants, with mixed results. Many of these studies found that RSV subgroup A strains are associated with greater disease severity than subgroup B strains (78-86). Conversely, two reports described subgroups B strains linked to more severe disease than subgroup A strains (87, 88), while a third group of studies determined no significant differences between disease severity among RSV strains (89-97). The divergent results described in these reports are likely due to differences in study design, including severity determinants and population sizes used.

The following chapters describe our efforts to determine how specific differences between RSV strains may result in differential pathogenesis in BALB/c mice. To study differential pathogenesis, we first generated an improved reverse genetics system for RSV, employing bacterial artificial chromosome technology and recombination-mediated mutagenesis. After establishing this system, we focused our investigations on variability in fusion activity between A strains or on variability in attachment protein sequence among B strains. In each case, we were able to describe variations that result in enhanced glycoprotein activity of one strain compared to another, and determined how these enhanced activities correlated to alterations in pathogenesis.

Chapter 2

A Stabilized Respiratory Syncytial Virus Reverse Genetics System Amenable to Recombination-Mediated Mutagenesis

The work of this chapter was published in October, 2012 in *Virology*

Full article citation:
Hotard, AL, FY Shaikh, S Lee, D Yan, MN Teng, RK Plemper, JE Crowe Jr., ML Moore. A stabilized respiratory syncytial virus reverse genetics system amenable to recombination-mediated mutagenesis. *Virology* 2012 434:129-136.

A Stabilized Respiratory Syncytial Virus Reverse Genetics System Amenable to Recombination Mediated Mutagenesis

Anne L. Hotard[1,2], Fyza Y. Shaikh[3], Sujin Lee[1,2], Dan Yan[1,2], Michael N. Teng[5], Richard K. Plemper[1,2], James E. Crowe Jr.[3,4], and Martin L. Moore[1,2]*

[1]Department of Pediatrics, Emory University, Atlanta, GA 30322, USA

[2]Children's Healthcare of Atlanta, Atlanta, GA 30322, USA

[3]Department of Pathology, Microbiology and Immunology, Vanderbilt University School of Medicine, Nashville, TN 37232, USA

[4] Department of Pediatrics, Vanderbilt University School of Medicine, Nashville, TN 37232, USA

[5]Division of Allergy and Immunology, Department of Internal Medicine, University of South Florida College of Medicine, Tampa, FL 33612, USA

*Correspondence should be addressed to M.L.M. (martin.moore@emory.edu)

Division of Pediatric Infectious Diseases, Emory University School of Medicine, 2015 Uppergate Dr NE Room 514, Atlanta, GA 30322

Phone: 404-727-9162

Fax: 404-727-9223

Abstract

We describe the first example of combining bacterial artificial chromosome (BAC) recombination-mediated mutagenesis with reverse genetics for a negative strand RNA virus. A BAC-based respiratory syncytial virus (RSV) rescue system was established. An important advantage of this system is that RSV antigenomic cDNA was stabilized in the BAC vector. The RSV genotype chosen was A2-line19F, a chimeric strain previously shown to recapitulate in mice key features of RSV pathogenesis. We recovered two RSV reporter viruses, one expressing the red fluorescent protein monomeric Katushka 2 (A2-K-line19F) and one expressing *Renilla* luciferase (A2-RL-line19F). As proof of principle, we efficiently generated a RSV gene deletion mutant (A2-line19FΔNS1/NS2) and a point mutant (A2-K-line19F-I557V) by recombination-mediated BAC mutagenesis. Together with sequence-optimized helper expression plasmids, BAC-RSV is a stable, versatile, and efficient reverse genetics platform for generation of a recombinant *Pneumovirus*.

Keywords: RNA virus, reverse genetics, recombineering, bacterial artificial chromosome, respiratory syncytial virus

Disclosure Statement

M. Moore and A. Hotard disclose that they are listed as inventors on a patent application for the RSV recombination-mediated mutagenesis system, submitted by Emory University.

Introduction

Respiratory syncytial virus (RSV) is the most important lower respiratory tract pathogen of infants, but there are no effective vaccines or antivirals in use. RSV is a member of the *Paramyxoviridae* family, genus *Pneumovirinae*, containing a non-segmented, negative-sense RNA genome (98). Plasmid-based reverse genetics and virus rescue is a cornerstone of RSV research and vaccinology (99, 100). However, plasmid-based virus rescue systems for the *Pneumovirinae* are plagued by cDNA instability (77, 101). RSV rescue involves co-transfection of an antigenomic cDNA plasmid in addition to four expression plasmids encoding the RSV nucleoprotein (N), phosphoprotein (P), large polymerase (L), and matrix 2-1 protein (M2-1) (99, 102). Current published rescue cDNA plasmids encode antigenome of the reference A2 strain of RSV (99, 102). The proteins expressed from the helper plasmids also are based on the genes from strain A2 (99, 102). We chose RSV strain A2-line19F for reverse genetics because infection with this chimeric strain better recapitulates RSV pathogenesis in the mouse model (77). We chose a bacterial artificial chromosome (BAC) as the backbone vector because BACs and other low copy vectors enhance stability of cDNAs that are difficult to clone (103-107). Our BAC-RSV was used successfully to directly transfect mammalian cells and recover recombinant virus. We utilized this new BAC-RSV construct for recombination-mediated genetic engineering to generate RSV mutants (Fig. 1). This BAC-RSV mutagenesis system provides an improved platform for RSV reverse genetics that could be applied to other RNA viruses as well.

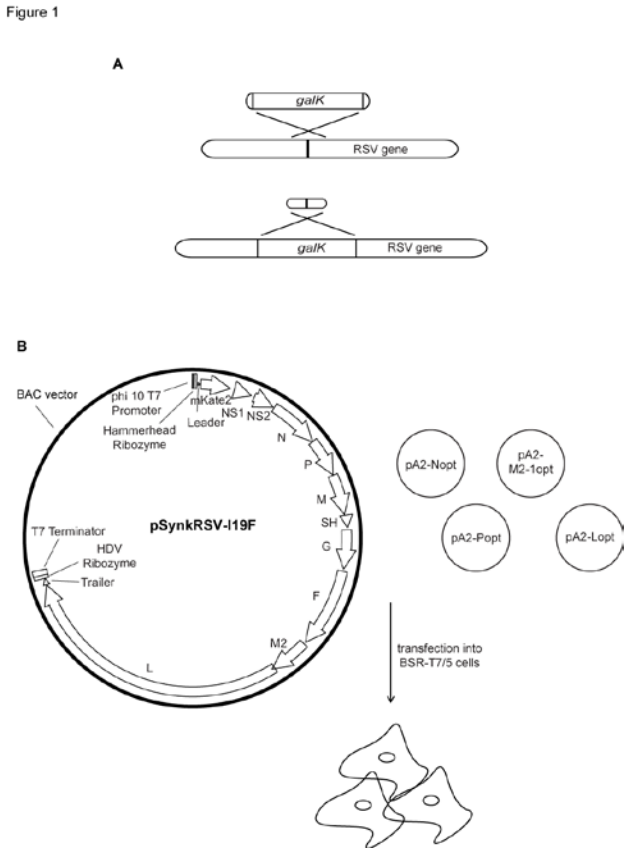

Figure 1. Model of RSV-BAC recombination-mediated mutagenesis and reverse genetics. (A) First recombination step in which a double-stranded PCR product containing the *galK* cassette recombines with RSV antigenome sequence, based on 50 base-pair homology sequence flanking *galK*. In the second step, annealed oligonucleotides containing the desired mutation flanked by the same 50 base-pair homology arms recombines with the RSV antigenome to displace galK. (B) RSV reverse genetics scheme. The RSV-BAC and sequence-optimized helper plasmids encoding RSV N, P, M2-1, and L are transfected into BSR-T7/5 cells, and infectious virus is recovered.

Results

Sequence-Optimized RSV N, P, M2-1, and L Genes Direct Greater RSV Transcription than Wild-Type RSV Genes

Efficient recombinant RSV recovery requires co-transfection with helper plasmids encoding the RSV N, P, M2-1, and L proteins (99, 102, 108). Sequence optimization of RSV cDNA for human codon bias and other optimal features enhances cDNA expression in mammalian cells (109). Plasmids encoding the wild-type (non-optimized) N, P, M2-1, and L genes have been used previously to drive minigenome expression (110). Using a RSV-luciferase minigenome assay in BSR-T7/5 cells (111), we compared the activity of these wild-type helper plasmids to the activity of plasmids that encode sequence-optimized N, P, M2-1, and L genes (111). Compared to wild-type RSV cDNAs, the sequence-optimized helper plasmids yielded approximately 3 fold higher polymerase activity, based on a RSV minigenome containing a luciferase reporter gene (Fig. 2).

Figure 2

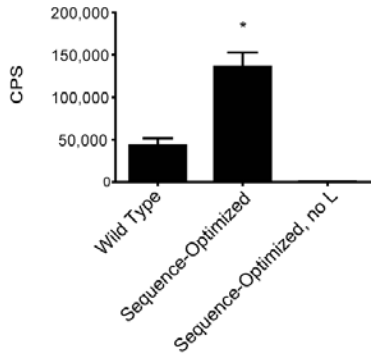

Figure 2. Sequence-optimized RSV helper plasmids drive more minigenome activity than wild-type RSV helper plasmids.

Minigenome activity driven by wild-type or sequence-optimized helper plasmids. Results are from transfection using 0.8, 0.4, 0.4, 0.4, and 0.2 µg of minigenome, N, P, M2-1, and L respectively. Data are shown as mean ± SEM. $P < 0.05$ by ANOVA of sequence-optimized relative to other conditions.

Generation of BAC-RSV Reporter Viruses

Antigenomic cDNA of A2-line19F was synthesized in three segments. We cloned the three segments sequentially into the BAC vector pKBS2 to generate the plasmid pSynkRSV-line19F. An additional gene was included in the RSV antigenomic cDNA to enhance detection of infection. The gene for the far-red fluorescent protein monomeric Katushka 2 (*mKate2*) lies in the first gene position flanked by RSV regulatory elements (112). The features of pSynkRSV-line19F are delineated by nucleotide position in Table 1. We compared recovery efficiency of the previously published RSV strain A2 antigenomic clone D46/6120 with recovery of pSynkRSV-line19F, and there was no difference in the recovery efficiency as measured by time (in days) to rescue (data not shown). We also compared the efficiency of pSynkRSV-line19F rescue using wild-type or sequence-optimized helper plasmids. In replicate experiments, sequence-optimized helpers yielded two-fold higher levels (0.5% of cells compared to 0.2%) of mKate2 fluorescence three days after transfection, but there was no significant difference in time to rescue between wild-type and sequence-optimized helpers. We used the sequence-optimized helper plasmids and pSynkRSV-line19F to recover recombinant virus A2-K-

line19F. Virus-encoded mKate2 serves as a marker for infected cells and provides means to assay infected cells by fluorescence (Fig. 3A and B). HEp-2 cell monolayer cultures were infected with RSV A2-line19F or A2-K-line19F then fixed and immunostained 48 hours post-infection (Fig. 3A). In addition, the percentage of cells expressing RSV F (fusion protein) and mKate2 was quantified using flow cytometric analysis at 24 hours post-infection (Fig. 3B). F protein positive cells were detected by indirect immunofluorescence using a monoclonal antibody to RSV F, while mKate2 fluorescence was directly detected in infected cells. mKate2 is a rapid and sensitive marker of infected cells, and is detectable using fluorescence microscopy and flow cytometry (Fig. 3).

Figure 3

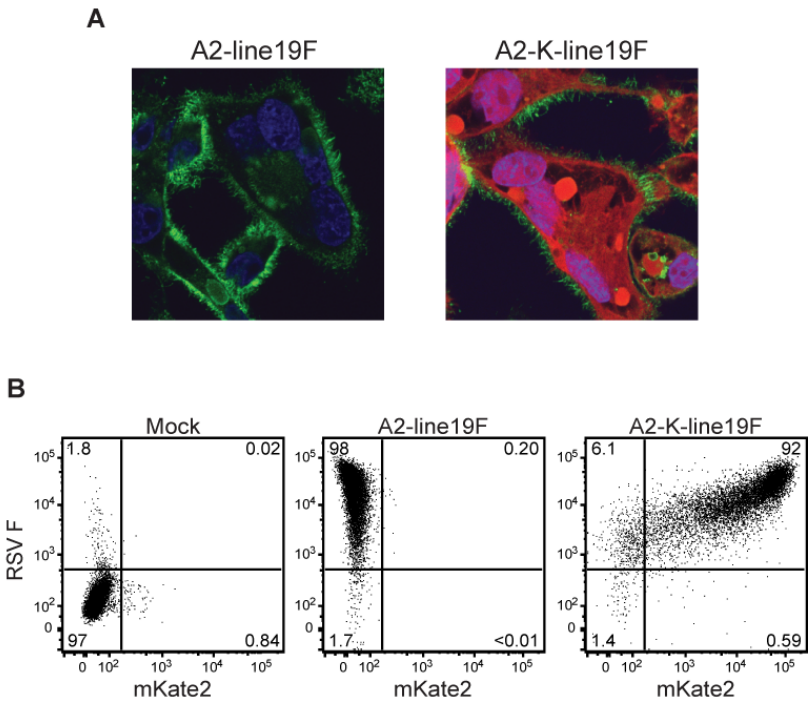

Figure 3. A2-K-line19F encoded mKate2 serves as a marker for RSV infected cells.

(A) HEp-2 cell monolayer cultures were infected with indicated virus at MOI 1.0 and incubated for 48 hours. RSV F protein was detected using indirect immunostaining and cell nuclei were detected using TO-PRO-3 iodide stain. RSV F is in green, mKate2 in red, and nuclei in blue. (B) HEp-2 cell culture monolayers were inoculated with indicated virus at MOI 3.0 and incubated for 24 hours. Panels show scatter plots from representative samples with a percentage of total cells detected as indicated for each quadrant.

Introduction of foreign genes into the RSV genome can attenuate RSV growth (113). We performed virus high and low multiplicity replication analyses of A2-K-line19F and A2-line19F. A2-K-line19F grew to similar titers as A2-line19F in HEp-2 cell monolayer cultures (Fig. 4A and B). We inserted the *Renilla* luciferase gene into pSynkRSV-line19F in place of the gene for mKate2 and recovered A2-RL-line19F virus. Multi-step replication analysis in HEp-2 cell monolayer cultures showed that A2-RL-line19F grew to similar titers as A2-K-line19F in this cell line.(Fig. 4C). We then used the A2-RL-line19F virus in a replication assay to determine how the titer of live virus detected as plaque forming units correlated with luciferase activity. The lowest levels of luciferase activity correlated with the lowest viral titers, and the highest levels of luciferase activity correlated with the peak viral titers (Fig. 4C). Virus-directed protein expression occurs prior to virus particle assembly, consequently, luciferase activity neared its maximum levels more quickly than virus titers (Fig. 4C). We next compared

the lung viral loads of A2-K-line19F, A2-RL-line19F, and A2-line19F in BALB/c mice. The lung viral load of A2-K-line19F was significantly lower than A2-line19F at day 4 post-infection, while lung viral load of A2-RL-line19F was significantly lower than both A2-line19F and A2-K-line19F (Fig. 4D). These results indicate that while mKate2 did not cause growth restriction *in vitro*, it did cause a slight restriction of RSV growth *in vivo*. In addition, the luciferase encoded by A2-RL-line19F provides a useful tool for detecting virus infection *in vitro*, even though the A2-RL-line19F was restricted in replication in BALB/c mice.

Figure 4

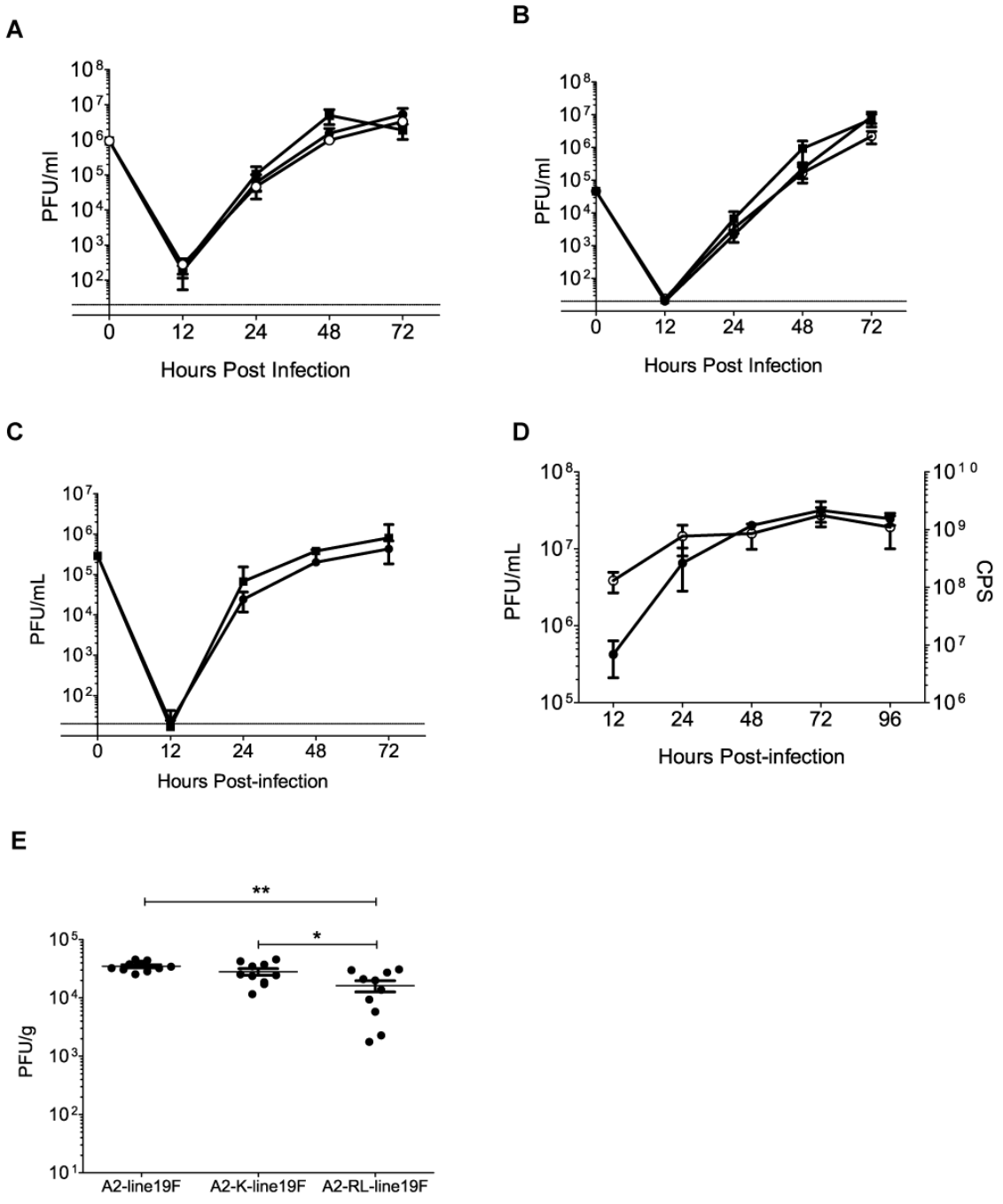
A
PFU/ml
Hours Post Infection
B
PFU/ml
Hours Post Infection
C
PFU/mL
Hours Post-infection
D
PFU/mL
CPS
Hours Post-infection
E
PFU/g
A2-line19F
A2-K-line19F
A2-RL-line19F

Figure 4. *In vitro* and *in vivo* growth characteristics of A2-K-line19F and A2-RL-line19F.

(A and B) Growth curves of A2 (■), A2-line19F (●), and A2-K-line19F (○) in HEp-2 cell monolayer cultures infected at MOI 2.0 (A) or MOI 0.1 (B). (C) Growth curve of A2-K-line19F (■) and A2-RL-line19F (●) in HEp-2 cell monolayer cultures infected at MOI 0.5. (D) Viral titers and luciferase activity in HEp-2 cell monolayer cultures infected with A2-RL-line19F at an MOI of 0.5. Titers are indicated by plaque forming units per mL (●) and luciferase activity is indicated by counts per second (○). Data for panels A-D are indicated as mean ± SEM. (E) BALB/c mice were infected with 5 x 10^5 PFU/mouse (5 mice per group) of A2-line19F, A2-K-line19F, or A2-RL-line19F and viral load was determined day 4 post infection via immunodetection plaque assay. *P = 0.05, **P = 0.01 by ANOVA.

BAC-RSV is a Stable Platform for Subcloning and for Recombination-Mediated Genetic Engineering

We determined the efficiency of cloning for an unstable fragment of RSV cDNA. A high-copy number cloning vector containing RSV cDNA including part of the small hydrophobic (SH) gene, the attachment glycoprotein (G), F, and M2 genes, and part of the L gene was transformed into two competent *E. coli* cell strains. None of the transformants selected contained the correct vector/insert. In contrast, when the same cDNA fragment of RSV cDNA was cloned into BAC vector pKBS2, all of the transformant colonies analyzed contained the correct vector/insert DNA. The enhanced stability of RSV cDNA provided by the BAC allowed for more efficient cloning.

We sought to develop recombination-mediated mutagenesis for RSV using a method relying on positive and negative selection of the *galK* cassette (114). To demonstrate its utility for RSV reverse genetics, we used this method to delete the genes for the RSV nonstructural proteins NS1 and NS2. The gene deletions were confirmed by nucleotide sequence determination, and lack of NS1 and NS2 production was confirmed by Western blot analysis of infected cell lysates (Fig. 5). We also used this recombination-based mutagenesis to generate a point mutation in the F protein of pSynkRSV-line19F, creating mutant I557V. The sequence of the F gene was confirmed to contain the correct mutation, demonstrating that recombination-mediated mutagenesis is a powerful tool for reverse genetic manipulations.

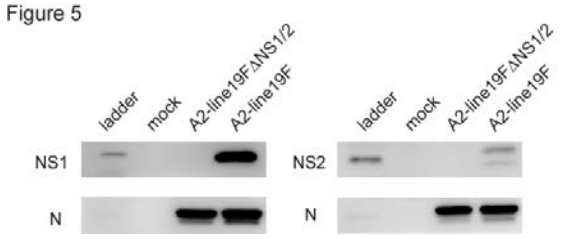

Figure 5. Recombination-mediated mutagenesis derived mutant viruses. Western blots of cell lysates from Vero cell monolayer cultures infected with A2-line19F or A2-line19FΔNS1/NS2. Polyclonal antisera for NS1 or NS2 were used to detect protein expression. Anti-RSV N was used to detect RSV N as a loading control.

Discussion

We have assembled the first BAC recombination-mediated mutagnenesis system for reverse genetics of a negative strand RNA virus. pSynkRSV-line19F is a RSV cDNA-containing BAC that is highly stable and enhances the efficiency of RSV reverse genetics. Recombination-mediated genetic engineering is commonly used for large BAC clones and reverse genetics of DNA viruses (115, 116). We demonstrated the utility of the BAC-RSV mutagenesis system by generating viruses with either gene deletions or a point mutation. We demonstrated the advantage of using sequence-optimized helper plasmids for virus recovery. These aspects of our reverse genetics system are likely to enhance rescue of attenuated mutants. We recovered two reporter viruses, A2-K-line19F and A2-RL-line19F, which express mKate2 and *Renilla* luciferase, respectively. Although these recombinant viruses encoding reporter genes were attenuated in mice, we were able to demonstrate their utility *in vitro*.

Stable and efficient mutagenesis of the RSV-BAC construct will facilitate RSV research and vaccine development. Despite the high clinical significance of RSV, reverse genetics reagents for this virus are not in widespread use relative to other members of the *Mononegavirales*, potentially due to cloning obstacles. BAC-RSV cloning alleviates cDNA instability, enhances the efficiency of traditional cloning, and enables recombination-mediated mutagenesis. This is particularly efficient for generating point mutations and deletions in the full-length antigenomic cDNA where convenient restriction enzyme sites are not available. This system will be useful for manipulation of RSV and may be useful for rescue and mutagenesis of *Pneumovirinae* or other RNA viruses with cDNA that is difficult to clone.

Experimental Procedures

Plasmids

Using published RSV sequences, we designed an antigenomic cDNA of a chimeric RSV strain A2 harboring the F gene of RSV strain line 19 (Table 1) (77). The cDNA was synthesized (GeneArt, Regensberg, Germany) in three separate fragments. In order 5´ to 3´, the first fragment contains a T7 promoter, a hammerhead ribozyme, RSV leader sequence, and genes encoding monomeric Katushka 2 (a red fluorescent protein mKate2) (112), RSV NS1, NS2, N, P, M, and a portion of SH flanked by appropriate RSV gene start, intergenic, and gene end sequences. This fragment is flanked by restriction sites BstBI and SacI. The second segment is flanked by restriction sites SacI and ClaI, and it contains the continuation of the SH gene followed by the RSV G, RSV line 19 strain F, and M2 genes, as well as a portion of the L gene. The third fragment contains the rest of the L gene followed by the RSV A2 trailer sequence, the hepatitis delta virus ribozyme, and a T7 terminator. This segment is flanked by ClaI and MluI restriction enzyme sites. We obtained a BAC vector (pKBS2) harboring the mouse adenovirus type 1 (MAV-1) genome (Katherine Spindler, University of Michigan). The MAV-1 DNA was removed, and the three RSV cDNA fragments were inserted sequentially in the BAC vector. This synthetic, mKate2-expressing BAC-RSV construct was termed pSynkRSV-line19F. The nucleotide features contained in pSynkRSV-line19F are shown in Table 1 with references.

Table 1. Nucleotide Sequence Positions of Features in pSynkRSV-line19F		
Nucleotide Position	**Feature**	**Reference**
1-26	phi 10 T7 promoter	(117)
30-77	Hammerhead ribozyme	(118) (119)
78-121	RSV leader	(120)
122-131	NS1 gene start	(121)
132-163	NS1 non-coding	(121)
164-874	mKate2 gene	(112)
875-886	L noncoding	(122)
887-898	L gene end	(122)
899-917	NS1/NS2 intergenic	(123)
918-1391	NS1 gene	(121)
1392-1468	NS1/NS2 intergenic	(123)
1469-1971	NS2 gene	(121)
1972-1996	NS2/N intergenic	(99)
1997-3200	N gene	(123)
3201-4115	P gene	(123)
4116-4124	P/M intergenic	(124)
4125-5081	M gene	(123)
5082-5100	M/SH intergenic	(123)
5101-5399	SH gene	(125)
5400-5445	SH/G intergenic	(123)
5446-6368	G gene	(123)
6369-6419	G/F intergenic	(123)
6420-8322	F gene	(77)
8323-8368	F/M2 intergenic	(126)
8369-9329	M2 gene	(123)
9261-15839	L gene	(122)
15840-15993	RSV trailer	(118) (120)
15994-16078	Hepatitis delta virus ribozyme	(127)
16079-16201	T7 terminator	(117)

We developed mammalian expression vectors for the RSV N, P, M2-1, and L proteins (111). Briefly, the sequences of the wild-type genes encoding these proteins in the RSV strain A2 were obtained from GenBank. We optimized the sequences for expression using computational algorithms to reduce the use of rare codons, occult splice sites, mRNA instability sequences, and RNA secondary structural elements. The

optimized cDNA sequences were synthesized (GeneArt) and then cloned into the pcDNA3.1 mammalian expression plasmid vector (Invitrogen, Grand Island, New York, USA). Plasmids were used to transfect 293F cells, then cells were fixed and permeabilized for immunofluorescence staining or lysed for analysis of expression by SDS-PAGE and Western blot. Each of the proteins were expressed in mammalian cells with the predicted molecular weight, as detected using polyclonal antisera to RSV (data not shown). The four helper plasmids pTM1-N, pTM1-P, pTM1-M2-1, and pTM1-L, each containing the gene under control of a T7 promoter, were obtained from Peter Collins (99).

cDNA Stability

To determine the stability of RSV antigenomic cDNA in cloning plasmids, a high-copy number vector (pMA, GeneArt) or single-copy number (pKBS2) vector containing the same piece of RSV antigenomic cDNA (corresponding to nucleotides 5382-9949 in pSynkRSV-line19F) were transformed into NEB-10β (New England BioLabs, Ipswitch, Massachusetts, USA) or One Shot Stbl-3 (Invitrogen) *E. coli* following manufacturer's protocols. *E. coli* were cultured at 32° C. The high-copy number vector was the GeneArt vector pMA, while the single-copy vector was pKBS2, as described above. pMA has a ColE1 origin of replication and carries an ampicillin resistance gene. Ten transformants from each were selected at random, and restriction digests were used to determine if plasmids contained in the transformants displayed the expected digestion pattern.

RSV-BAC Mutations

We used recombination-mediated mutagenesis to generate a point mutation in the F gene of pSynkRSV-line19F. Our protocol was based a method using positive and negative selection of the galactokinase expression cassette (*galK*) (114). The *galK* cassette was amplified from plasmid pgalK using primers 557galK F 5´-CATTAATTGCTGTTGGACTGCTCCTATACTGTAAGGCCAGAAGCACACCA*CCTGTTGACAATTAATCATCGGCA*-3´ and 557galK R 5´-ACTAAATGCAATATTATTTATACCACTCAGTTGATCCTTGCTTAGTGTGA*TCAGCACTGTCCTGCTCCTT*-3´. pSynkRSV-line19F homology arms are underlined and *galK* sequence is italicized. The PCR conditions were 94°C denaturation for 30 seconds followed by 30 cycles (94°C for 15 seconds, 60°C for 30 seconds, and 72°C for 1 minute) and a final 6 minute, 72°C extension. The resulting double stranded product was the *galK* cassette flanked by RSV homology arms. Upon recombination, the *galK* cassette replaced the nucleotide to be changed in pSynkRSV-line19F. For the second recombination step to replace *galK* with the desired mutation, we used annealed oligonucleotide adapters with the following sequences: 557inF 5´-CATTAATTGCTGTTGGACTGCTCCTATACTGTAAGGCCAGAAGCACACCA**G**TCACACTAAGCAAGGATCAACTGAGTGGTATAAATAATATTGCATTTAGT-3´ and 557inR 5´-ACTAAATGCAATATTATTTATACCACTCAGTTGATCCTTGCTTAGTGTGA**C**TGGTGTGCTTCTGGCCTTACAGTATAGGAGCAGTCCAACAGCAATTAATG-3´. 557inF and 557inR are entirely homologous to pSynkRSV-line19F except for the bold nucleotide, which designates the mutation.

The NS1 and NS2 genes were deleted from a version of the BAC-RSV without the gene for mKate2. The primers for *galK* amplification from pgalK were NS1startF 5´-ATAAGAATTTGATAAGTACCACTTAAATTTAACTCCCTTGGTTAGAGATG*CCTGTTGACAATTAATCATCGGCA*-3´ and NS2stopR 5´-TATGCATAGAGTTGTTGTTTTAGATTGTGTGAATATTGTGTTGAAATTTA*TCAGCACTGTCCTGCTCCTT*-3´. RSV antigenome homology arms are underlined and *galK* sequence is italicized. The PCR conditions were the same as described above. To complete the NS1/NS2 deletion and replace *galK*, the following oligonucleotides were annealed and used for recombination. dNS12F 5´-ATAAGAATTTGATAAGTACCACTTAAATTTAACTCCCTTGGTTAGAGATGGCTCTTAGCAAAGTCAAGTTGAATGATACACTCAACAAAGATCAACTTCT-3´ and dNS12R 5´-AGAAGTTGATCTTTGTTGAGTGTATCATTCAACTTGACTTTGCTAAGAGCCATCTCTAACCAAGGGAGTTAAATTTAAGTGGTACTTATCAAATTCTTAT-3´. dNS12F and dNS12R are entirely homologous sequences to the RSV antigenome.

A double recombination-PCR strategy was employed to generate cDNA copies of pSynkRSV-Luc$_{Ren}$ in pSynkRSV-line19F. First, individual segments of pSynkRSV-line19F flanking the luciferase insertion site and harboring unique BstBI and AvrII restrictions sites were amplified using oligonucleotide primer pairs 5´-CCCAGGCCGTGCCGGC/5´-GCTAAGCAAGGGAGTTAAATTTAAGTGG. The *Renilla* luciferase gene was amplified from pGL4.74[*hRluc*/TK] (Promega, Madison, Wisconsin, USA) with oligonucleotide primer pairs 5´-CCACTTAAATTTAACTCCCTTGCTTAGCATGGCTTCCAAGGTGTACG/5´-

CTGTTAAGTTTTTAATAACTAT

AATTGAATACTCACTGCTCGTTCTTCAGCACGC (underlined nucleotides are complementary to the RSV genomic sequences flanking the insertion site). In two consecutive PCR reactions, the luciferase-encoding amplicon was then recombined with the pSynkRSV-line19F-derived segments, and the final amplicon subcloned into the pCR2.1-TOPO (Invitrogen) vector. Transfer of BstBI/AvrII segments harboring the luciferase gene into the similarly opened pSynkRSV-line19F produced pSynkRSV-Luc_{Ren}.

We modified the protocol from Warming *et al.* for our recombination-mediated mutagenesis procedure (114). Most notably, we used 50 µL electrocompetent *E. coli* and 100-200 ng of PCR product or annealed oligonucleotides for each electroporation event. In addition, *E. coli* containing pSynkRSV-line19F routinely took 4-5 days to form colonies on both positive and negative *galK* selection plates.

Recombinant Virus Recovery

Recombinant viruses were recovered by modifying the protocol from previous reports (99, 108). BHK cells constitutively expressing the T7 polymerase (BSR-T7/5 cells) were transfected with BAC-RSV plasmids as well as the sequence-optimized helper plasmids encoding N, P, M2-1, and L, all under T7 control (108). Using Lipofectamine 2000 (Invitrogen), the plasmids were transfected at concentrations of 0.8 µg, 0.4 µg, 0.4 µg, 0.4 µg, and 0.2 µg, respectively. Prior to transfection, BSR-T7/5 cells were maintained in Glasgow's minimal essential media (GMEM, Invitrogen) supplemented with 10% FBS, 1% penicillin, streptomycin sulfate, amphotericin B

solution (Invitrogen), and 2% minimal essential amino acids (Invitrogen), with 1 mg/mL Geneticin (Invitrogen) added every other passage. Cells were plated to be confluent in 6 well plates at the time of transfection. Cells were incubated with transfection complexes of 500 µL at room temperature for 2 hours on a rocking platform. Following this incubation, 500 µL of GMEM supplemented as described above, except that FBS concentration was 3%, was added to each well and the cells were incubated overnight at 37°C. The next morning, the transfection complexes were removed from the wells and replaced with 2 mL of GMEM + 3% FBS. Cells were passed into 25 cm^2 flasks 2 days post-transfection, and every 2-3 days following until cytopathic effect was seen, at which time the cells were scraped from the flasks, aliquoted, and frozen. After thawing to release to virus, the cells and cell debris were pelleted at 1800 x g for 5 min at 4°C, and the supernatant was used to infect subconfluent HEp-2 cell monolayer cultures in order to propagate recovered virus.

RSV Minigenome Luciferase Reporter Assay

Construction of the RSV minigenome reporter plasmid has been described (111). BSR-T7/5 cells were transfected with the RSV minigenome reporter and the helper plasmids encoding N, P, M2-1, and L in either sequence-optimized or non-optimized forms. Using Lipofectamine 2000, the plasmids were transfected in the following quantities: 0.8 µg minigenome, 0.4 µg N, P, and M2-1, and 0.2 µg L. The transfection procedure was identical to that for recombinant virus recovery, except that two hours post-transfection 1.5 ml of GMEM supplemented with 3% FBS was added to cells. Approximately 24 hours post-transfection, the supernatant was removed, the cells washed

once in phosphate buffered saline (PBS), and lysed in 300 µL 1x reporter lysis buffer (Promega). Samples were diluted 1:100 and luciferase activity was determined using a Perkin Elmer Top Count scintillation and luminescence counter.

Virus Growth Curves and Quantification of Lung Viral Load

Subconfluent HEp-2 cell monolayer cultures in 6-well plates were infected in triplicate with RSV A2, A2-line19F, or A2-K-line19F at an MOI of 0.1 or 2.0. The virus was adsorbed for one hour at room temperature with rocking. Unbound inoculum was washed off with PBS and EMEM supplemented with 10% FBS and 1% penicillin, streptomycin sulfate, amphotericin B solution (Invitrogen) was added to the cells. Samples of the supernatant were taken at 12, 24, 48, and 72 hours post-infection and frozen until plaque titration by immunodetection plaque assay (76). For the A2-RL-line19F growth curve, HEp-2 cell monolayer cultures were infected at an MOI of 0.5. 12, 24, 48, 72, and 96 hours post infection, cells were washed in PBS and either 1ml of MEM or 200 µL of Renilla-Glo lysis buffer (Promega) was added. The cells in MEM were scraped and frozen until plaque titration. The cells in lysis buffer were scraped and frozen until luciferase activity was determined using the Renilla-Glo system (Promega).

To determine lung viral load, 6-8 week old BALB/c mice (The Jackson Laboratory, Bar Harbor, Maine, USA) were infected intranasally with 5×10^5 pfu of RSV per mouse as described (77). On day four post-infection, the left lung was harvested and viral load was determined as described previously (76). The procedures for all experiments involving mice were approved by the Emory University Institutional Animal Care and Use Committee.

NS1/NS2 Western Blotting

Vero cells maintained in EMEM supplemented with 10% FBS and antibiotic/antimycotic were infected with A2-line19F and A2-line19FΔNS1/NS2 and infected cell lysates were harvested 24 hours post infection in RIPA buffer (Sigma-Aldrich, St. Louis, Missouri, USA). Lysates were mixed 1:1 with Laemmli sample buffer prior to loading on SDS 4-20% polyacrylamide gels (Bio-Rad, Hercules, California, USA). Proteins were transferred to polyvinylidene fluoride membranes. NS1 and NS2 were detected using polyclonal rabbit sera raised to recombinant NS1 or NS2 proteins. The NS2 antisera slightly cross-reacts with NS1. Secondary incubation with horse radish peroxidase (HRP) coupled goat anti-rabbit (Jackson Immunoresearch Laboratories, West Grove, Pennsylvania, USA) IgG antibodies followed by chemiluminescent detection using SuperSignal West Femto Substrate (Thermo Scientific, Rockford, Illinois, USA) on a ChemiDoc imaging system (Bio-Rad) enabled visualization of proteins. Antibodies were stripped from membranes using Restore Western Blot Stripping Buffer (Thermo Scientific) and re-probed using an anti-N RSV antibody (clone D14, a gift from Dr. Ed Walsh) and HRP-coupled donkey anti-mouse secondary (Jackson Immunoresearch Laboratories) (128).

Immunofluorescence Microscopy

HEp-2 cell monolayer cultures on 6-well plates were inoculated with RSV at MOI 1.0. 48 hrs later cells were fixed with 3.7% (w/v) paraformaldehyde in PBS for 10 min then permeabilized with 0.3% (w/v) Triton X-100 and 3.7% paraformaldehyde in PBS for

10 min at RT. After fixation, cells were blocked in 3% (w/v) BSA in PBS for 60 min followed by addition of primary antibody in the blocking solution for 60 min. Cells then were washed three times in PBS, and species-specific anti-IgG Alexa Fluor conjugated antibodies (Invitrogen) were added at a dilution of 1:1,000 in block solution for 60 min to detect primary antibodies. Cells were washed three times in PBS and fixed on glass slides using Prolong Antifade kit (Invitrogen). All steps were performed at room temperature. Images were obtained on a Zeiss inverted LSM510 confocal microscope using a 63x/1.40 Plan-Apochromat oil lens. Anti-RSV F protein humanized mouse monoclonal antibody (palivizumab; MedImmune) was obtained from the Vanderbilt Pharmacy, and TO-PRO-3 iodide stain (Invitrogen) was used to visualize the nucleus.

Flow Cytometric Assay for Quantitative Surface Expression of RSV F Protein

HEp-2 cell monolayer cultures on 6-well plates were inoculated with RSV at MOI 3.0. After 24 hours, cells were treated with 20 mM EDTA in PBS to form a single cell suspension. Cells were washed twice in wash buffer (2% FBS in PBS) and then incubated with RSV F-specific monoclonal antibody (palivizumab) at 1 µg/mL for 30 min at RT. Cells again were washed twice with wash buffer and immunostained with an Alexa Fluor 488 labeled goat anti-mouse secondary antibodies at a final concentration of 2 µg/mL. Cells were washed twice in wash buffer and analyzed on a 5-laser LSRFortessa™ flow cytometer (Becton Dickinson, Franklin Lakes, New Jersey, USA) in the Vanderbilt Medical Center Flow Cytometry Shared Resource. Data analysis was performed using FlowJo version 7.6.5 (Treestar Inc., Ashland, Oregon, USA).

Statistical Analyses

Groups were compared by one way analysis of variance (ANOVA) and Tukey multiple comparison tests unless otherwise noted. $P < 0.05$ was considered significant.

Acknowledgements

We thank Kathy Spindler (University of Michigan Medical School) for pKBS2-MAV-1. We thank Peter Collins (NIH) for the D46/6120 RSV antigenomic cDNA clone and the pTM1-N, pTM1-P, pTM1-L, and pTM1-M2-1 helper plasmids. We thank Ursula Buchholz (NIH) for BSR-T7/5 cells. We thank Ed Walsh for the anti-N mAb. This work was supported by the following grants awarded to MLM: NIH 1R01AI087798, NIH 1U19AI095227, and a Children's Healthcare of Atlanta (CHOA) Center for Immunology and Vaccines Pilot Grant. This work was also supported by the Vanderbilt Medical Scientist Training Program NIGMS/NIH T32 GM007347 and by a grant from the March of Dimes to JEC, as well as NIAID 5R01AI081977 to MNT, and NIH R01 AI071002 to RKP.

Chapter 3

Identification of Residues in the Human Respiratory Syncytial Virus Fusion Protein That Modulate Fusion Activity and Pathogenesis

The work of this chapter is in press as of October, 2014, in *Journal of Virology*

Full article citation:
Hotard, AL, S Lee, MG Currier, JE Crowe Jr., K Sakamoto, DC Newcomb, RS Peebles, RK Plemper, ML Moore. Identification of residues in the human respiratory syncytial virus fusion protein that modulate fusion activity and pathogenesis. *J Virol*. *In press*.

Identification of Residues in the Human Respiratory Syncytial Virus Fusion Protein That Modulate Fusion Activity and Pathogenesis

Anne L. Hotard[a,b], Sujin Lee[a,b], Michael G. Currier[a,b], James E. Crowe Jr.[c,d,e], Kaori Sakamoto[f], Dawn C. Newcomb[g], R. Stokes Peebles Jr.[g], Richard K. Plemper[h], Martin L. Moore[a,b,#]

[a]Department of Pediatrics, Emory University School of Medicine, Atlanta, GA, USA

[b]Children's Healthcare of Atlanta, Atlanta, GA, USA

[c]Department of Pathology, Microbiology and Immunology, Vanderbilt Medical Center, Nashville, TN, USA

[d]Department of Pediatrics, Vanderbilt Medical Center, Nashville, TN, USA

[e]The Vanderbilt Vaccine Center of Vanderbilt Medical Center, Nashville, TN, USA

[f]Department of Pathology, College of Veterinary Medicine, University of Georgia, Athens, GA, USA

[g]Department of Medicine, Vanderbilt University School of Medicine, Nashville, TN, USA

[h]Institute for Biomedical Sciences, Georgia State University, Atlanta, GA, USA

[#]Address correspondence to Martin L. Moore, martin.moore@emory.edu

Abstract

Human respiratory syncytial virus (RSV) lower respiratory tract infection can result in inflammation and mucus plugging of airways. RSV strain A2-line19F induces relatively high viral load and mucus in mice. The line19 fusion (F) protein harbors five unique residues compared to the non-mucus-inducing strains A2 and Long, at positions 79, 191, 357, 371, and 557. We hypothesized that differential fusion activity is a determinant of pathogenesis. In a cell-cell fusion assay, line19 F was more fusogenic than Long F. We changed the residues unique to line 19 F to the corresponding residues in Long F and identified residues 79 and 191 together as responsible for high fusion activity. Surprisingly, mutation of residues 357 or 357 with 371 resulted in gain of fusion activity. Thus, we generated RSV F mutants with a range of defined fusion activity and engineered these into recombinant viruses. We found a clear, positive correlation between fusion activity and early viral load in mice, however, we did not detect a correlation between viral loads and levels of airway mucin expression. The F mutant with the highest fusion activity, A2-line19F-K357T/Y371N, induced high viral loads, severe lung histopathology, and weight loss, but did not induce high levels of airway mucin expression. We defined residues 79/191 as critical for line19 F fusion activity and 357/371 as playing a role in A2-line19F mucus induction. Defining the molecular basis of the role of RSV F in pathogenesis may aid vaccine and therapeutic strategies aimed at this protein.

Importance

Human respiratory syncytial virus (RSV) is the most important lower respiratory tract pathogen of infants for which there is no vaccine. Elucidating mechanisms of RSV pathogenesis is important for rational vaccine and drug design. We defined specific amino acids in the fusion (F) protein of RSV strain line19 critical for fusion activity, and elucidated a correlation between fusion activity and viral load in mice. Further, we identified two distinct amino acids in F as contributing to the mucogenic phenotype of the A2-line19F virus. Taken together, these results illustrate a role for RSV F in virulence.

Introduction

Human respiratory syncytial virus (hRSV according to the International Committee on Taxonomy of Viruses, often abbreviated RSV) is a negative-sense, non-segmented, and single-stranded RNA virus in the *Paramyxoviridae* family. RSV is the most important viral lower respiratory tract pathogen for infants, causing 16 times more hospitalizations than influenza virus in children under one year old (129). There is currently no vaccine licensed to prevent RSV infections, there is also a need for additional therapies, and further knowledge of RSV pathogenesis will enhance efforts toward these goals.

Strains of RSV exhibit differential pathogenesis in the BALB/c mouse model of RSV disease (75-77). A strain called line 19 was originally isolated in 1967 and then passaged in primary chick kidney cells, as well as primary chick lung cells, prior to 72 passages in human MRC-5 fibroblast cells (130). Line 19 exhibits enhanced pathogenesis in mice compared to commonly studied laboratory strains A2 and Long (75, 77). This virus strain was sequenced and found to encode ten amino acids differing from RSV strain Long, six of which are located in the fusion (F) protein (77). Of those six amino acids, five remained unique to line 19 F when the sequence was additionally compared to the A2 F protein (77). Furthermore, these five point mutations are exclusive to line 19 F when compared to virtually all other complete RSV F protein sequences in GenBank, suggesting that line 19 is derived from a unique passage history (Fig. S1). None of the residues unique to line 19 F are located in the currently described RSV F antigenic sites (68). Based on the overall striking degree of identity of strains line 19 and Long (16

nucleotide, ten amino acid differences), it is likely that line 19 is a laboratory passage variant strain derived from the Long strain.

Figure S1

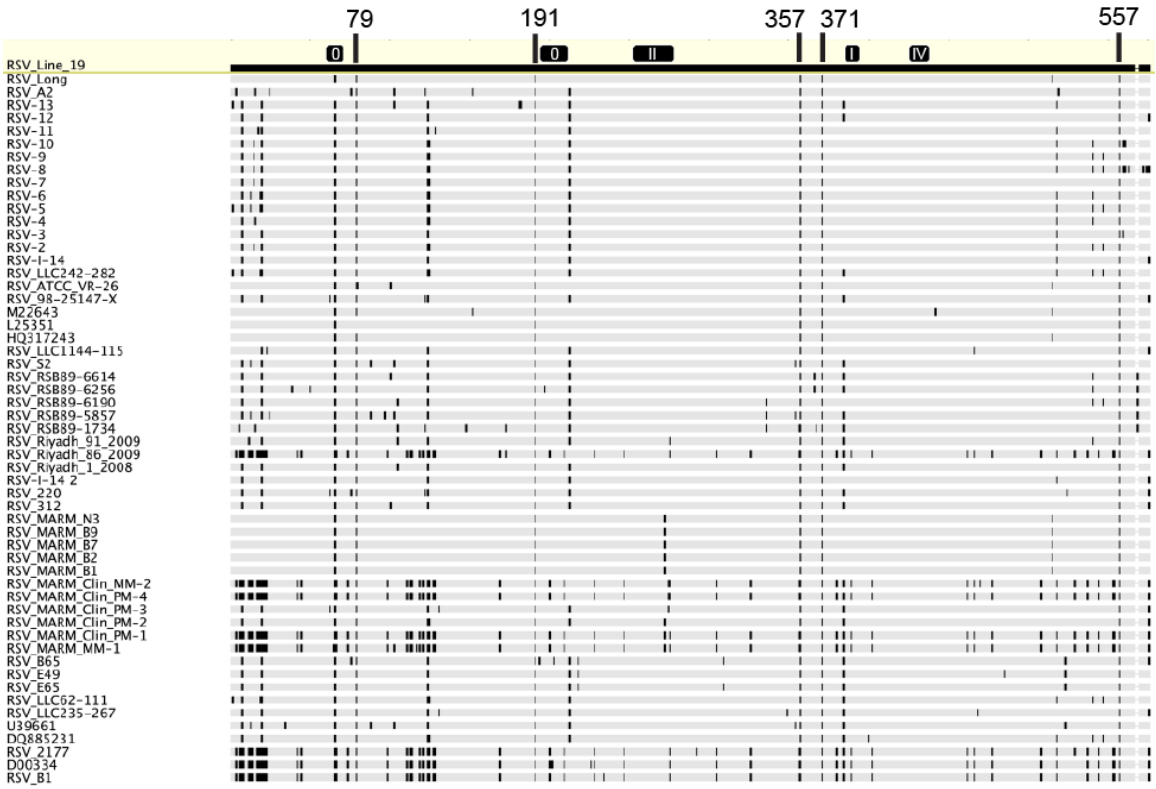

Figure S1. Amino acid alignment of RSV F. Amino acid alignment of RSV strain line 19 F with 2 55 complete RSV subgroup A F sequences obtained from GenBank, aligned using ClustalW, and 3 visualized using Geneious Pro software (Geneious, Auckland, New Zealand). Vertical black 4 lines indicate residues differing from line 19 F. Positions of antigenic sites 0, I, II, and IV are 5 indicated with horizontal black bars.

Chimeric strain A2-line19F, composed of the F protein of strain line 19 in the genetic background of strain A2, displays disease symptoms in BALB/c mice that more closely mimic human disease than that of other RSV strains (77). Features of A2-line19F pathogenesis in BALB/c mice include high levels of airway goblet cell hyperplasia,

relatively higher peak viral load, airway hyperreactivity, and increased breathing effort compared to the A2 strain and a chimeric virus harboring the F protein of the Long strain in an A2 strain genetic background (77, 131). Airway mucin induction leading to airway plugging is considered an important sequelae of RSV disease in infants (6, 7). The F mutations unique to line 19 are located at F positions 79 in the F_2 subunit, 191 in heptad repeat A, 357 and 371 in the F_1 subunit, and 557 in the cytoplasmic tail. We hypothesize that these residues singly or in combination contribute to the differential pathogenesis of chimeric RSV strains A2-line19F and A2-LongF by a fusion activity-based mechanism.

The RSV F protein, like other paramyxovirus F proteins, is responsible for virus-cell fusion as well as for fusion of infected cells with neighboring cells (98). A generally accepted model for paramyxovirus fusion involves insertion of a hydrophobic fusion peptide into the opposing cell membrane in conjunction with major conformational changes, which lead to refolding into a post-fusion conformation and membrane merger (66-68, 132, 133). Studies have defined domains and specific residues important for fusion activity of RSV F (63, 69, 134-137), however, the impact of fusion activity on paramyxovirus pathogenesis is not well understood. A pair of reports on Sendai virus demonstrated residues in heptad repeat A of F that enhance or dampen fusion activity and modulate pathogenesis (138, 139). A hyperfusogenic mutation in Sendai virus F resulted in greater pathogenesis and mortality than the wild type virus in the DBA/2 mouse model used, while a hypofusogenic mutation resulted in lessened mortality and pathogenesis than wild type virus (138).

The A2-line19F BALB/c mouse model of RSV pathogenesis recapitulates airway mucin induction seen in human disease. Using this model and reverse genetics, we

changed, singly or in combinations, the unique F residues in line 19 F to the corresponding residues in the Long strain F, a laboratory strain that is non-mucogenic. We identified residues in F that modulate fusion activity. Higher fusion activity *in vitro* correlated with greater lung viral load in mice. We also identified F residues that contribute to airway mucin expression and found that mucin induction did not correlate with fusion activity or viral load, suggesting an alternative mechanism for this aspect of pathogenesis. Defining RSV F residues that affect fusion and pathogenesis may guide targeted therapies and rational vaccine designs.

Materials and Methods

Cells and mice

HEp-2 and 293T cells were obtained from ATCC and cultured in minimal essential medium (MEM) containing 10% FBS and 1 µg/mL penicillin, streptomycin, and amphotericin B (PSA). BEAS-2B bronchial epithelial cells were cultured in RPMI containing 10% FBS and 1 µg/mL PSA, as described (76). BSR-T7/5 cells were a gift from Ursula Buchholz (National Institutes of Health, Bethesda, MD) and Karl-Klaus Conzelmann (Ludwig-Maximilians University Munich, Munich, Germany) and were cultured in Glasgow's minimal essential medium (GMEM) containing 10% FBS, 1 µg/mL PSA, and supplemented with 1 mg/mL geneticin every other passage, as described (140).

Seven-week-old female BALB/c mice were obtained from the Jackson Laboratory (Bar Harbor, ME). Mice were housed in specific pathogen free facilities, and all animal

procedures were conducted according to the guidelines of the Emory University Institutional Animal Care and Use Committee.

Plasmids

Human codon bias-optimized line 19 F and Long F cDNAs were obtained from GeneArt (Life Technologies, Grand Island, NY) and cloned into pcDNA3.1+ expression vector (Life Technologies). Sequences were based on GenBank nucleotide accession numbers FJ614813 (line 19) and FJ614815 (Long) (77). Site-directed mutagenesis was used to mutate residues 79, 191, 357, 371, and 557 in the pcDNA-line19F plasmid to the corresponding residues in the Long F sequence. Plasmids used to express codon-optimized RSV N, P, M2-1, and L were described (141). DSP_{1-7} and DSP_{8-11} plasmids were a gift of Naoyuki Kondo (142).

A bacterial artificial chromosome (BAC), which harbors the A2-line19F antigenomic cDNA, was previously described (141). We generated mutants of the A2-line19F virus strain at positions F79, F191, F357, F371, F557, F79/191, and F357/371 using the recombination-mediated mutagenesis method we described previously (141). Sequences of primers used to amplify *galK* with RSV homology arms and oligonucleotides homologous to RSV antigenome flanking nucleotides undergoing mutagenesis are available upon request. M79I/R191K and K357T/Y371N double mutants were made by sequential mutagenesis of the BAC at each residue. The RSV F sequence of each BAC was confirmed to contain only the desired mutation prior to proceeding with virus rescue.

Rescue of recombinant viruses

Recombinant RSV rescue using the BAC constructs and codon-optimized helper plasmids has been described (141). Briefly, each BAC was co-transfected into BSR-T7/5 cells with helper plasmids encoding codon-optimized RSV N, P, M2-1, and L using Lipofectamine 2000 (Life Technologies). Transfected cells were passaged until visible cytopathic effect affected a majority of the cells. The transfected cells were then scraped in their media and frozen. The harvested material was passaged onto HEp-2 cells at 37 °C to generate master and working stocks, as described elsewhere (76). Viral RNA was extracted from working stock samples using the QiaAmp Viral RNA Mini Kit (Qiagen, Valencia, CA), and F-specific RNA was reverse transcribed using primer F-r (77). F cDNA was amplified using primers F-f and F-r, followed by sequencing to confirm that only the desired mutations were present (77). All viruses rescued, but after 4 failed attempts to grow at 37°C, A2-line19F-K357T/Y371N master and working stocks were grown at 32°C to generate virus titers high enough for experimentation. High titer (1×10^8 PFU/mL) working stocks of A2-line19F-K357T/Y371N were generated similarly to virus stocks grown at 32°C, except at time of harvest, media was removed until only 5 mLs of growth medium remained in the T-175 flask. Cells were scraped in that 5 mL and then sonicated, centrifuged, and aliquoted as previously described (76).

Generation of F protein models

F structure models are based on the recently published pre- or post-fusion F coordinates in the Protein Data Bank (PDB, accession numbers 4jhw and 3rrr) (66, 68).

Mac PyMol and UCSF Chimera programs were used for modeling and presentation (143).

Multi-step virus growth curves

Subconfluent BEAS-2B cells in 6-well plates were infected at a MOI of 0.01 with each virus at room temperature with rocking for one hour. After the hour incubation, the inoculum was removed and cells were washed with PBS before 2 mLs RPMI supplemented with 10% FBS and 1 µg/mL PSA was added to each well. At 12, 24, 48, 72, 96, or 120 hours post-infection, one well of cells infected with each virus was scraped in the medium, aliquoted, and frozen at -80°C. After all samples were collected, viral titers were determined by immunodetection plaque assay, as previously described (76).

Dual-split protein fusion assay

The dual-split protein (DSP) cell-cell fusion assay was previously described (69, 140). Nearly confluent 293T cells in 6-well plates were transfected using Lipofectamine 2000 with 2 µg each of either DSP_{1-7} and F-expression construct or with DSP_{8-11} in the presence of the fusion inhibitor BMS-433771 (provided by Jin Hong, Alios Biopharma, San Francisco, CA) (144). Twenty-four hours post-transfection, DSP_{1-7}/F containing cells were washed in PBS and harvested by pipetting in media containing EnduRen Live Cell Substrate (Promega, Madison, WI). DSP_{8-11}-transfected cells were similarly harvested. Equal volumes of each set of cells were mixed and aliquoted into four wells each of an opaque 96-well plate or clear 96-well plate. The plates were incubated at 37 °C, and luciferase activity in the opaque plate was recorded on a TopCount Luminescence

counter (Perkin Elmer, Waltham, MA) 4, 6, and 8 hours post-cell plating. In addition, images of GFP-expressing syncytia were captured 8 hours post-cell plating in the clear plate.

F protein total and surface expression determination

Nearly confluent 293T cells in 6-well plates were transfected using Lipofectamine 2000 with 2 µg of each F construct in the presence of BMS-433771 RSV F inhibitor. Twenty-four hours post-transfection, cells were washed in PBS and harvested for either Western blotting or flow cytometry. For Western blots, cells were lysed in 200 µL radioimmunoprecipitation assay buffer (RIPA; Sigma Aldrich, St. Louis, MO) buffer containing Halt protease inhibitor cocktail (Thermo Scientific, Waltham, MA). Lysates were cleared by centrifugation at 12,000 × *g* for 5 minutes and frozen until use. Lysates were loaded onto 10% SDS polyacrylamide gels (SDS-PAGE) and separated via gel electrophoresis. Proteins were transferred to polyvinylidine fluoride (PVDF; Bio-Rad, Hercules, CA) membranes and detected using an RSV F-specific monoclonal antibody, motavizumab (generously provided by Nancy Ulbrandt, MedImmune), and a horseradish peroxidase (HRP)-conjugated anti-human secondary antibody (Jackson ImmunoResearch, West Grove, PA) (145). SuperSignal West Femto chemiluminescent substrate (Thermo Scientific) was used for signal detection. Antibodies were stripped and membranes reprobed with anti-GAPDH clone 6C5 (Life Technologies) and HRP-conjugated anti-mouse secondary antibody (Jackson ImmunoResearch). For flow cytometry, the transfected 293T cells were harvested in PBS by pipetting from the well and transferred to FACS tubes. Cells were washed in PBS containing 2% FBS and 0.1%

sodium azide and stained using the RSV F-specific monoclonal antibody palivizumab and a phycoeryhtrin (PE)-conjugated anti-human secondary antibody or human IgG1, K isotype control (both from Southern Biotech, Birmingham, AL) (146). Flow cytometric analysis was performed using a Becton Dickinson LSRII flow cytometer and data were analyzed using FlowJo software (Tree Star Inc., Ashland, OR).

In vivo *viral load determination, pathology, and mucus induction*

For viral load determination, histopathology, and mucus induction, seven-week-old BALB/c mice were infected with 10^5 PFU (hypofusogenic viruses) or 10^6 PFU (hyperfusogenic viruses) of virus. On days 1, 2, 4, 6, or 8 post-infection, mice were euthanized and the left lung was harvested for viral load. Lungs were homogenized using a mini-beadbeater and virus was titrated by immunodetection plaque assay as previously described (76). For quantification of airway mucin and histopathology analysis, 7-week-old female BALB/c mice were infected with 10^6 PFU of virus or mock-infected. On days 2, 4, or 8 post-infection, both lungs were harvested and fixed in 10% formalin overnight. Following embedding in paraffin blocks, 5 micron thick sections of each pair of lungs were mounted onto slides and stained with Periodic acid Schiff (PAS) stain or hematoxylin-eosin (H&E). A pathologist blinded to the experimental groups scored the H&E-stained slides for histopathological changes. Scoring for eosinophil recruitment (numbers surrounding arterioles) was as follows: 1 = 1-10, 2 = 11-30, 3 = 21-30, 4 = 31-40. Perivascular cuffing was scored as follows: 1 = 1 cell layer, 2 = 2-4 cell layers, 3 = 5-9 cell layers, 4= 10+ cell layers. Interstitial pneumonia was scored as based on how thick the alveolar septa appeared, each score representing number leukocyte thickness. Slides

were scanned using a Mirax-Midi microscope (Zeiss, Thornwood, NY), as described (76). PAS staining was quantified by annotation using HistoQuant software (3D Histotech, Budapest, Hungary), as previously described (76).

For weight monitoring, groups of 10 eight-week-old BALB/c mice were infected with 5×10^6 (data not shown) or 1×10^6 PFU A2-line19F, varying doses of A2-line19F-K357T/Y371N (5×10^5, 1×10^6, 5×10^6, or 1×10^7 PFU), or mock-infected. Weights were measured daily, and body weight was calculated as a percentage of day 0 pre-infection weight. On day 8 post-infection, mice were euthanized and left lungs were harvested for homogenization by mini-beadbeater. Right lungs were sectioned and PAS stained to determine mucin induction. Homogenates from 5×10^6 groups were used in a mouse 20-plex Luminex assay (Invitrogen). Assays were performed as directed by the manufacturer and detection was performed on a Luminex 200 analyzer. Day 1 post-infection lung homogenates from the hyperfusogenic virus viral load time course (see above) were pooled and used in an ELISA to determine interferon alpha levels. PBL Assay Science (Piscataway, NJ) mouse interferon alpha ELISA was performed as directed by the manufacturer's instructions.

R**esults**

In vitro *fusion activity*

Previous work showed that RSV expressing the F protein of strain line 19 exhibits greater viral load and airway mucin induction in BALB/c mice than RSV expressing the F protein of strain Long, and identified five amino acids unique to the line 19 F protein compared to the F proteins of RSV strains A2 and Long (Fig. 1A and Ref. (77)). We sought to understand how the line 19 F protein was responsible for the differences in pathogenesis between strains A2-line19F and A2-LongF. Modeling the unique line 19 F residues on the recently crystallized structures of pre- or post-fusion RSV F posits residues 79 and 191 at a lateral face of the pre-fusion F head, which undergoes major conformational changes during the fusion process (Fig. 1B and Ref. (66, 68)). In contrast, residues 357 and 371 are predicted to reside in close proximity in the base of the F head that remains conformationally intact during F refolding. Accordingly, the F rearrangements do not reposition these residues relative to each other in the structural models. Based on these predictions, we also chose to study 79/191 and 357/371 double mutants due to the location of these residues in the pre- and post-fusion structures of F (Fig. 1B).

Figure 1

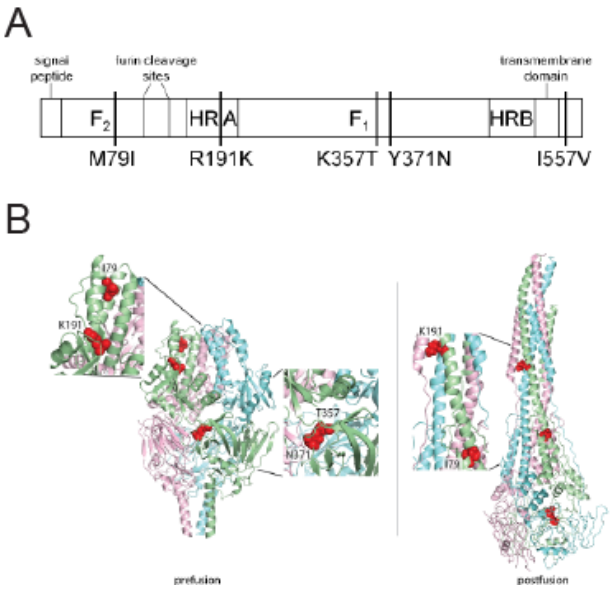

Figure 1. Amino acid residues unique to line 19 F. (A) Schematic of RSV F with major domains and line 19 unique residues indicated. Residues are identified by the amino acid in line 19 F, the position in F, and the amino acid in A2 and Long F (e.g. M79I is methionine in line 19 F and isoleucine in A2 and Long F at position 79). (B) Pre- and post-fusion structures of RSV strain A2 F with residues unique to line 19 F indicated.

In order to test our hypothesis that the F proteins from line 19 and Long strains have different fusion activities, we employed a dual-reporter cell-to-cell fusion assay (69, 140). We first determined if the line 19 and Long F proteins exhibit any differences in total or surface F expression. We measured total F expression by Western blot (Fig. 2A) and surface F expression by flow cytometry (Fig. 2B). While total and surface expression of Long F was slightly greater than line 19 F, these differences were not statistically significant (Fig. 2A and B). We quantified the cell-to-cell fusion activity of these two

proteins using a dual-split protein (DSP) fusion assay. The DSP assay was initially described for use in HIV research (147), but has been used for determining RSV fusion activity (69, 140). In brief, one DSP plasmid expresses the amino terminal portion of *Renilla* luciferase as well as a portion of GFP, while the other DSP plasmid expresses the remaining portions of both proteins. Major benefits to this system are that the F proteins themselves are not modified by attachment of reporter constructs, and that fusion is monitored both visually and quantitatively. When cell content mixing occurs via F-mediated fusion, the two DSPs associate and both GFP expression and luciferase activity are measurable. Using this assay, we found that line 19 F had higher fusion activity than Long F (Fig. 2C and D), consistent with our primary hypothesis that fusion activity of line 19 F is a determinant of pathogenesis.

We next determined which residue differences between line 19 F and Long F are critical for the differential fusion activity observed by changing the residues in the line 19 F protein to the corresponding residues in Long F. We found no significant differences from line19 F in total or surface expression of the F mutants (Fig. 2A and B). Western blots also indicated no deficiencies in cleavage of the F mutants (data not shown). Quantification of the cell-cell fusion activity of these mutants revealed that mutations M79I, R191K, Y371N and I557V had no effect on the cell-to-cell fusion activity of line 19 F (Fig. 2C). The double mutant M79I/R191K displayed fusion activity lower than line 19 F, similar to Long F, indicating that these residues in combination are important for the fusion activity of line 19 F (Fig. 2C and D). Mutation K357T increased the fusion activity of line 19 F (Fig. 2C and D). This finding was an unexpected gain of function. Additionally, the K357T/Y371N double mutant exhibited even greater fusion activity

than the K357T mutant. Taken together, we determined that residues M79 and R191 in combination contribute to the high fusion activity of line 19 F compared to Long F. We also identified residues K357 and K357/Y371 as dampening line 19 F fusion activity relative to residues T357 and T357/N371 in F.

Figure 2

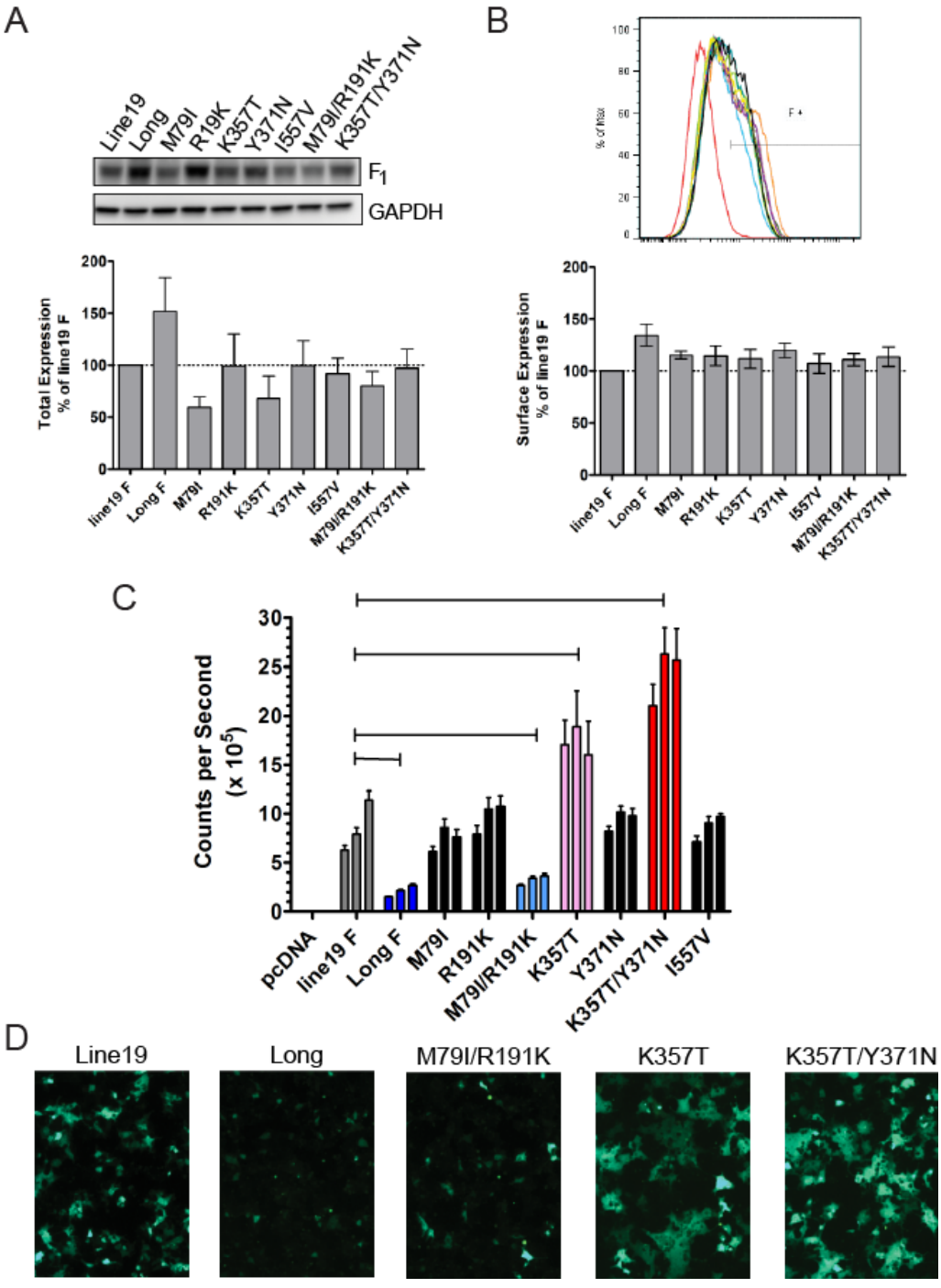
A
Line19
Long
M79I
R19K
K357T
Y371N
I557V
M79I/R191K
K357T/Y371N
F1
GAPDH
Total Expression
% of line19 F
line19 F
Long F
M79I
R191K
K357T
Y371N
I557V
M79I/R191K
K357T/Y371N
B
% of Max
F+
Surface Expression
% of line19 F
C
Counts per Second
(x 10^5)
pcDNA
line19 F
Long F
M79I
R191K
M79I/R191K
K357T
Y371N
K357T/Y371N
I557V
D
Line19
Long
M79I/R191K
K357T
K357T/Y371N

Figure 2. F expression and cell-cell fusion activity. (A) 293T cells were transfected with F mutant plasmids in the presence of the fusion inhibitor BMS-433771, and lysates were harvested 24 hours post-transfection for F-specific Western blot. A representative F blot is shown with GAPDH loading control. The bar graph shows expression as a percentage of line 19 F for three experiments combined. (B) Surface expression of the F mutants determined by flow cytometry of 293T cells harvested 24 hours post-transfection with F mutant plasmids in the presence of BMS-433771. The histogram displays results from a single experiment and the bar graph shows expression as a percentage of line 19 F from three experiments combined. (C and D) F expression plasmids were transfected into 293T cells in the presence of fusion inhibitor, and the cell-cell fusion activity was quantified by luciferase activity or monitored by GFP expression. Representative results are shown for luciferase activity (C) and GFP expression (D). Luciferase activity was measured 4, 6, and 8 hours post-cell mixing, indicated from left to right by the three bars for each F construct. Cross bars in (C) indicate groups significantly different compared to line 19 F. $*P < 0.05$ by one-way ANOVA and Tukey multiple comparison test. Images of GFP-expressing cells (D) were taken 8 hours post-cell mixing.

Viral replication in vitro *and in BALB/c mice*

We focused our further studies on those mutants that altered line 19 F fusion activity by generating recombinant viruses in the A2-line19F backbone with the K357T, M79I/R191K, or K357T/Y371N mutations. We tested viral growth at a low multiplicity of infection (MOI) in a human bronchial epithelial cell line, BEAS-2B. A2-LongF

exhibited an initial delay in replication, but reached peak viral titers similar to A2-line19F (Fig. 3). A2-line19F-K357T and A2-line19F-M79I/R191K replicated similarly to A2-line19F (Fig. 3). We did not test the double mutant A2-line19F-K357T/Y371N for growth in BEAS-2B at 37°C because growth at 32°C was required to generate the stocks for this virus (see Materials and Methods). The A2-line19F-K357T/Y371N mutant generated large syncytia *in vitro*, and we used a lower growth temperature in order to limit fusion and increase yield.

Figure 3

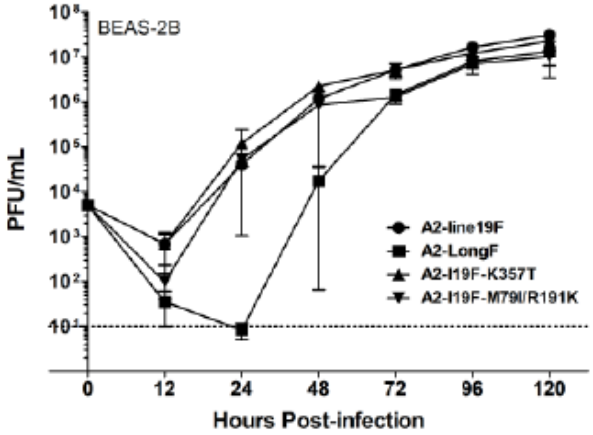

Figure 3. Virus replication in BEAS-2B cells. BEAS-2B cells were infected at a MOI of 0.01 with each virus, and cells were harvested at the designated time points for viral titer quantification. Input virus titer is represented as the zero time point. A composite of three experiments is shown. There were no significant differences between viruses at each time point by one-way ANOVA.

We investigated how modulation of line19 F fusion activity affected lung viral load in BALB/c mice. We infected mice with either the highly fusogenic viruses, A2-line19F-K357T and A2-line19F-K357T/Y371N, or the minimally fusogenic viruses, A2-line19F-M79I/R191K and A2-LongF, and quantified viral load relative to A2-line19F. Based on peak virus stock titers obtainable in cell culture, we used a lower dose (1×10^5 PFU/mouse) of the minimally fusogenic viruses than of the highly fusogenic viruses (1×10^6 PFU/mouse). The A2-line19F-K357T/Y371N mutant, which displayed the highest F protein fusion activity, exhibited lung viral loads greater than A2-line19F and A2-line19F-K357T on days 1 and 2 post-infection, while both highly fusogenic mutants (K357T and K357T/Y371N) had lung viral loads greater than A2-line19F on day 4 post-infection (Fig. 4A). Conversely, the viruses with the F proteins exhibiting the lowest fusion activities, A2-line19F-M79I/R191K and A2-LongF, had lower lung viral loads than A2-line19F on days 1 and 2 post-infection (Fig. 4B). Interestingly, the A2-line19F-M79I/R191K mutant did not have reduced viral load relative to A2-line19F on day 4 post-infection, indicating that fusion activity does not correlate with peak viral loads (Fig. 4B). Sequence analysis of A2-line19F-M79I/R191K isolated from these lungs at day 4 revealed that the F gene did not revert to parental line 19. There was no difference in viral clearance of any of the strains, which were cleared (as measured by plaque assay) by day 8 post-infection (data not shown). Taken together, these RSV fusion mutant viruses show that *in vitro* fusion activity correlates with early, but not peak, lung viral loads in BALB/c mice.

Figure 4

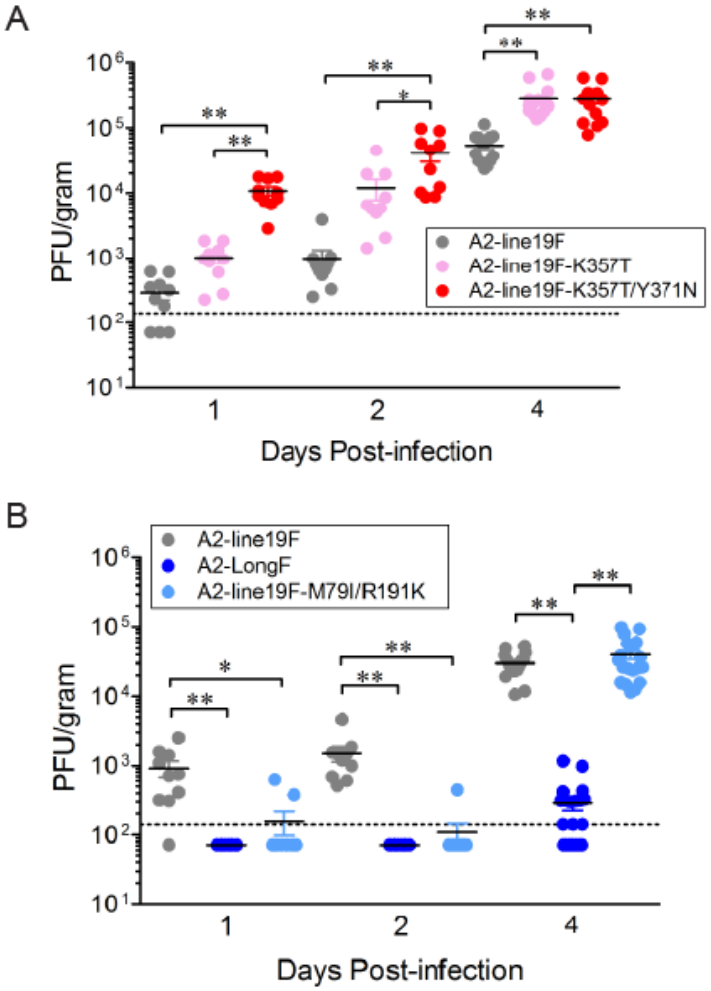

Figure 4. Lung viral load in BALB/c mice. (A and B) BALB/c mice were inoculated with 10^6 (A) or 10^5 (B) PFU of the indicated viruses, and left lungs were harvested on days 1, 2, or 4 post-infection. Viral titers were determined by immunodetection plaque assay. The dotted lines represent the limit of detection. Groups significantly different compared to A2-line19F are indicated by cross bars. Data are combined from three independent experiments, each with 4-5 mice per group. For (B), $*P < 0.05$ and $**P < 0.001$ by one-way ANOVA with Tukey multiple comparison test. For (C) $*P < 0.01$ and $**P < 0.001$ by one-way ANOVA with Tukey multiple comparison test.

Airway mucin expression in BALB/c mice

We investigated the ability of these viruses to induce airway mucin expression by infecting BALB/c mice and performing periodic acid Schiff (PAS) stains on lung sections. PAS stains mucin and mucin producing cells, and PAS positivity per airway can be quantified as a measure of mucus induction, as previously published (76, 140). As previously reported, A2-line19F induced greater airway mucus than A2-Long F (Fig. 5A and C and Ref. (77)). Both viruses A2-line19F-K357T and A2-line19F-M79I/R191K induced greater airway mucus than A2-line19F (Fig. 5A and C). Thus, fusion activity and viral load did not correlate with levels of airway mucin expression. The virus displaying the greatest fusion activity and viral load (A2-line19F-K357T/Y371N) induced levels of mucus lower than A2-line19F and similar to mock-infected mice (Fig. 5B and D), indicating that residues 357 and 371 act in concert to promote airway mucin expression in this model, though the mechanism is currently unknown. Taken together, these data suggest that neither early viral load nor peak viral load are critical determinants of airway mucin induction in the RSV BALB/c model.

Figure 5

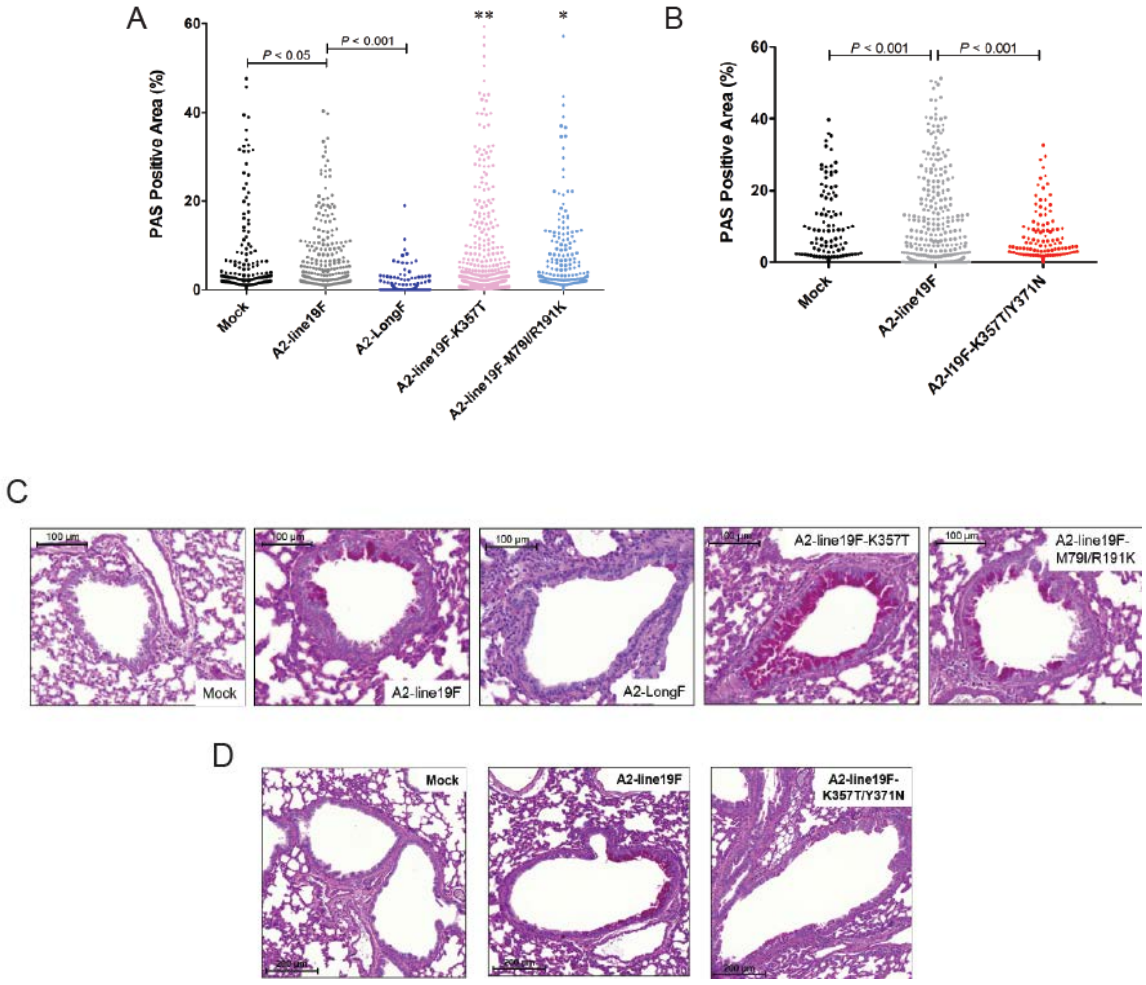
A
PAS Positive Area (%)
P < 0.05
P < 0.001
**
*
Mock
A2-line19F
A2-LongF
A2-line19F-K357T
A2-line19F-M79I/R191K
B
PAS Positive Area (%)
P < 0.001
P < 0.001
Mock
A2-line19F
A2-l19F-K357T/Y371N
C
Mock
A2-line19F
A2-LongF
A2-line19F-K357T
A2-line19F-M79I/R191K
D
Mock
A2-line19F
A2-line19F-K357T/Y371N

Figure 5. Airway mucus induction in BALB/c mice. BALB/c mice were inoculated with 10^5 (A and C) or 10^6 (B and D) PFU of the indicated viruses and whole lungs were harvested day 8 post-infection. Lungs were fixed, sectioned, and stained with periodic acid Schiff (PAS). Magenta coloring indicated PAS positive airway cells (C and D). Mucus induction was quantified using 3D Histotech software as percentage of airway positive for PAS staining (A and B). In (A), cross bars indicate groups significantly lower than A2-line19F and * indicate groups significantly greater than A2-line19F. *$P < 0.05$ and **$P < 0.001$. In (B), cross bars indicate groups significantly lower than A2-line19F. Data are a combination of 3 (A) or 2 (B) experiments, and images in (C) and (D) are representative from experiments in (A) and (B), respectively. All data were normalized using an arcsine transformation and analyzed using a one-way ANOVA with Bonferonni multiple comparison test.

As we observed a marked increase in early viral load in A2-line19F-K357T/Y371N infected mice compared to A2-line19F infected mice, we analyzed other parameters of pathogenesis in mice infected with this hyperfusogenic mutant. We infected BALB/c mice with varying doses of A2-line19F-K357T/Y371N, a single dose of A2-line19F, or a mock inoculum. By day 2 post-infection, all A2-line19F-K357T/Y371N infected mice lost significantly more weight than mock-infected or A2-line19F infected mice (Fig. 6A). This weight loss and subsequent weight recovery in A2-line19F-K357T/Y371N infected mice was dose dependent (Fig. 6A). On day 8 post-infection, we harvested the lungs of the mice infected with multiple doses of A2-line19F-K357T/Y371N and performed PAS staining, and found no differences in mucin induction

between the groups (data not shown), suggesting that the initial viral inoculum is not directly responsible for the induction of mucin.

Although A2-line19F-K357T/Y371N displayed reduced airway mucin induction compared to A2-line19F on day 8 post-infection, mice infected with A2-line19F-K357T/Y371N exhibited enhanced lung lesions on days 2 and 4 post-infection (Fig. 6B and C). A2-line19F-K357T/Y371N infected mice had higher levels of eosinophils, perivascular cuffing (PVC), and interstitial pneumonia (IP) compared to A2-line19F or mock-infected mice on days 2 and 4 post-infection (Fig. 6C). The enhanced scores reflect greater numbers of eosinophils surrounding arterioles, and thickened leukocyte layers surrounding the vasculature and expanding the alveolar septa. The IP and PVC were characterized by infiltration of neutrophils, monocytes, and lymphocytes, with eosinophils also present in the PVC.

A2-line19F was previously shown to induce the T_h2 cytokine interleukin-13 (IL-13), which mediates RSV-induced airway mucus expression (75, 77). Using a multiplex Luminex assay, we measured the levels of the T_h2 cytokines IL-4, IL-5, and IL-13 in lung homogenates from mock, A2-line19F, or A2-line19F-K357T/Y371N infected mice on day 8 post-infection. Levels of these T_h2 cytokines were lower in A2-line19F-K357T/Y371N lung homogenates compared to A2-line19F, while there was no difference between the groups in levels of the T_h1 cytokine interferon gamma (Fig. 6D). Although IL-10 was previously shown to be important in regulating a myriad of cytokines during RSV infection (reviewed in Ref. (148)), we found no differences in IL-10 or IL-12p70 levels induced in A2-line19F and A2-line19F-K357T/Y371N infected mice (data not shown). Lower IL-13 levels correlate with the lower levels of airway

mucus induced by the A2-line19F-K357T/Y371N virus at this time point (Fig. 5B and D). Although A2-line19F-K357T/Y371N induced eosinophils early after infection, the eosinophil numbers abated by day 8 (data not shown), correlating with the lack of IL-5 at this time point. These data show that infection of mice with the hyperfusogenic A2-line19F-K357T/Y371N results in high viral load and pathogenicity, but an altered host response compared to A2-line19F.

Because the differences in A2-line19F/A2-line19F-K357T and A2-line19F-K357T/Y371N were established by day 2 post-infection (Fig. 6), we hypothesized that differences in innate immune responses could be responsible for the altered pathogenesis. To this end, we measured interferon alpha levels by ELISA in lung homogenates from day 1 post-infection, but found no significant differences between the A2-line19F-K357T and A2-line19F-K357T/Y371N infected groups (data not shown). These results do not rule out differential innate immune recognition as the cause of altered pathogenesis between the strains, but suggest that the differences are not mediated by type I interferon.

Figure 6

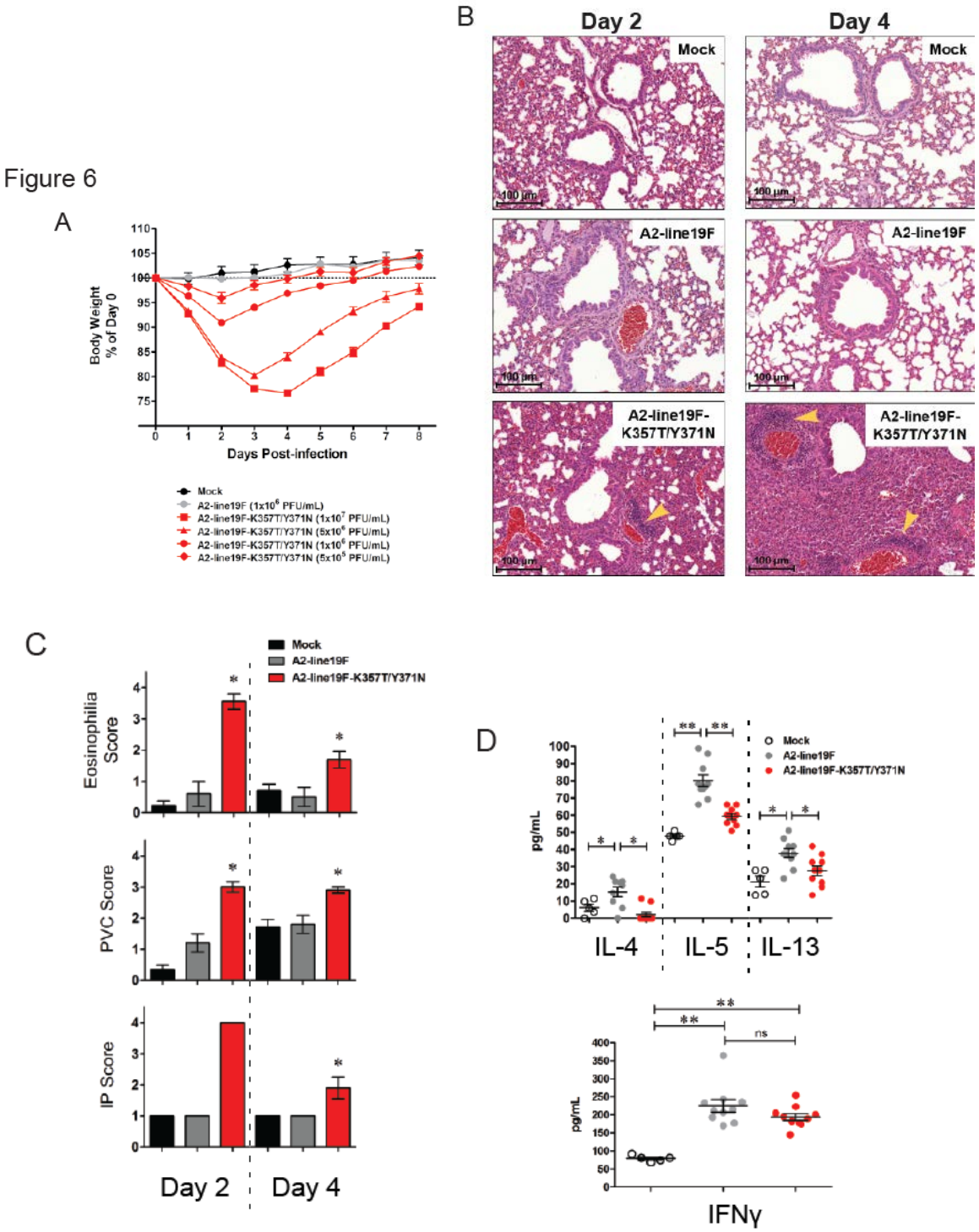
A
Body Weight % of Day 0
Days Post-infection
Mock
A2-line19F (1x10^6 PFU/mL)
A2-line19F-K357T/Y371N (1x10^7 PFU/mL)
A2-line19F-K357T/Y371N (5x10^6 PFU/mL)
A2-line19F-K357T/Y371N (1x10^6 PFU/mL)
A2-line19F-K357T/Y371N (5x10^5 PFU/mL)
B
Day 2
Day 4
Mock
A2-line19F
A2-line19F-K357T/Y371N
100 µm
C
Mock
A2-line19F
A2-line19F-K357T/Y371N
Eosinophilia Score
PVC Score
IP Score
Day 2
Day 4
D
Mock
A2-line19F
A2-line19F-K357T/Y371N
pg/mL
IL-4
IL-5
IL-13
IFNγ
ns

Figure 6. Pathogenesis of A2-line19F-K357T/Y371N. (A) Groups of 10 BALB/c mice were infected with the indicated doses of A2-line19F, A2-line19F-K357T/Y371N, or mock-infected, and their weights monitored daily. (B) Hematoxylin and eosin (H&E) stained lung sections from BALB/c mice infected with 10^6 PFU of A2-line19F, A2-line19F-K357T/Y371N, or mock-infected. Lungs were harvested on day 2 or 4 post-infection. Yellow arrowheads indicate areas of perivascular cuffing (PVC). (C) H&E stained lung tissues from the infections in (B) were scored by a pathologist blinded to the groups. Scoring for eosinophilia indicates numbers around arterioles. PVC, as indicated in (B), described thickness of the leukocyte layer surrounding the vasculature. Interstitial pneumonia (IP) score reflects thickened alveolar septa. See materials and methods for a description of the individual scoring guideline. $*P < 0.05$ by one-way ANOVA and Tukey multiple comparison test. (D) Luminex assay performed on lung homogenates harvested day 8 post-infection from mice infected with 5×10^5 PFU A2-line19F, A2-line19F-K357T/Y371N, or mock infected. $*P < 0.05$ and $**P < 0.01$ by one-way ANOVA and Tukey multiple comparison test.

Discussion

We utilized RSV strain A2-line19F to identify amino acids critical to the fusion activity of the RSV F protein, and showed that modulating fusion activity can result in changing the dynamics of viral load in BALB/c mice. We used an *in vitro* cell-to-cell fusion assay to identify residues 79/191 in line 19 F as directly contributing to its fusion activity. We hypothesize the location of these residues in the F structure impacts their influence on fusion activity. Both residues are located in regions that undergo conformational changes during the pre-fusion to post-fusion transition (Fig. 1B). A recent report highlighted F residue 66, which lies in the same loop as residue 79, as contributing to the fusion activity of RSV strain A2 F (134). In that study, pathogenesis was not tested, but fusogenicity of A2 F could be increased or decreased depending on the residue at position 66 (134). Based on this recent work along with our results and reports on other paramyxovirus proteins, the loop region of F_2 containing residue 79 appears to be involved in the mechanism of fusion (134, 149, 150). An individual residue in F_2 was implicated in the differential fusogenicity of wild type measles virus compared to the Edmonston strain of measles virus (150). In 2007, Gardner and Dutch demonstrated that in non-*Pneumovirus* paramyxoviruses, a conserved region in F_2 encompassing residue 79 drastically affected fusion activity *in vitro* (149). In addition, for human parainfluenza virus 5, they postulated a potential interaction of this region with heptad repeat A (149). Our data are consistent with these findings. A single mutation of RSV line 19 F residue 79 in F2 and single mutation of residue 191 in heptad repeat A had no effect on fusion, but mutating both residues resulted in a decrease in fusion activity of line 19 F. In our study, decreasing the fusion activity of A2-line19F by mutations M79I/R191K affected

the day 1 and 2 viral load in mice, suggesting that a certain threshold of fusion activity is important for early pulmonary infection.

We found that residues F357 or F357 together with F371 impacted RSV fusion activity. Mutating F357 from the lysine (K) in line 19 to the threonine (T) in Long unexpectedly resulted in a gain in fusion activity. Based on the core position of this residue in the F structure (Fig. 1B), our current working hypothesis is that this residue functions as an important determinant for overall conformational stability of the F protein. In our study, we mutated this residue from a basic amino acid, lysine, to uncharged, polar threonine. We speculate that the K to T mutation destabilizes the pre-fusion conformation of RSV F, resulting in a more readily triggered (hyperfusogenic) F protein. The possibility of residue 357 interacting with other internal F residues is implied by our *in vitro* cell-to-cell fusion assay results with a K357T/Y371N mutant F, which exhibited an even greater hyperfusogenic phenotype. In contrast to the low fusion activity A2-line19F-M79I/R191K, the highly fusogenic A2-line19-K357T/Y371N exhibited greater viral load than A2-line19F on days 1 and 2 post-infection, leading us to the conclusion that RSV *in vitro* fusion activity is a determinant of early viral load in mice. The higher viral load, more severe lung lesions, and weight loss caused by A2-line19F-K357T/Y371N make it potentially useful as a RSV challenge strain. Viral load, lung lesions, and weight loss peaked concomitantly at day 4 post-infection with this mutant, whereas RSV peak viral load typically peaks before disease manifestations in mice infected with other RSV strains. Thus, A2-line19F-K357T/Y371N may be practical for efficacy studies.

Based on several reports implicating viral load as a predictor of disease severity in infants (90, 151-153), we hypothesized that in mice, viruses exhibiting high fusion would also exhibit high viral load and be those that induced severe disease. Using mucus expression alone as a marker of pathogenesis, we found this not to be the case, but when we investigated pathogenesis parameters in addition to mucus, the hypothesis was supported. Neither early nor peak viral load correlated with mucus induction. Mutant virus A2-line19F-K357T/Y371N, with the highest viral load at all time points tested, induced mucus similar to levels in mock-infected mice (Fig. 4A and 5B). While these results point against viral load predicting mucus induction in BALB/c mice, the data do implicate residues K357 and Y371 together as critical for mucus induction by A2-line19F. It is possible that a threshold of viral load is necessary to induce airway mucin expression but that the high viral loads of A2-line19F-K357T/Y371N down-regulate a pathway leading to airway mucin-expression that lower viral loads fail to down-regulate.

In contrast to early lung viral load, the mucus response to RSV did not correlate with F protein activity and likely involves orchestrated innate and adaptive immune responses. RSV strain line 19-induced airway mucin expression in mice has been shown to be modulated by immune regulators, such as CXCR2 (154), IL-12 (155), TLR3 (156), CCR1 (157), MyD88 (158), IL-25 (159), and Beclin-1 (160). In our study, compared to A2-line19F, the hypofusogenic A2-line19F-M79I/R191K had lower early viral loads, recovered to peak viral load equivalent to A2-line19F, and induced slightly but significantly more airway mucin expression than A2-line19F. Our working hypothesis is that early innate immune responses in part dictate the later IL-13-dependent mucus

response. We speculate that lower antiviral innate responses to A2-line19F-M79I/R191K pave the way for a somewhat exacerbated mucus response.

In the case of hyperfusogenic A2-line19F-K357T/Y371N, which establishes high early viral loads and lung lesions, our working hypothesis is that robust innate immune responses prime for lower T_h2 cytokines we observed day 8 post-infection. We initially suspected that the T_h1 cytokine IFN-γ may be elevated in A2-line19F-K357T/Y371N-infected mice, but this was not the case. We are currently investigating what type of innate immune regulators might be differentially activated by A2-line19F-K357T/Y371N compared to A2-line19F. Initial studies measuring early type I interferon levels point away from a type I interferon-mediated difference. Additional studies are needed to characterize the host response to this pathogenic RSV strain. In the case of A2-line19F-K357T, a mutant with higher fusion activity than A2-line19F but not as high as the 357/371 mutant, we observed higher peak viral load and higher mucin expression levels than A2-line19F. As the early (day 1 and day 2) viral load of the K357T mutant did not differ significantly from A2-line19F, we speculate that the innate response to this mutant is not qualitatively altered and that the exacerbated mucus response may be due to elevated peak antigen load and a quantitative T_h2 response. Thus, our model posits that a substantial peak viral load is required for airway mucin expression, consistent with A2-LongF being non-mucogenic, but that early host responses to a more virulent strain (A2-line19F-K357T/Y371N) can set the stage for lower T_h2 cytokines and mucin expression.

Single amino acid mutations in F resulting in modulated fusion activity and alterations in pathogenesis are not unprecedented for paramyxoviruses. A study published in 2010 showed that mutation of a single amino acid in Sendai virus F, which created a

hyperfusogenic mutant, was also linked to enhanced pulmonary inflammation *in vivo* (138). A more recent report on parainfluenza virus 5 described a mechanism by which a single amino acid mutation in F causing greater fusion activity also resulted in differential recognition of the virus by the complement pathway (161). We showed that two amino acid changes in F dramatically altered the host response to RSV. Furthermore, we identified regions of F (residues 79/191 and 357/371) outside of the 5 described antigenic sites (68) that modulate F function and RSV pathogenesis. This work highlights the need for additional studies on the role of F in RSV pathogenesis, specifically how small sequence changes can cause large alterations in pathogenesis.

Acknowledgements

This work was supported by NIH grants 1R01AI087798 (to M.L.M.), 1U19AI095227 (to R.S.P.), the Children's Center for Immunology and Vaccines, and public health service grant AI083402 from the NIH/NIAID (to R.K.P.).

We thank Carla Shoffeitt for histology technical assistance. We thank Nancy Ulbrandt (MedImmune LLC) for the motavizumab mAb. We thank Ursula Buchholz and Karl-Klaus Conzelmann for the BSR-T7/5 cells. We thank Naoyuki Kondo and Zene Matsuda for the $DSP_{1\text{-}7/8\text{-}11}$ plasmids. We thank Jin Hong at Alios Biopharma for the BMS-433771 fusion inhibitor. We also thank the Emory Children's Pediatric Research Center flow cytometry core and immunology core, which are supported by Children's Healthcare of Atlanta.

Chapter 4

Role of the 60 Nucleotide Duplication in the Respiratory Syncytial Virus Buenos Aires Strain Attachment Glycoprotein

The work of this chapter is in preparation as a research article to be submitted to *Journal of Virology*.

Role of the 60 Nucleotide Duplication in the Respiratory Syncytial Virus Buenos Aires Strain Attachment Glycoprotein

Anne L. Hotard[a,b], Elizabeth Laikhter[a,b], Kelsie Brooks[a,b], Martin L. Moore[a,b,#]

[a]Department of Pediatrics, Emory University School of Medicine, Atlanta, GA, USA

[b]Children's Healthcare of Atlanta, Atlanta, GA, USA

[#]Address correspondence to Martin L. Moore, martin.moore@emory.edu

Abstract

The attachment protein (G) of respiratory syncytial virus (RSV) is used to determine the phylogeny of newly isolated RSV strains. There are two subgroups of RSV, A and B, and within each subgroup isolates are further divided into clades. Several years ago, subgroup B isolates were described which contained a duplication of 60 nucleotides in the G gene. These isolates were given a new clade designation of BA based on the site of isolation, Buenos Aires, Argentina. BA RSV strains have since become the predominant circulating clade of RSV B viruses. We hypothesized that the duplicated region in G served to enhance the function of G in the context of the virus. To investigate this, we generated recombinant viruses which expressed a consensus BA G gene, or a consensus BA G gene lacking the duplication ($G_{\Delta dup}$). We determined that the duplicated region functions during virus attachment to cells in a glycosaminoglycan-dependent mechanism. Additionally, we showed that *in vitro*, the virus containing the duplication has a fitness advantage compared to the virus without the duplication. *In vivo*, the virus expressing BA G exhibited higher peak viral loads than the virus expressing BA $G_{\Delta dup}$. Taken together, our data indicate that the duplicated region in the BA strain G protein functions to augment the attachment function of G.

Introduction

The attachment glycoprotein (G) of RSV is the most variable protein between strains (98). The G protein is a type II transmembrane protein, consisting of an N-terminal cytoplasmic tail, a transmembrane domain, and a C-terminal ectodomain. The ectodomain of RSV G is characterized by two hypervariable, mucin-like domains which flank a central conserved region. As the name implies, most of the variability between G proteins of different strains is located in the hypervariable regions. The final 270 nucleotides (nt) of the G gene, encompassing part of the second hypervariable region, are commonly used to determine classification of RSV strains as belonging to subgroup A or B. Phylogenetic analysis of this region of G also classifies clades within each subgroup.

In the late 1990's, several isolates of RSV subgroup B strains from Buenos Aires, Argentina, were identified to contain an as yet undescribed duplication of 60 nt in the second hypervariable region of the G gene (58). The duplication was exact, such that an additional sequence of 20 amino acids followed the first run of those residues. The specific genotype of strains containing the duplication was termed "BA" for Buenos Aires, the site of the first described isolation events (59). Since those original isolates, B strains of RSV harboring the same duplication or derivatives thereof have been isolated globally (57, 162, 163). In multiple studies, the only B strains isolated contained the duplicated region in G (164, 165). Due to the global spread of these strains, and the decrease in the isolation events of B strains lacking the duplication, RSV BA strains are seen as the predominant circulating RSV B strains (57).

Perhaps as interesting as the emergence of BA strains as the predominant circulating RSV B strains was the appearance of an RSV A genotype harboring a similar

duplication in G (15). These strains, termed “ON1” for their original isolation in Ontario, Canada, were first described in 2012 (15). As with BA strains, since their original description, ON RSV strains have been isolated globally, and are trending towards predominating among circulating A strains (166-168).

While multiple investigators have hypothesized what the potential advantage of the duplicated region is for these strains, the role of the duplication has not been directly studied. The most conventional role of G is in virus attachment to host cells (43), but G also serves an immunomodulatory role during RSV infection (49, 169, 170), and has been shown to contribute to some of the pathogenesis of strain A2-line19F (131). The original description of the second hypervariable region of G identified the possibility of positive selection occurring in this region of the protein (171), and a more recent study described positively selected sites in this region of G (172). These reports imply that RSV G mutates to contain residues changes that are advantageous for the virus. We chose to study whether the duplication found in BA RSV strains had an advantage for RSV, either *in vitro* or *in vivo*.

We focused our study on the duplication found in the BA strains because these were the first reported RSV isolates with the duplication (as opposed to the ON1 subtype A strains). We hypothesized that the duplicated region serves to enhance one or more of the functions of the G protein. Due to the small number of full length BA G and BA F sequences, and even smaller number of full length BA genomes available, we designed consensus BA G and BA F nucleotide sequences and cloned them into the A2 or A2-line19F genetic background. Additionally, we generated a BA G with the duplicated sequence deleted, termed BA $G_{\Delta dup}$, to directly address the role of the duplication in RSV

pathogenesis. Using these recombinant viruses, we were able to show that the duplication plays a role in virus attachment to cells which is associated with a slight advantage of the virus *in vivo*. While not specifically testing transmissibility of the viruses, our results suggest a possible role for the duplication in enhancing the function of the G protein to aid in the spread and infectivity of RSV.

Materials and Methods

Cloning and Rescue of Recombinant Viruses

For generating the consensus sequence of BA G, the full G gene nucleotide sequences from GenBank accession numbers AB117522, DQ270227, HQ699287-HQ699310, JN032115-JN032117, and JN032119-JN032120 were obtained. The sequences were aligned using MegAlign from the DNASTAR Lasergene Suite. A construct harboring the SacI to SacII fragment of pSynkRSVline19F (described in Chapter 2 and Ref. (141)) with the consensus sequence generated by the BA G alignment in place of A2 G was obtained from GeneArt. For BA $G_{\Delta dup}$, the same consensus sequence was used, except the duplicated 60 nucleotides were deleted from the consensus. A similar construct was obtained from GeneArt. The A2 G encoding SacI-SacII fragment was cloned out of pSynkRSVline19F and replaced with either the BA G SacI-SacII fragment or BA $G_{\Delta dup}$ SacI-SacII fragment. Both constructs were confirmed to contain the correct G constructs by restriction fragment length polymorphism (RFLP) analysis.

To generate the BA F consensus sequence, the 5 GenBank entries with a full length F gene from a BA strain with a full length G gene were obtained and aligned using MegAlign. These sequences were accession numbers JF714712, JN032115, JN032117, JN032119, and JN032120. A fragment of pSynkRSVline19F from SacII to SalI restriction sites with line 19 F replaced with the BA F consensus was obtained from GeneArt. The line 19 F encoding SacII-SalI fragment was cloned out of pSynk-BAG-line19F and pSynk-BA$G_{\Delta dup}$-line19F and replaced with the BA F SacII-SalI fragment. Both constructs were confirmed to contain the correct F construct by RFLP analysis.

The four antigenomic plasmids harboring BA G, BA $G_{\Delta dup}$, BA G-BA F, or BA $G_{\Delta dup}$-BA F were used to rescue the corresponding viruses as previously described (141). Briefly, the antigenome containing bacterial artificial chromosomes were transfected into BSR-T7/5 cells in 6-well plates along with codon-optimized expression plasmids encoding RSV N, P, M2-1, and L. After 48 hours, the cells were passaged into T-25 flasks, and subsequently passaged every other day until 70% cytopathic effect and mKate2 fluorescence were visible throughout the flask. At that time the cells were scraped in their media and frozen at -80ºC. Master and working stocks were generated from the frozen BSR-T7/5 suspensions as previously described (76). After working stocks were generated, viral RNA was isolated using the QIAamp Viral RNA Mini Kit (Qiagen, Valencia, CA). Reverse transcription was performed using G and F specific primers, and PCR primers specific to G or F were used to amplify the G and F genes. Primer sequences are available upon request. The sequences of the G and F genes from the four working stocks were determined to be the expected sequences.

Cells and Mice

HEp-2 cells were maintained in Eagle's modified essential media (EMEM) containing 10% FBS and 1 µg/mL ampicillin/streptomycin/amphotericin B (PSA) solution. BEAS-2B cells were maintained in RPMI containing 10% FBS and 1 µg/mL PSA. CHO-K1 and CHO pgsD-677 cells were maintained in F12-K with 10% FBS and 1 µg/mL PSA.

Seven to eight week old female BALB/c mice were obtained from the Jackson Laboratories (Bar Harbor, ME). Mice were housed in specific-pathogen free facilities and

all experiments were performed according to rules and regulations set by the Emory University Institutional Animal Care and Use Committee (IACUC).

Multi-cycle Growth Analyses

Subconfluent BEAS-2B cells in 6-well plates were infected, in duplicate, with MOI 0.01 of A2-K-BAG-BAF, A2-K-BAG-line19F, A2-K-BAG$_{\Delta dup}$-BAF, or A2-K-BAG$_{\Delta dup}$-line19F. After one hour rocking at room temperature, inoculum was washed from cells, and 2 mLs complete growth media was added to each well. At 12, 24, 48, 72, and 96 hours post-infection, cells were scraped in the media, aliquoted, and frozen at -80ºC. Titration of virus in samples was performed by focus-forming unit assay on HEp-2 cells in 96-well plates, as described previously (22). Samples were titrated in triplicate.

Binding Assays

Subconfluent BEAS-2B cells in 6-well plates were inoculated, in duplicate, with MOI 1.0 of A2-K-BAG-BAF, A2-K-BAG-line19F, A2-K-BAG$_{\Delta dup}$-BAF, or A2-K-BAG$_{\Delta dup}$-line19F. Virus was adsorbed to cells for 2 hours at 4ºC. Extra inoculum was frozen at -20ºC for further use. After the 2 hour incubation, the inoculum was removed, and the cells were washed 3 times in cold PBS. 200 µL radioimmunoprecipitation assay buffer (RIPA) containing HALT protease inhibitor cocktail (Thermo Scientific, Waltham, MA)) was added to each well. Cells were removed from wells by pipetting in lysis buffer and lysates were transferred to microcentrifuge tubes and frozen at -20ºC.

Prior to Western blot analysis, lysates were cleared by centrifugation at 12,000 x *g* for 5 minutes. Protein in lysates, as well as in saved inoculum samples, were separated

via sodium dodecyl sulfide-polyacrylamide gel electrophoresis (SDS-PAGE). Proteins were transferred to polyvinylidine fluoride (PVDF) membranes. Membranes were probed for N using a monoclonal antibody against the RSV N protein (clone D14, a gift from Edward Walsh, University of Rochester), followed by a peroxidase conjugated anti-mouse secondary antibody. Chemiluminscent signal was developed using Western Bright Quantum substrate (Advansta, Menlo Park, CA) and detected on a ChemiDoc XRS analyzer (BioRad, Hercules, CA). Antibodies were stripped from membrane using Restore Western Protein Stripping Buffer (Thermo Scientific), and membranes were reprobed for GAPDH using antibody clone 6C5 (Life Technologies) and a peroxidase conjugated anti-mouse secondary antibody. Signal was again detected using Western Bright Quantum and a ChemiDoc XRS. Densitometry was performed using Image Lab software (BioRad). Densitometry of N in lysates (bound virus) was normalized to N in inoculum as well as to GAPDH in lysates prior to comparison between groups.

Quantification of Lung Viral Load

Seven to eight-week old female BALB/c mice were inoculated intranasally with 1×10^5 PFU of A2-K-BAG-line19F or A2-K-BAG$_{\Delta dup}$-line19F. On days 4, 6, and 8 post-infection, mice were euthanized and the left lung was collected and homogenized for viral load determination as previously described (76). Titration was performed on HEp-2 cells in 24-well plates using an immunodetection plaque assay.

Glycosaminoglycan (GAG) Dependency Index

Infectivity of A2-K-BAG-line19F and A2-K-BAG$_{\Delta dup}$-line19F was determined in CHO-K1 cells and in CHO pgs-D677 cells by fluorescent focus assay, as described (22). The ratio of infectivity in K1 to pgs-D677 cells was determined for each virus and termed the GAG Dependency Index, as defined previously (173).

Competitive Infection Assay

Subconfluent BEAS-2B cells in 6-well plates were infected singly with A2-K-BAG-line19F or A2-K-BAG$_{\Delta dup}$-line19F at MOI 1.0, or were infected with both viruses at ratios of 1:1 (MOI 0.5 of each), 10:1 (MOI 1 and MOI 0.1, respectively), or 1:10 (MOI 0.1 and MOI 1.0, respectively). Twenty-four or forty-eight hours post-infection, supernatant was removed, and RNA was extracted from cells using Trizol (Life Technologies) reagent according to the manufacturer's instructions. After RNA extraction, RNA was quantified and 1 µg total RNA was used as template in a reverse transcription reaction for G messenger or antigenomic RNA using a G specific primer and SuperScript III reverse transcriptase. Equal volumes of each cDNA generated from reverse transcription were used as templates in PCR amplification of a portion of the G gene encoding the duplicated region. Expected PCR product sizes were 709 nt for A2-K-BAG-line19F and 649 nt for A2-K-BAG$_{\Delta dup}$-line19F. Equal volumes of PCR products were separated by agarose gel electrophoresis.

Results

Design of Consensus BA G and BA F Sequences

To design the full gene consensus nucleotide sequence of the BA G gene, we aligned the full length G nucleotide sequences from 31 BA isolates present in the GenBank nucleotide database which displayed the full length G gene, and we excluded the sequences of the original BA isolates. Our reasoning for excluding the original isolates from the design was that the duplication has mutated since those original strains were isolated. Initially, the duplicated region was an exact copy of 60 nt. Over time, the duplicated region in most BA isolates harbored one to four mutated amino acids which differed from the original sequences. We chose to generate our consensus based on sequences that were most closely related to strains that were currently circulating at the time of design. Similarly, the consensus BA F gene was generated by aligning the only 5 full length BA F sequences found in the GenBank nucleotide database. One weakness of the F design is that 4 of the 5 isolates were from one study, which limits the global representation of our F sequence.

We obtained BA G, BA $G_{\Delta dup}$, and BA F subclones from GeneArt, and cloned the genes into our bacterial artificial chromosome construct containing the antigenome of strain A2-line19F (clone construction shown in Fig. 1). We generated four viruses with these constructs, A2-K-BAG-BAF, A2-K-BA$G_{\Delta dup}$-BAF, A2-K-BAG-line19F, and A2-K-BA$G_{\Delta dup}$–line19F. Additionally, we generated expression plasmids with mammalian codon-optimized BA G, BA $G_{\Delta dup}$, and BAF sequences for transient expression of the three proteins.

Figure 1

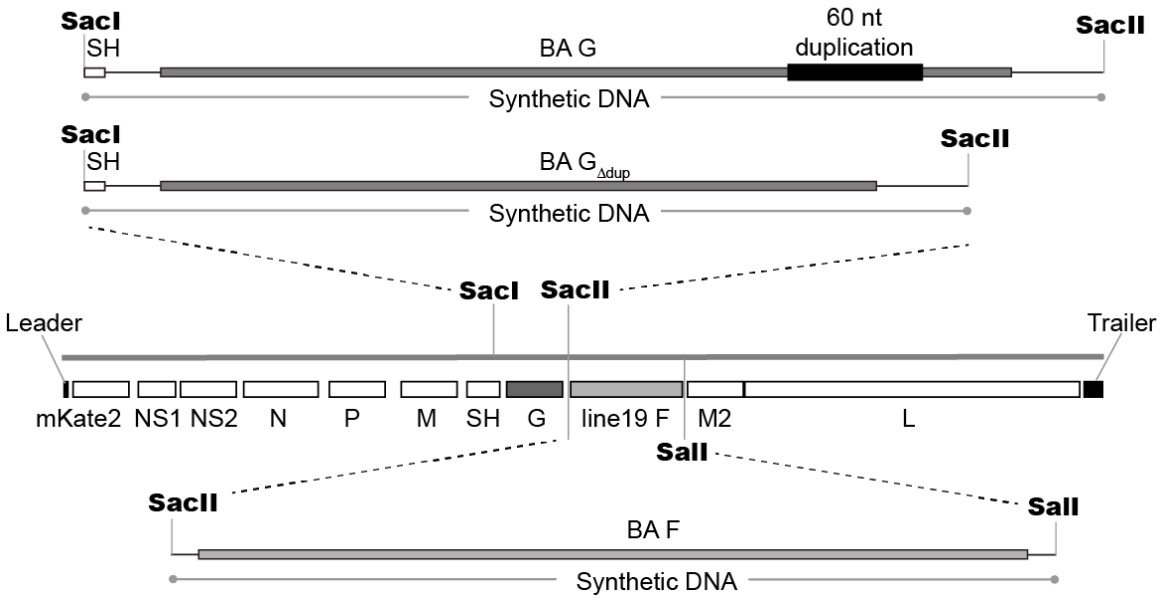

Figure 1. **BA Strain Cloning Scheme**. Subclones harboring the designed consensus sequences of BA G, BA $G_{\Delta dup}$, or BA F were obtained from GeneArt. SacI and SacII restriction sites flanking the G genes were utilized to clone the G constructs into pSynkRSVline19F in place of A2 G. Additionally, SacII and SalI restriction sites flanking the F gene were used to clone BA F in place of line 19 F. The rest of the RSV genes, shown in white, are from strain A2.

Replication of the Recombinant BA Strains in vitro

We initially tested the ability of the four viruses to replicate in a human bronchial epithelial cell line, BEAS-2B, by performing multi-step growth curves with an initial multiplicity of infection (MOI) of 0.01 for each virus. The viruses harboring line 19 F replicated with remarkably increased kinetics compared to viruses harboring the BA F gene (Fig. 2). Regardless of the F gene present in the virus, there were no distinguishable differences between the viruses expressing BA G and those expressing BA $G_{\Delta dup}$ (Fig. 2).

These data indicate that in BEAS-2B cells, there is no difference in replication of viruses with or without the duplication in G. Additionally, our data implicate BA F as attenuating compared to the A strain F, line 19 (line 19 F is discussed in greater detail in Chapter 3).

Figure 2

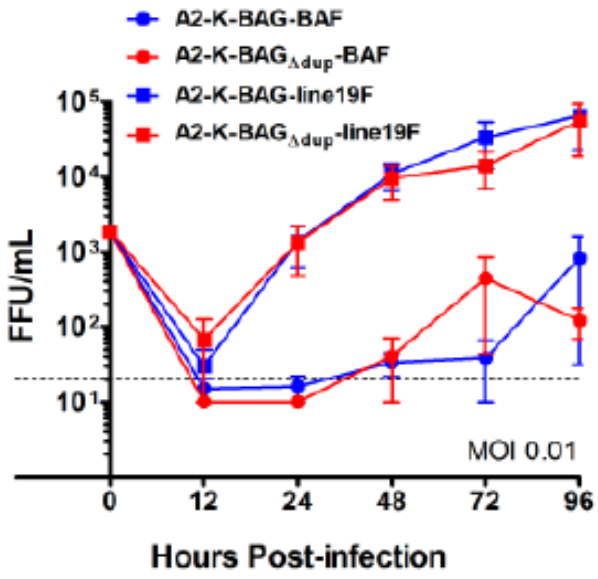

Figure 2. **Recombinant BA Strain Replication in BEAS-2B Cells**. BEAS-2B cells were infected with the four viruses indicated at an MOI of 0.01. Cells were scraped in media at the indicated time points, and virus was titered by fluorescent focus unit assay in HEp-2 cells. Duplication-containing viruses are in red, and viruses expressing line 19 F are denoted by squares. The data are a combination of three experiments combined. There are no significant differences in the paired F strains between the virus with the duplication and the virus lacking the duplication (i.e. A2-K-BAG-BAF vs. A2-K-BAG$_{\Delta dup}$-BAF) by 2-way ANOVA.

While growth curve analyses are one means to determine virus fitness, we sought to better appreciate whether the duplication in G provides an advantage to RSV. To address this in a more direct approach, we performed a competitive infection experiment by infecting HEp-2 cells simultaneously with A2-K-BAG-line19F and A2-K-BAG$_{\Delta dup}$-line19F, and assessing G RNA levels in the cells by reverse transcription followed by PCR (Fig. 3). When cells were infected with both viruses at MOI 0.5 (1:1 ratio), even as early as 24 hours post-infection, most of the G-specific RNA in the cells was from BA G, not BA G$_{\Delta dup}$. During infection with a 10:1 ratio of A2-K-BAG-line19F to A2-K-BAG$_{\Delta dup}$-line19F, virtually no BA G$_{\Delta dup}$ G RNA was detectable, whereas with a 1:10 infection ratio of the two viruses, BA G specific G was readily visible. These results suggest that A2-K-BAG-line19F has an advantage when in direct competition with A2-K-BAG$_{\Delta dup}$-line19F.

Figure 3

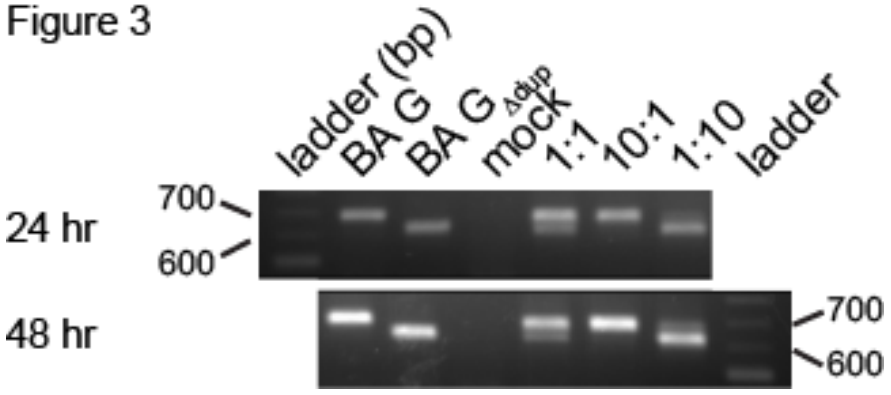

Figure 3. **Competitive Infection Assay**. HEp-2 cells were infected with A2-K-BAG-line19F, A2-K-BAG$_{\Delta dup}$-line19F, or both viruses at ratios of 1:1, 10:1, or 1:10. Twenty-four and 48 hours post-infection, RNA was harvested from cells and subjected to RT-PCR to amplify a portion of the G gene. Equal RNA amounts were used for the reverse transcription, and equal volumes of cDNA were used as templates for the PCR. Gels are representative of two experiments. Expected PCR product sizes are 709 bp for A2-K-BAG-line19F, and 649 bp for A2-K-BAG$_{\Delta dup}$-line19F.

Role of the G Duplicated Region in Virus-Cell Binding

We next sought to determine if the duplicated region played a role in the function of G as the RSV attachment protein. We inoculated BEAS-2B cells at MOI 1.0 at 4°C to allow virus binding to cells, but prevent virus fusion with cells. After sufficient time for virus binding, the cells were lysed and the amount of bound virus compared by Western blotting for N expression in the cell lysates. N expression levels were normalized to N levels in the inoculum, as well as to GAPDH levels in the cell lysates, to control for equal protein loading. We found that both A2-K-BAG-BAF and A2-K-BAG-line19F bound more efficiently to BEAS-2B cells than A2-K-BAG-G$_{\Delta dup}$-BAF and A2-K-BAG$_{\Delta dup}$-line19F (Fig. 4A-D). We saw no difference in binding between A2-K-BAG-BAF and A2-K-BAG-line19F (Fig. 4E). These data strongly support a role for the duplicated region of BA G in enhancing the attachment function of the RSV BA G protein.

Figure 4

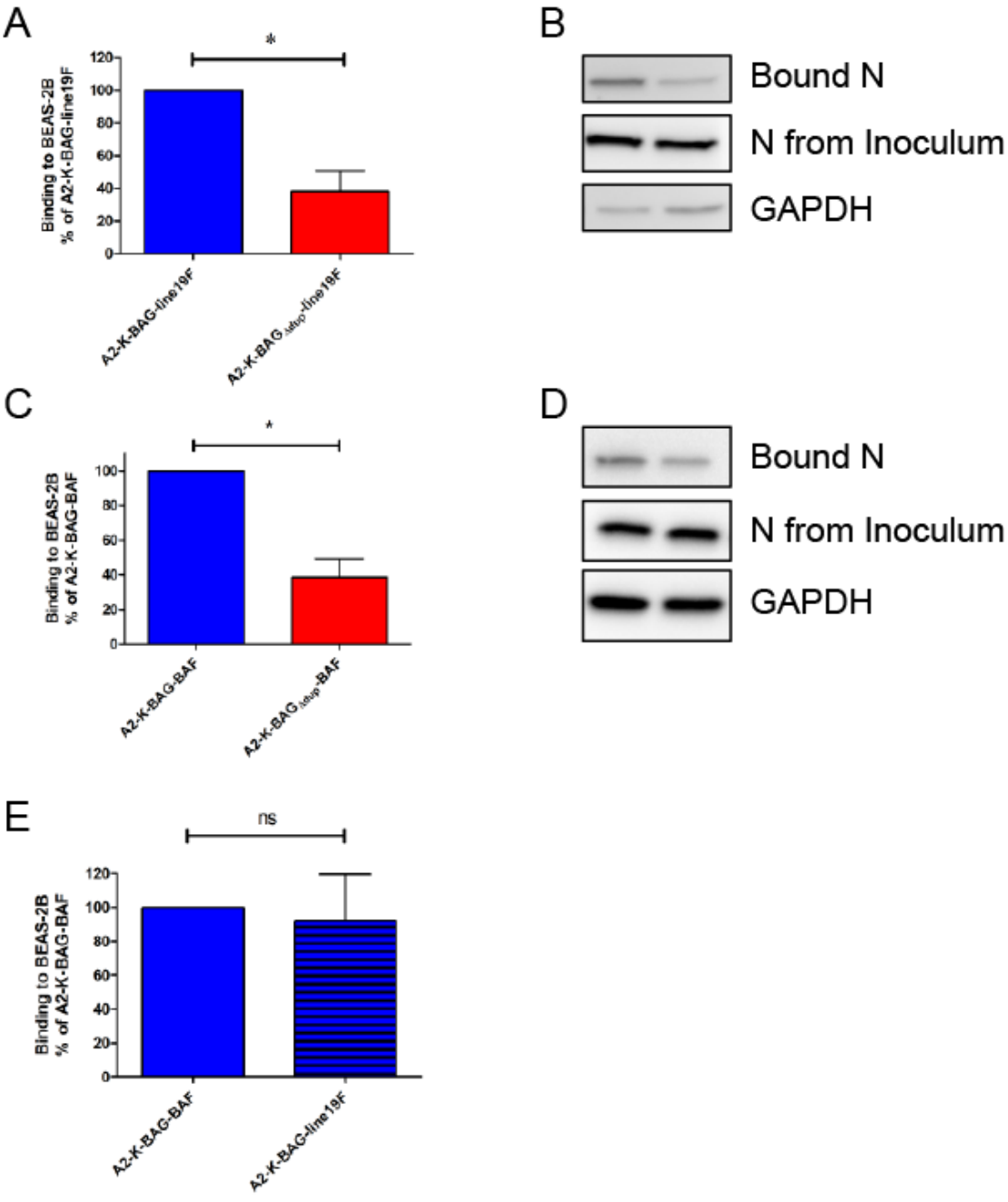
A
*
Binding to BEAS-2B
% of A2-K-BAG-line19F
120
100
80
60
40
20
0
A2-K-BAG-line19F
A2-K-BAG$_{step}$-line19F
B
Bound N
N from Inoculum
GAPDH
C
*
Binding to BEAS-2B
% of A2-K-BAG-BAF
100
80
60
40
20
0
A2-K-BAG-BAF
A2-K-BAG$_{step}$-BAF
D
Bound N
N from Inoculum
GAPDH
E
ns
Binding to BEAS-2B
% of A2-K-BAG-BAF
120
100
80
60
40
20
0
A2-K-BAG-BAF
A2-K-BAG-line19F

Figure 4. **Recombinant BA Strain Binding to BEAS-2B Cells**. BEAS-2B cells were inoculated with the indicated viruses at an MOI of 1.0, and virus was allowed to adsorb to cells at 4°C. Inoculum was removed and cells were washed three times in cold PBS to remove unbound virus. Cells were lysed and lysates, along with an aliquot of original inoculum, was subjected to SDS-PAGE and Western blotting with an anti-N monoclonal antibody. GAPDH was also probed as a loading control. (A), (C), and (E) are combinations of three experiments each, and amount of bound N was normalized to N in inoculum as well as GAPDH prior to comparison between groups. (B) and (D) are representative Western blots from experiments in (A) and (C), respectively. *$P < 0.05$ by one-way ANOVA with Tukey multiple comparison test.

As mentioned in Chapter 1, RSV G has been shown to bind many cell surface proteins, but the majority of G binding to cells is thought to occur through attachment to glycosaminoglycans (GAGs), specifically heparan sulfate. We measured the GAG dependency of A2-K-BAG-line19F and A2-K-BAG$_{\Delta dup}$-line19F. We chose to continue our studies with only the viruses expressing line 19 F because of the poor replication kinetics of the BA F expressing viruses. In a GAG dependency assay utilizing Chinese hamster ovary (CHO) cells and CHO cells deficient in generating heparan sulfate (pgs-D677), the A2-K-BAG-line19F virus exhibited a greater GAG dependency than A2-K-BAG$_{\Delta dup}$-line19F (Fig. 4), suggesting that the enhanced attachment function provided by the duplication is dependent on binding to GAGs.

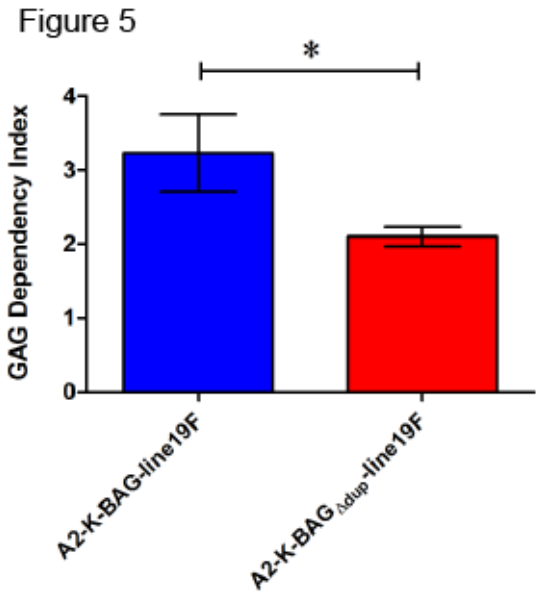

Figure 5. **Glycosaminoglycan (GAG) Dependency of Recombinant BA Strains**. Infectivity in CHO-K1 and CHO pgsD-677 cells was determined for the two indicated viruses. GAG dependency was defined as the ratio of infectivity in CHO-K1 cells to infectivity in pgsD-677 cells. Graph shows a combination of three experiments. *P < 0.05 by one-way ANOVA and Tukey multiple comparison test.

Role for the Duplicated Region in G in vivo

We ultimately investigated whether the attachment enhancement provided by the duplication in BA G contributes to advantages *in vivo*. We measured the lung viral load in BALB/c mice infected with either A2-K-BAG-line19F or A2-K-BAG$_{\Delta dup}$-line19F. While the A2-K-BAG-line19F exhibited greater lung viral load at every time point tested, the only significant difference occurred on day 6 post-infection, at the peak of viral load (Fig. 6). While only a modest enhancement over A2-K-BAG$_{\Delta dup}$-line19F, these results suggest that the duplication in G present in RSV BA strains has the ability to enhance viral infectivity *in vivo*.

Figure 6

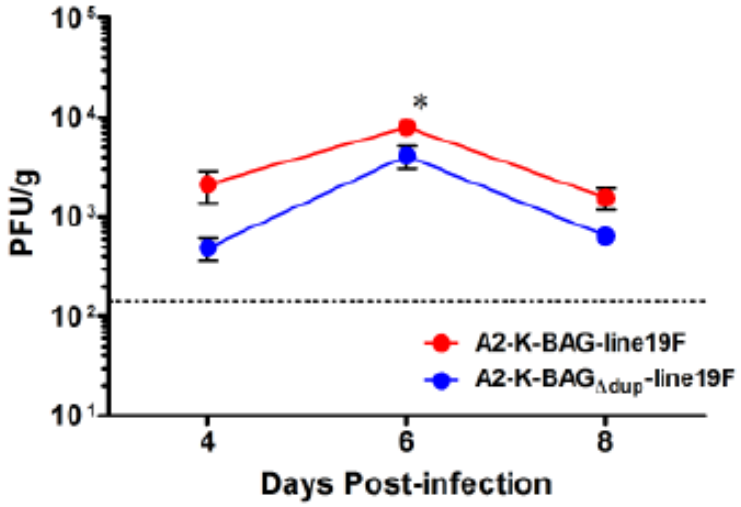

Figure 6. **Recombinant BA Strain Lung Viral Load in BALB/c Mice.** BALB/c mice were infected with 1 x 10^5 PFU of either A2-K-BAG-line19F or A2-K-BAG$_{\Delta dup}$-line19F and lungs were harvested on days 4, 6, and 8 post-infection. Viral load was quantified by immunodetection plaque assay. *$P < 0.05$ by one-way ANOVA and Tukey multiple comparison test.

Discussion

The RSV attachment glycoprotein, G, is the most variable RSV protein between strains, and is capable of tolerating many mutations. G sequences have evolved over time, with perhaps the greatest change occurring in the last two decades with the introduction of a 60 nt duplication in B strains and a 72 nt duplication in A strains. We generated recombinant virus strains expressing consensus G proteins from the BA subgroup with or without the 60 nt duplication to determine a role for the duplication in the context of the virus. We also generated a consensus F gene from BA strains, and cloned this F into our BA G and BA $G_{\Delta dup}$ expressing viruses.

We found that the BA F gene did not support replication of the viruses to the extent that the A strain line 19 F protein did. The possibility exists that the F consensus we designed does not properly reflect a homotypic BA F protein paired with the BA G protein we designed, due to the small number of sequences used to generate the F consensus relative to the G consensus (5 F sequences, to 31 G sequences). Alternatively, preliminary results suggest that the BA F protein is deficient in fusion activity compared to line 19 F (data not shown), which could contribute to the inability of BA F expressing viruses to grow to the same levels as line 19 F expressing viruses in BEAS-2B cells.

In the context of viruses expressing line 19 F, we were able to show a role for the duplication in G in virus attachment to cells (Fig. 4). We also showed that this enhanced attachment by BA G relative to BA $G_{\Delta dup}$ expressing viruses was dependent on heparan sulfate containing glycosaminoglycans (GAGS; Fig. 5). Although the duplicated region does not encompass the linear heparin binding domain characterized on RSV G (174), there are 11 potential O-glycosylation sites in the duplicated region (serine and threonine

residues). One study suggested that heparin-like structures on G were critical for the role of G in attachment progressing to viral infection (175). These two characteristics of G result in our working hypothesis that the extra glycans likely present on BA G are responsible for the enhanced binding of BA G relative to BA $G_{\Delta dup}$. Studies are needed to determine whether the two G proteins are indeed differentially glycosylated, and whether mutagenesis of the additional 11 glycosylation sites abrogates the BA G enhanced cell-binding phenotype.

In addition to a general enhancement of binding efficiency to BEAS-2B cells, we showed that the duplication provides an advantage in both a competitive infection assay as well as in BALB/c mice (Figs. 3 and 6). The advantages we identified both *in vitro* and *in vivo* suggest one reason that BA strains expanded so drastically after their initial introduction to circulating RSV strains. It is conceivable that a slight growth advantage *in vivo* could lead to greater transmission and dissemination of a virus strain in the human population. Due to limitations of RSV animal models, direct contact transmission studies with RSV are rare if not nonexistent, but might provide further clues to the selective advantage of the duplication in BA strain G genes if they could be performed.

Attachment is only one function of G during the course of RSV infections. The secreted form of the G protein was shown to serve in an antigen-decoy mechanism (169). We did not address what role the duplication may play in this type of immune modulation. For an A strain of RSV, binding of G by a monoclonal antibody reduced pathogenesis parameters including breath distension and mucus induction (131). Results from that study suggest a further role for G in pathogenesis. Our study was limited to

measuring viral load *in vivo*, and further work would be required to investigate the role of the duplication on these other functions of G.

While our study did not include an A strain RSV exhibiting the duplication in G, we hypothesize a similar binding enhancement and mechanism to be at play. The duplication in the original ON1 isolates also resulted in 11 additional potential O-glycosylation sites (15), providing feasibility to this hypothesis. Further studies specifically on the duplication in A strains are needed to confirm this, but could easily be performed based on the results and reagents established here.

Acknowledgements

This work was supported by NIH grant 1R01AI087798 (to M.L.M.) and the Children's Center for Immunology and Vaccines. We thank Ursula Buchholz and Karl-Klaus Conzelmann for the BSR-T7/5 cells. We thank Edward Walsh for the D14 monoclonal antibody.

Chapter 5

Summary and Conclusions

The respiratory syncytial virus (RSV) attachment (G) and fusion (F) glycoproteins are arguably the most well-studied of the RSV proteins, however, the effect of sequence variations in the two glycoproteins between RSV strains on viral pathogenesis has not been thoroughly characterized. Elucidating mechanisms of pathogenesis directed by these two proteins is critical to identifying therapeutics and targeted RSV vaccines. In the preceding chapters, we demonstrated that enhancing the basic activities attributed to each of these glycoproteins can result in worsened pathogenesis in the BALB/c mouse model. In the case of F, augmenting fusion activity caused drastic changes in viral pathogenesis, including greater viral load, weight loss, and altered cytokine production in the A2-line19F model of RSV disease (Chapter 3). Boosting the attachment function of G also resulted in a virus exhibiting enhanced viral load in the RSV mouse model (Chapter 4).

In order to investigate how modulating the activities of the glycoproteins affected pathogenesis, we first developed an easily manipulated mutagenesis system. Recombination-mediated mutagenesis is a new tool to the RSV field, but has been used for decades to mutagenize DNA viruses (105, 176), and we believe it can be utilized in future studies of specific RSV mutants. We generated both point and deletion mutants (Chapters 3 and 2, respectively) within the system, which has been used by our group to generate close to twenty mutants currently under study. Rescue of viruses has also been supplemented by our development of sequence-optimized expression plasmids for the helper proteins. We believe this set of tools provides strong framework for future studies with RSV mutants, and acts as a platform from which to develop specifically mutated live-attenuated vaccine candidates.

Several reports suggest that viral load is a predictor for disease severity in infants (90, 151-153). Severe cases of RSV-induced bronchiolitis in infants result in mucus plugs in small airways (7). The RSV strain line 19 and the chimeric strain A2-line19F present a more human-like model of RSV infection (greater mucus induction and airway hyper-reactivity) in mice than do commonly studied lab strains A2 and Long (75, 77). We hypothesized that in the context of the A2-line19F mouse model of RSV, fusion activity, viral load, and mucus induction were linked. Through mutagenesis studies with F expression plasmids, we found that residues 79 and 191 together are critical for the fusion function of the line 19 F protein. While a virus expressing F with mutations at these residues exhibited decreased early viral load relative to A2-line19F, peak viral load and mucus induction were unaffected. Additionally, residues 357 and 371 together were identified as critical for the mucus induction of A2-line19F, but when mutated actually resulted in a gain of function in fusion activity. Together, these results suggest that fusion activity, viral load, and mucus induction are not correlated in a linear fashion. Instead, our results show that fusion activity and early viral load correlate with one another, and suggest a threshold of viral load necessary for differential immune responses to RSV.

The greater fusion activity of the K357T/Y371N mutant compared with line 19 F could be the result of either a change in the ability of F to interact with other proteins, or an intrinsic difference between the F proteins of the two strains. If the first scenario is at play, it is possible that the K357T/Y371N mutant F is more easily triggered for fusion than line 19 F. This could be due to a differential interaction with a host cell protein (receptor/co-receptor) or with the RSV attachment protein G. In either case, the K357T/Y371N mutant may require less activation energy initiated by a protein-protein

interaction to transition from the pre-fusion to post-fusion conformation. The differential interaction with G is less likely, since G was not a part of the dual-split protein (DSP) fusion assay used to determine the fusion activities of the two F proteins, and G is not required for fusion to occur. RSV F was shown to interact with multiple proteins, including nucleolin (71), TLR-4 (177), and ICAM-1 (178). A future study could test the interactions of line 19 versus the K357T/Y371N mutant with these known F-interacting partners to determine if there are differences, and to tease out how these might affect fusion activity.

A second possibility is that the A2-line19F-K357T/Y371N virus has a greater proportion of prefusion F compared to postfusion F on the virus cell or virus surface than A2-line19F, allowing more F to be available for fusion activation. If F is already in the postfusion conformation on the cell surface, those proteins would not be able to cause cell-cell or virus-cell fusion, as the pre- to postfusion transition is irreversible. The amount of F in the prefusion and postfusion conformations is testable by ELISA with prefusion F-specific monoclonal antibodies (179), and is an area of ongoing follow-up research. In preliminary experiments, it appears that A2-line19F actually has a greater proportion of prefusion F out of the total F than does A2-line19F-K357T/Y371N. These results support the hypothesis that the K357T/Y371N F is more easily triggered to undergo the pre- to postfusion conformational changes. Similar explanations are likely responsible for the greater fusion activity of line 19 F compared to the M79I/R191K mutant F or Long F.

Interestingly, the residues responsible for fusion activity in line 19 F (79/191) were not the same residues responsible for the mucus induction caused by line 19 F

(357/371). This was contrary to our hypothesis, and indicates a complex role for F in infection, where different domains of F may function in different roles for the protein. Many studies focusing on RSV as well as other paramyxoviruses have identified residues or domains in F critical for fusion activity (63, 69, 134-137, 149, 150, 180), but domains important for pathogenesis are not defined. We have identified residues 357 and 371 as important to the pathogenesis of RSV strain line 19. In an alignment of 46 RSV A strain F proteins (not including line 19), these particular residues are conserved, but lie in a region with a good amount of variability, given the overall conservation of F between strains (Fig. 1). While not a part of defined antigenic sites (68), this region may present a site of immune selection that has not yet been defined. Mouse passage studies using the K357T/Y371N mutant could elucidate whether this is actually occurring. Furthermore, expanding the sites of mutagenesis to a broader set of surrounding residues may shed light on whether 357 and 371 are actually located in an F protein-domain necessary for pathogenesis. Another supporting factor for this hypothesis is that altering residue 357 alone had a modest effect on pathogenesis, while mutating both 357 and 371 together resulted in drastic changes, suggesting more of a domain-dependent mechanism.

Figure 1

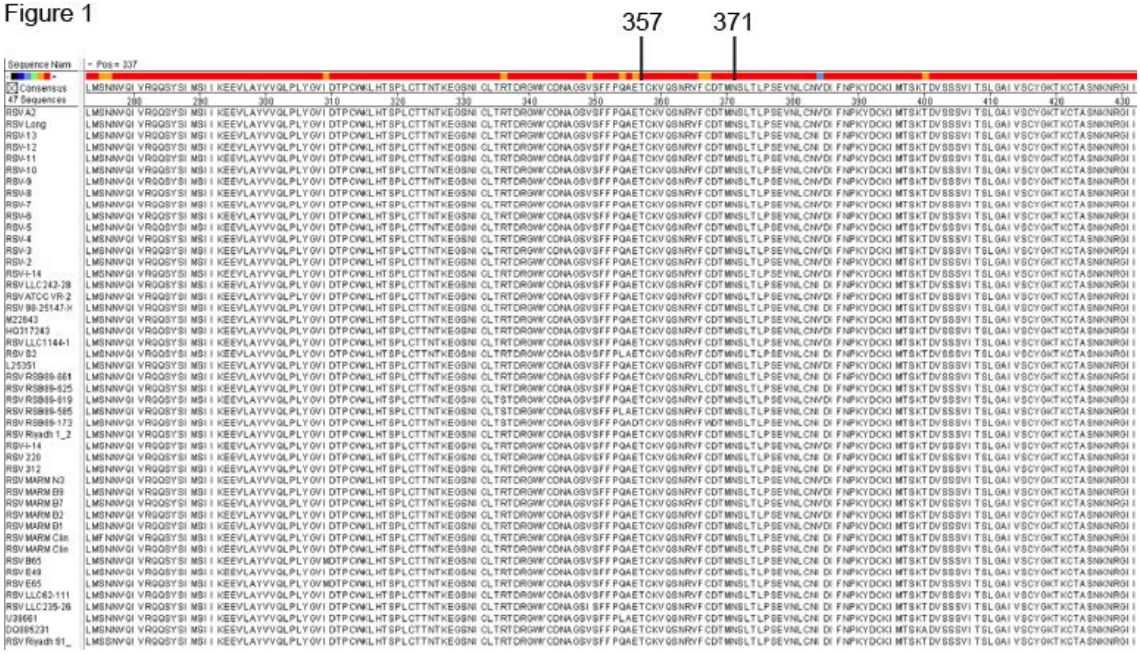

Figure 1. **RSV A Strain F Protein Alignment.** Forty-seven RSV A protein sequences obtained from GenBank were aligned using MegAlign in the DNAStar Lasergene Software suite. Residues 273-431 are shown. Variability from the consensus is indicated by the colored bar across the top, where red is conserved, orange is an amino acid difference across 1-3 strains, and blue is an amino acid difference across at least half of the strains.

The differential pathogenesis of the K357T/Y371N mutant compared to A2-line19F occurs early during infection, as mice begin losing greater amounts of weight by days 1 and 2 post-infection, and have severe lung pathology by day 2 post-infection (Chapter 3, Fig. 6). These results suggest a differential activation of the innate immune response during K357T/Y371N infection. As discussed previously, this could be due to a change in a direct protein-protein interaction. An alternative hypothesis is that the higher viral load induced by this virus on days 1 and 2 post-infection results in a higher antigen burden in the mice, and therefore upregulates innate immune responses. This could be

directly tested by inoculating mice with increasing doses of A2-line19F or decreasing doses the K357T/Y371N mutant such that the day 1 and 2 viral loads are the same. A potential flaw with this experiment, however, is that if early viral load is truly dependent on fusion activity, as we have concluded, it may never be possible to achieve comparable day 1 and 2 viral loads between the two viruses. Another hyperfusogenic strain of RSV would be needed to test this hypothesis.

Assuming that an increase in early viral load is responsible for the disparate immune response to the two strains, the question still remains as to what immune cells are activated by the K357T/Y371N mutant that are not activated by A2-line19F and most other RSV strains. One potential cell subset are the group 3 innate lymphoid cells (ILC3s). Three groups of ILCs have been identified to date, and respond to various forms of infection (bacterial, viral, parasitic) in the lungs, gut, and even the skin (181). A hallmark of ILCs is their ability to respond to pathogens with transcription factor and cytokine output commonly associated with T helper cell subtypes, but without an antigen specific T-cell receptor (181).

ILC3s were shown to produce interleukin 22 (IL-22) in a model of allergic airway inflammation, and the IL-22 served to downregulate mediators of the inflammation, such as IL-13 and IL-5 (182). Interestingly, IL-22 presence or absence did not affect IFN-γ levels in this model (182). We saw similar trends in IL-13, IL-5, and IFN-γ expression induced upon infection with the K357T/Y371N mutant compared to A2-line19F (Chapter 3, Fig. 6). It is possible that the K357T/Y371N mutant is inducing ILC3s, which in turn produce IL-22 that can dampen the normal T_h2 response seen with A2-line19F. IL-22 was not one of the cytokines tested in our Luminex panel (Chapter 3), but could easily be

tested by Luminex or ELISA. Additional studies investigating whether ILC3s are activated in response to infection with the K357T/Y371N mutant would be needed to test this hypothesis.

The M79I/R191K mutant, which we demonstrated to have low fusion activity *in vitro*, had a very interesting phenotype *in vivo*. This virus exhibited low early viral load, but had peak viral load similar to A2-line19F (Chapter 3). We sequenced the F gene of the virus from lung homogenates at day 4 post-infection and found no reversion mutations in F. One possibility to explain these findings is that a mutation occurred elsewhere in the virus and enabled it to reproduce to A2-line19F levels by day 4 post-infection. While this is feasible, it implies that a similar mutation occurred in the virus in each mouse, since the variation in the measured viral load between samples was small (Chapter 3, Fig. 4).

An alternative hypothesis is that early viral load and peak viral load have different determinants. We established that early viral load is dependent on fusion activity (Chapter 3), although none of the mutants described to have differential fusion activity from line 19 F exhibited a reduction in peak viral load. To investigate this further, I attempted replication studies in several mouse cell lines but none that were tested sustained replication of RSV (epithelial cells MLE-12 and LA-4, and fibroblast cells NIH-3T3). Instead, I measured growth of A2-line19F and A2-LongF in baby hamster kidney cells (BHK-21), as a representative rodent cell line. Here, A2-LongF exhibited lower peak titers than A2-line19F (Fig. 2A). In these cells, the Y371N mutant virus displayed a replication phenotype similar to A2-LongF, not A2-line19F (Fig. 2A). When peak lung viral load was measured on day 4 post-infection from BALB/c mice, this

mutant displayed statistically significantly lower viral load than A2-line19F, albeit not reduced to the level of A2-LongF (Fig. 2B). Together these results indicate the tyrosine residue at position 371 in line 19 F is important for viral replication in rodent cells *in vitro* as well as *in vivo*.

Figure 2

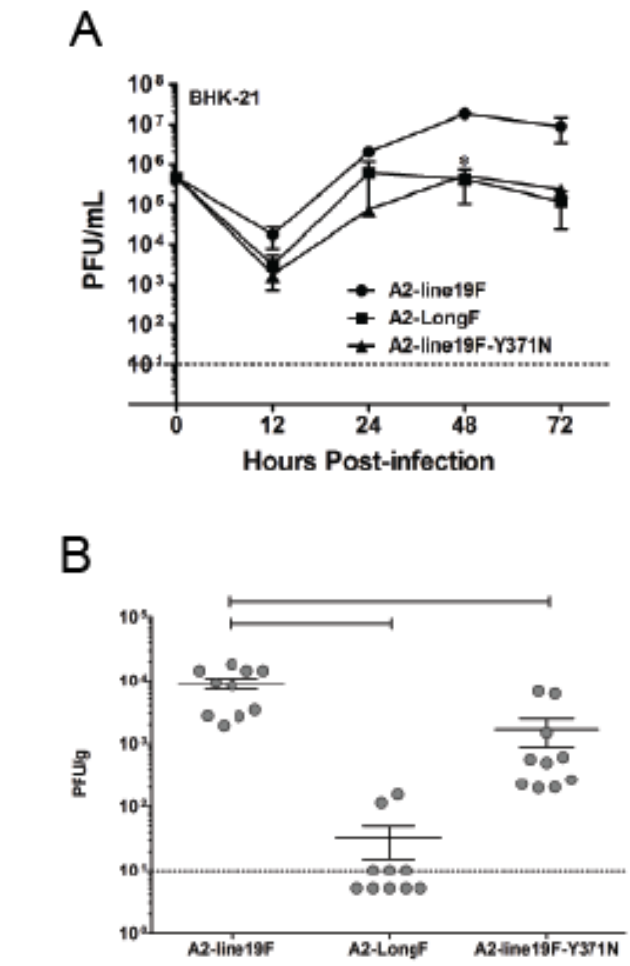

Figure 2. **A2-line19F-Y371N Replication in BHK-21 Cells and BALB/c Mice.** (A) BHK-21 cells were infected in duplicate with each virus and samples were harvested at indicated timepoints by scraping cells in media. Virus was titrated by immunodetection plaque assay. Graph is combination of three experiments. *$P < 0.05$ compared to A2-line19F by two-way ANOVA and Tukey multiple comparison test. (B) Groups of 5 BALB/c mice were infected with 3 x 105 PFU per mouse. Left lungs were harvested on day 4 post-infection, homogenized, and virus was titrated by immunodetection plaque assay. Graph is a combination of two experiments. Cross bars indicate groups significantly different from A2-line19F. *$P < 0.001$ by one-way ANOVA and Tukey multiple comparison test.

Based on these results, any of our mutants with a tyrosine at position 371 should have viral load similar to A2-line19F. This was seen for all mutant viruses tested (data not shown), and is exemplified in this dissertation by mutants K357T and M79I/R191K (Chapter 3, Figure 4). The one virus of intrigue, if residue 371 is truly a determinant of peak viral load, is K357T/Y371N, which exhibits even greater peak viral load than A2-line19F (Chapter 3, Figure 4). While this virus has a mutated residue 371, my hypothesis is that the increase in fusion activity afforded by the addition of the mutation at 357 (and thus high early viral load) supersedes any phenotype contributed by a 371 mutation, allowing the virus to gain a foothold in the mouse, and replicate to high peak titers. Further evidence suggesting this might be the case is demonstrated by my efforts to generate a M79I/R191K/Y371N triple mutant. I hypothesized that by mutating both the residues responsible for line 19 F fusion activity as well as the residue I believe to be responsible for A2-line19F peak viral load, I would generate a virus similar to A2-LongF

on all fronts. Unfortunately, although this mutant was able to be rescued in BSR-T7 cells, three attempts at generating master stocks in HEp-2 cells have yielded no visible cytopathic effect up to 7 days post-infection (data not shown). It is possible that additional mutation of this construct at residue 357 could rescue the virus, but I have not tested whether this is the case. If so, it would support the epistasis, or dominant nature, of the K357T mutation relative to the Y371N mutation hypothesized above.

In addition to showing that enhanced F activity results in augmented pathogenesis, we defined a role for the 60 nucleotide duplication in the G protein of RSV BA strains in virus-cell attachment. The duplicated region of 20 amino acids in our construct contains 11 potential O-glycosylation sites. I hypothesize a link between the addition of these potential glycosylation sites and the enhanced binding efficiency of viruses with the duplication. Initially, it needs to be determined whether the potential glycosylation sites are actually glycosylated. In the study first describing strains with the duplication, Western blots were performed in the presence and absence of tunicamycin to identify the size difference in G conferred by the additional 20 amino acids (58). The blot without tunicamycin was poorly resolved at the level of mature, glycosylated G, so it is unclear whether additional glycosylation events occurred in the presence of the duplication (58). Once it is determined whether the duplicated region includes newly glycosylated residues, the effect of the additional glycosylation could be tested by mutating each potentially glycosylated amino acid to a non-modifiable one and determining the effect of the mutants on virus to cell binding.

Whether additional glycosylation sites are the reason for enhanced binding or some other mechanism is at play, the prevalence of RSV strains containing duplications

in G suggest that the virus is able to tolerate fairly large insertions in order to maintain a fitness advantage in nature. We demonstrated that the virus with the duplication exhibited greater peak viral loads in BALB/c mice. Due to limitations of human studies, it remains to be determined whether this holds true in humans. An additional possibility which we are unable to test in current animal model systems of RSV is that the enhanced binding is important for transmission of the virus. The prevalence of strains with duplications in G could simply be due to the ability of these viruses to transmit more readily than viruses without the duplication in G. Until an effective animal model of RSV transmission is established, however, this is likely to remain a mystery.

Another possible advantage for viruses with the duplication in G that is not simply based on virus to cell binding or transmission, is that extra glycosylation of G serves to shield the F protein from neutralization by antibodies. This could be tested by using the viruses we generated to measure neutralization by both F-specific and non F-specific anti-RSV antibodies. I speculate that the viruses lacking the duplication and additional glycosylation sites in G would be more sensitive to F-specific antibody neutralization, based simply on the ability of the antibodies to attach to the F protein (183). If G shielding of F is indeed occurring, it should considered when rationally designing prophylaxis and treatment for RSV, much of which is currently being designed to target the F protein (184). It is likely that a combination G and F targeting vaccine or treatment will be needed to effectively prevent RSV infections or reduce disease burden.

Our work describes how specific strain variations, including those found in currently circulating RSV strains, can lead to differential pathogenesis of RSV. Given the ever increasing number of vaccine candidates making their way through the pipeline for

RSV (51 as of July 8, 2014, according to PATH, Ref (185)), it is critical to understand how specific genetic characteristics of different strains and specific proteins can contribute to pathogenesis. Incomplete understanding of potential pitfalls of a formalin-inactivated vaccine candidate led to disastrous consequences in the 1960s. I believe our work provides a better foundation for understanding how two of the eleven RSV proteins can affect pathogenesis, and can contribute to rational vaccine design. Additionally, our research on the duplicated region in BA strain G proteins points toward a type of selective advantage that RSV is using in nature. Understanding how some strains become dominant over time could help the field to determine what types of mutations RSV might undergo when faced with the selective pressure of widely used drugs or vaccination currently in development.

References

1. **Blount RE, Jr., Morris JA, Savage RE.** 1956. Recovery of cytopathogenic agent from chimpanzees with coryza. Proc Soc Exp Biol Med **92:**544-549.
2. **Chanock R, Finberg L.** 1957. Recovery from infants with respiratory illness of a virus related to chimpanzee coryza agent (CCA). II. Epidemiologic aspects of infection in infants and young children. American journal of hygiene **66:**291-300.
3. **Chanock R, Roizman B, Myers R.** 1957. Recovery from infants with respiratory illness of a virus related to chimpanzee coryza agent (CCA). I. Isolation, properties and characterization. American journal of hygiene **66:**281-290.
4. **Nair H, Nokes DJ, Gessner BD, Dherani M, Madhi SA, Singleton RJ, O'Brien KL, Roca A, Wright PF, Bruce N, Chandran A, Theodoratou E, Sutanto A, Sedyaningsih ER, Ngama M, Munywoki PK, Kartasasmita C, Simoes EA, Rudan I, Weber MW, Campbell H.** 2010. Global burden of acute lower respiratory infections due to respiratory syncytial virus in young children: a systematic review and meta-analysis. Lancet **375:**1545-1555.
5. **Hall CB, Weinberg GA, Iwane MK, Blumkin AK, Edwards KM, Staat MA, Auinger P, Griffin MR, Poehling KA, Erdman D, Grijalva CG, Zhu Y, Szilagyi P.** 2009. The burden of respiratory syncytial virus infection in young children. N Engl J Med **360:**588-598.
6. **Aherne W, Bird T, Court SD, Gardner PS, McQuillin J.** 1970. Pathological changes in virus infections of the lower respiratory tract in children. J Clin Pathol **23:**7-18.
7. **Johnson JE, Gonzales RA, Olson SJ, Wright PF, Graham BS.** 2007. The histopathology of fatal untreated human respiratory syncytial virus infection. Mod Pathol **20:**108-119.
8. **Committee On Infectious D, Bronchiolitis Guidelines C, Committee On Infectious D, Bronchiolitis Guidelines C.** 2014. Updated guidance for palivizumab prophylaxis among infants and young children at increased risk of hospitalization for respiratory syncytial virus infection. Pediatrics **134:**415-420.
9. **Committee On Infectious D, Bronchiolitis Guidelines C, Committee On Infectious D, Bronchiolitis Guidelines C.** 2014. Updated guidance for palivizumab prophylaxis among infants and young children at increased risk of hospitalization for respiratory syncytial virus infection. Pediatrics **134:**e620-638.
10. **Gardinassi LG, Simas PV, Gomes DE, do Bonfim CM, Nogueira FC, Garcia GR, Carareto CM, Rahal P, de Souza FP.** 2012. Diversity and adaptation of human respiratory syncytial virus genotypes circulating in two distinct communities: public hospital and day care center. Viruses **4:**2432-2447.
11. **Hervas D, Reina J, Hervas JA.** 2012. Meteorologic conditions and respiratory syncytial virus activity. Pediatr Infect Dis J **31:**e176-181.
12. **Paynter S, Sly PD, Ware RS, Williams G, Weinstein P.** 2014. The importance of the local environment in the transmission of respiratory syncytial virus. The Science of the total environment **493:**521-525.
13. **Anderson LJ, Hierholzer JC, Tsou C, Hendry RM, Fernie BF, Stone Y, McIntosh K.** 1985. Antigenic characterization of respiratory syncytial virus strains with monoclonal antibodies. J Infect Dis **151:**626-633.

14. **Peret TC, Hall CB, Schnabel KC, Golub JA, Anderson LJ.** 1998. Circulation patterns of genetically distinct group A and B strains of human respiratory syncytial virus in a community. J Gen Virol **79 (Pt 9):**2221-2229.
15. **Eshaghi A, Duvvuri VR, Lai R, Nadarajah JT, Li A, Patel SN, Low DE, Gubbay JB.** 2012. Genetic variability of human respiratory syncytial virus A strains circulating in Ontario: a novel genotype with a 72 nucleotide G gene duplication. PLoS One **7:**e32807.
16. **Cowton VM, McGivern DR, Fearns R.** 2006. Unravelling the complexities of respiratory syncytial virus RNA synthesis. J Gen Virol **87:**1805-1821.
17. **Xu X, Zheng J, Zheng K, Hou Y, Zhao F, Zhao D.** 2014. Respiratory syncytial virus NS1 protein degrades STAT2 by inducing SOCS1 expression. Intervirology **57:**65-73.
18. **Hastie ML, Headlam MJ, Patel NB, Bukreyev AA, Buchholz UJ, Dave KA, Norris EL, Wright CL, Spann KM, Collins PL, Gorman JJ.** 2012. The human respiratory syncytial virus nonstructural protein 1 regulates type I and type II interferon pathways. Molecular & cellular proteomics : MCP **11:**108-127.
19. **Teng MN, Whitehead SS, Bermingham A, St Claire M, Elkins WR, Murphy BR, Collins PL.** 2000. Recombinant respiratory syncytial virus that does not express the NS1 or M2-2 protein is highly attenuated and immunogenic in chimpanzees. J Virol **74:**9317-9321.
20. **Whitehead SS, Bukreyev A, Teng MN, Firestone CY, St Claire M, Elkins WR, Collins PL, Murphy BR.** 1999. Recombinant respiratory syncytial virus bearing a deletion of either the NS2 or SH gene is attenuated in chimpanzees. J Virol **73:**3438-3442.
21. **Wright PF, Karron RA, Madhi SA, Treanor JJ, King JC, O'Shea A, Ikizler MR, Zhu Y, Collins PL, Cutland C, Randolph VB, Deatly AM, Hackell JG, Gruber WC, Murphy BR.** 2006. The interferon antagonist NS2 protein of respiratory syncytial virus is an important virulence determinant for humans. J Infect Dis **193:**573-581.
22. **Meng J, Lee S, Hotard AL, Moore ML.** 2014. Refining the balance of attenuation and immunogenicity of respiratory syncytial virus by targeted codon deoptimization of virulence genes. MBio **5**.
23. **Bakker SE, Duquerroy S, Galloux M, Loney C, Conner E, Eleouet JF, Rey FA, Bhella D.** 2013. The respiratory syncytial virus nucleoprotein-RNA complex forms a left-handed helical nucleocapsid. J Gen Virol **94:**1734-1738.
24. **Navarro J, Lopez-Otin C, Villanueva N.** 1991. Location of phosphorylated residues in human respiratory syncytial virus phosphoprotein. J Gen Virol **72 (Pt 6):**1455-1459.
25. **Asenjo A, Calvo E, Villanueva N.** 2006. Phosphorylation of human respiratory syncytial virus P protein at threonine 108 controls its interaction with the M2-1 protein in the viral RNA polymerase complex. J Gen Virol **87:**3637-3642.
26. **Castagne N, Barbier A, Bernard J, Rezaei H, Huet JC, Henry C, Da Costa B, Eleouet JF.** 2004. Biochemical characterization of the respiratory syncytial virus P-P and P-N protein complexes and localization of the P protein oligomerization domain. J Gen Virol **85:**1643-1653.

27. **Tran TL, Castagne N, Bhella D, Varela PF, Bernard J, Chilmonczyk S, Berkenkamp S, Benhamo V, Grznarova K, Grosclaude J, Nespoulos C, Rey FA, Eleouet JF.** 2007. The nine C-terminal amino acids of the respiratory syncytial virus protein P are necessary and sufficient for binding to ribonucleoprotein complexes in which six ribonucleotides are contacted per N protein protomer. J Gen Virol **88:**196-206.
28. **Yu Q, Hardy RW, Wertz GW.** 1995. Functional cDNA clones of the human respiratory syncytial (RS) virus N, P, and L proteins support replication of RS virus genomic RNA analogs and define minimal trans-acting requirements for RNA replication. J Virol **69:**2412-2419.
29. **Bajorek M, Caly L, Tran KC, Maertens GN, Tripp RA, Bacharach E, Teng MN, Ghildyal R, Jans DA.** 2014. The Thr205 phosphorylation site within respiratory syncytial virus matrix (M) protein modulates M oligomerization and virus production. J Virol **88:**6380-6393.
30. **Kiss G, Holl JM, Williams GM, Alonas E, Vanover D, Lifland AW, Gudheti M, Guerrero-Ferreira RC, Nair V, Yi H, Graham BS, Santangelo PJ, Wright ER.** 2014. Structural Analysis of Respiratory Syncytial Virus Reveals the Position of M2-1 between the Matrix Protein and the Ribonucleoprotein Complex. J Virol **88:**7602-7617.
31. **Liljeroos L, Krzyzaniak MA, Helenius A, Butcher SJ.** 2013. Architecture of respiratory syncytial virus revealed by electron cryotomography. Proc Natl Acad Sci U S A **110:**11133-11138.
32. **Gan SW, Tan E, Lin X, Yu D, Wang J, Tan GM, Vararattanavech A, Yeo CY, Soon CH, Soong TW, Pervushin K, Torres J.** 2012. The small hydrophobic protein of the human respiratory syncytial virus forms pentameric ion channels. J Biol Chem **287:**24671-24689.
33. **Masante C, El Najjar F, Chang A, Jones A, Moncman CL, Dutch RE.** 2014. The human metapneumovirus small hydrophobic protein has properties consistent with those of a viroporin and can modulate viral fusogenic activity. J Virol **88:**6423-6433.
34. **Bukreyev A, Whitehead SS, Murphy BR, Collins PL.** 1997. Recombinant respiratory syncytial virus from which the entire SH gene has been deleted grows efficiently in cell culture and exhibits site-specific attenuation in the respiratory tract of the mouse. J Virol **71:**8973-8982.
35. **McLellan JS, Ray WC, Peeples ME.** 2013. Structure and function of respiratory syncytial virus surface glycoproteins. Current topics in microbiology and immunology **372:**83-104.
36. **Blondot ML, Dubosclard V, Fix J, Lassoued S, Aumont-Nicaise M, Bontems F, Eleouet JF, Sizun C.** 2012. Structure and functional analysis of the RNA- and viral phosphoprotein-binding domain of respiratory syncytial virus M2-1 protein. PLoS Pathog **8:**e1002734.
37. **Bermingham A, Collins PL.** 1999. The M2-2 protein of human respiratory syncytial virus is a regulatory factor involved in the balance between RNA replication and transcription. Proc Natl Acad Sci U S A **96:**11259-11264.

38. **Jin H, Cheng X, Zhou HZ, Li S, Seddiqui A.** 2000. Respiratory syncytial virus that lacks open reading frame 2 of the M2 gene (M2-2) has altered growth characteristics and is attenuated in rodents. J Virol **74:**74-82.
39. **Fearns R, Collins PL.** 1999. Model for polymerase access to the overlapped L gene of respiratory syncytial virus. J Virol **73:**388-397.
40. **Cartee TL, Megaw AG, Oomens AG, Wertz GW.** 2003. Identification of a single amino acid change in the human respiratory syncytial virus L protein that affects transcriptional termination. J Virol **77:**7352-7360.
41. **Tang RS, Nguyen N, Zhou H, Jin H.** 2002. Clustered charge-to-alanine mutagenesis of human respiratory syncytial virus L polymerase generates temperature-sensitive viruses. Virology **302:**207-216.
42. **Roberts SR, Lichtenstein D, Ball LA, Wertz GW.** 1994. The membrane-associated and secreted forms of the respiratory syncytial virus attachment glycoprotein G are synthesized from alternative initiation codons. J Virol **68:**4538-4546.
43. **Levine S, Klaiber-Franco R, Paradiso PR.** 1987. Demonstration that glycoprotein G is the attachment protein of respiratory syncytial virus. J Gen Virol **68 (Pt 9):**2521-2524.
44. **Hallak LK, Collins PL, Knudson W, Peeples ME.** 2000. Iduronic acid-containing glycosaminoglycans on target cells are required for efficient respiratory syncytial virus infection. Virology **271:**264-275.
45. **Techaarpornkul S, Collins PL, Peeples ME.** 2002. Respiratory syncytial virus with the fusion protein as its only viral glycoprotein is less dependent on cellular glycosaminoglycans for attachment than complete virus. Virology **294:**296-304.
46. **Tripp RA, Jones LP, Haynes LM, Zheng H, Murphy PM, Anderson LJ.** 2001. CX3C chemokine mimicry by respiratory syncytial virus G glycoprotein. Nature immunology **2:**732-738.
47. **Hickling TP, Malhotra R, Bright H, McDowell W, Blair ED, Sim RB.** 2000. Lung surfactant protein A provides a route of entry for respiratory syncytial virus into host cells. Viral immunology **13:**125-135.
48. **Malhotra R, Ward M, Bright H, Priest R, Foster MR, Hurle M, Blair E, Bird M.** 2003. Isolation and characterisation of potential respiratory syncytial virus receptor(s) on epithelial cells. Microbes Infect **5:**123-133.
49. **Johnson TR, McLellan JS, Graham BS.** 2012. Respiratory syncytial virus glycoprotein G interacts with DC-SIGN and L-SIGN to activate ERK1 and ERK2. J Virol **86:**1339-1347.
50. **Teng MN, Whitehead SS, Collins PL.** 2001. Contribution of the respiratory syncytial virus G glycoprotein and its secreted and membrane-bound forms to virus replication in vitro and in vivo. Virology **289:**283-296.
51. **Wertz GW, Krieger M, Ball LA.** 1989. Structure and cell surface maturation of the attachment glycoprotein of human respiratory syncytial virus in a cell line deficient in O glycosylation. J Virol **63:**4767-4776.
52. **Choi Y, Mason CS, Jones LP, Crabtree J, Jorquera PA, Tripp RA.** 2012. Antibodies to the central conserved region of respiratory syncytial virus (RSV) G protein block RSV G protein CX3C-CX3CR1 binding and cross-neutralize RSV A and B strains. Viral immunology **25:**193-203.

53. **Kim S, Joo DH, Lee JB, Shim BS, Cheon IS, Jang JE, Song HH, Kim KH, Song MK, Chang J.** 2012. Dual role of respiratory syncytial virus glycoprotein fragment as a mucosal immunogen and chemotactic adjuvant. PLoS One **7:**e32226.
54. **Power UF, Plotnicky-Gilquin H, Huss T, Robert A, Trudel M, Stahl S, Uhlen M, Nguyen TN, Binz H.** 1997. Induction of protective immunity in rodents by vaccination with a prokaryotically expressed recombinant fusion protein containing a respiratory syncytial virus G protein fragment. Virology **230:**155-166.
55. **Mufson MA, Orvell C, Rafnar B, Norrby E.** 1985. Two distinct subtypes of human respiratory syncytial virus. J Gen Virol **66 (Pt 10):**2111-2124.
56. **Melero JA, Garcia-Barreno B, Martinez I, Pringle CR, Cane PA.** 1997. Antigenic structure, evolution and immunobiology of human respiratory syncytial virus attachment (G) protein. J Gen Virol **78 (Pt 10):**2411-2418.
57. **Trento A, Casas I, Calderon A, Garcia-Garcia ML, Calvo C, Perez-Brena P, Melero JA.** 2010. Ten years of global evolution of the human respiratory syncytial virus BA genotype with a 60-nucleotide duplication in the G protein gene. J Virol **84:**7500-7512.
58. **Trento A, Galiano M, Videla C, Carballal G, Garcia-Barreno B, Melero JA, Palomo C.** 2003. Major changes in the G protein of human respiratory syncytial virus isolates introduced by a duplication of 60 nucleotides. J Gen Virol **84:**3115-3120.
59. **Trento A, Viegas M, Galiano M, Videla C, Carballal G, Mistchenko AS, Melero JA.** 2006. Natural history of human respiratory syncytial virus inferred from phylogenetic analysis of the attachment (G) glycoprotein with a 60-nucleotide duplication. J Virol **80:**975-984.
60. **Agoti CN, Gitahi CW, Medley GF, Cane PA, Nokes DJ.** 2013. Identification of group B respiratory syncytial viruses that lack the 60-nucleotide duplication after six consecutive epidemics of total BA dominance at coastal Kenya. Influenza and other respiratory viruses **7:**1008-1012.
61. **Auksornkitti V, Kamprasert N, Thongkomplew S, Suwannakarn K, Theamboonlers A, Samransamruajkij R, Poovorawan Y.** 2014. Molecular characterization of human respiratory syncytial virus, 2010-2011: identification of genotype ON1 and a new subgroup B genotype in Thailand. Archives of virology **159:**499-507.
62. **White JM, Delos SE, Brecher M, Schornberg K.** 2008. Structures and mechanisms of viral membrane fusion proteins: multiple variations on a common theme. Critical reviews in biochemistry and molecular biology **43:**189-219.
63. **Gonzalez-Reyes L, Ruiz-Arguello MB, Garcia-Barreno B, Calder L, Lopez JA, Albar JP, Skehel JJ, Wiley DC, Melero JA.** 2001. Cleavage of the human respiratory syncytial virus fusion protein at two distinct sites is required for activation of membrane fusion. Proc Natl Acad Sci U S A **98:**9859-9864.
64. **Zimmer G, Budz L, Herrler G.** 2001. Proteolytic activation of respiratory syncytial virus fusion protein. Cleavage at two furin consensus sequences. J Biol Chem **276:**31642-31650.

65. **Krzyzaniak MA, Zumstein MT, Gerez JA, Picotti P, Helenius A.** 2013. Host cell entry of respiratory syncytial virus involves macropinocytosis followed by proteolytic activation of the F protein. PLoS Pathog **9:**e1003309.
66. **McLellan JS, Yang Y, Graham BS, Kwong PD.** 2011. Structure of respiratory syncytial virus fusion glycoprotein in the postfusion conformation reveals preservation of neutralizing epitopes. J Virol **85:**7788-7796.
67. **Swanson KA, Settembre EC, Shaw CA, Dey AK, Rappuoli R, Mandl CW, Dormitzer PR, Carfi A.** 2011. Structural basis for immunization with postfusion respiratory syncytial virus fusion F glycoprotein (RSV F) to elicit high neutralizing antibody titers. Proc Natl Acad Sci U S A **108:**9619-9624.
68. **McLellan JS, Chen M, Leung S, Graepel KW, Du X, Yang Y, Zhou T, Baxa U, Yasuda E, Beaumont T, Kumar A, Modjarrad K, Zheng Z, Zhao M, Xia N, Kwong PD, Graham BS.** 2013. Structure of RSV fusion glycoprotein trimer bound to a prefusion-specific neutralizing antibody. Science **340:**1113-1117.
69. **Baviskar PS, Hotard AL, Moore ML, Oomens AG.** 2013. The respiratory syncytial virus fusion protein targets to the perimeter of inclusion bodies and facilitates filament formation by a cytoplasmic tail-dependent mechanism. J Virol **87:**10730-10741.
70. **Oomens AG, Wertz GW.** 2004. trans-Complementation allows recovery of human respiratory syncytial viruses that are infectious but deficient in cell-to-cell transmission. J Virol **78:**9064-9072.
71. **Tayyari F, Marchant D, Moraes TJ, Duan W, Mastrangelo P, Hegele RG.** 2011. Identification of nucleolin as a cellular receptor for human respiratory syncytial virus. Nat Med **17:**1132-1135.
72. **Prince GA, Horswood RL, Berndt J, Suffin SC, Chanock RM.** 1979. Respiratory syncytial virus infection in inbred mice. Infection and immunity **26:**764-766.
73. **Taylor G, Stott EJ, Hughes M, Collins AP.** 1984. Respiratory syncytial virus infection in mice. Infection and immunity **43:**649-655.
74. **Graham BS, Perkins MD, Wright PF, Karzon DT.** 1988. Primary respiratory syncytial virus infection in mice. J Med Virol **26:**153-162.
75. **Lukacs NW, Moore ML, Rudd BD, Berlin AA, Collins RD, Olson SJ, Ho SB, Peebles RS, Jr.** 2006. Differential immune responses and pulmonary pathophysiology are induced by two different strains of respiratory syncytial virus. The American journal of pathology **169:**977-986.
76. **Stokes KL, Chi MH, Sakamoto K, Newcomb DC, Currier MG, Huckabee MM, Lee S, Goleniewska K, Pretto C, Williams JV, Hotard A, Sherrill TP, Peebles RS, Jr., Moore ML.** 2011. Differential Pathogenesis of Respiratory Syncytial Virus (RSV) Clinical Isolates in BALB/c Mice. J Virol **85:**5782-5793.
77. **Moore ML, Chi MH, Luongo C, Lukacs NW, Polosukhin VV, Huckabee MM, Newcomb DC, Buchholz UJ, Crowe JE, Jr., Goleniewska K, Williams JV, Collins PL, Peebles RS, Jr.** 2009. A chimeric A2 strain of respiratory syncytial virus (RSV) with the fusion protein of RSV strain line 19 exhibits enhanced viral load, mucus, and airway dysfunction. J Virol **83:**4185-4194.
78. **Hall CB, Walsh EE, Schnabel KC, Long CE, McConnochie KM, Hildreth SW, Anderson LJ.** 1990. Occurrence of groups A and B of respiratory syncytial

virus over 15 years: associated epidemiologic and clinical characteristics in hospitalized and ambulatory children. J Infect Dis **162:**1283-1290.

79. **Heikkinen T, Waris M, Ruuskanen O, Putto-Laurila A, Mertsola J.** 1995. Incidence of acute otitis media associated with group A and B respiratory syncytial virus infections. Acta paediatrica **84:**419-423.
80. **Imaz MS, Sequeira MD, Videla C, Veronessi I, Cociglio R, Zerbini E, Carballal G.** 2000. Clinical and epidemiologic characteristics of respiratory syncytial virus subgroups A and B infections in Santa Fe, Argentina. J Med Virol **61:**76-80.
81. **McConnochie KM, Hall CB, Walsh EE, Roghmann KJ.** 1990. Variation in severity of respiratory syncytial virus infections with subtype. J Pediatr **117:**52-62.
82. **Mufson MA, Belshe RB, Orvell C, Norrby E.** 1988. Respiratory syncytial virus epidemics: variable dominance of subgroups A and B strains among children, 1981-1986. J Infect Dis **157:**143-148.
83. **Papadopoulos NG, Gourgiotis D, Javadyan A, Bossios A, Kallergi K, Psarras S, Tsolia MN, Kafetzis D.** 2004. Does respiratory syncytial virus subtype influences the severity of acute bronchiolitis in hospitalized infants? Respir Med **98:**879-882.
84. **Salomon HE, Avila MM, Cerqueiro MC, Orvell C, Weissenbacher M.** 1991. Clinical and epidemiologic aspects of respiratory syncytial virus antigenic variants in Argentinian children. J Infect Dis **163:**1167.
85. **Taylor CE, Morrow S, Scott M, Young B, Toms GL.** 1989. Comparative virulence of respiratory syncytial virus subgroups A and B. Lancet **1:**777-778.
86. **Walsh EE, McConnochie KM, Long CE, Hall CB.** 1997. Severity of respiratory syncytial virus infection is related to virus strain. J Infect Dis **175:**814-820.
87. **Hornsleth A, Klug B, Nir M, Johansen J, Hansen KS, Christensen LS, Larsen LB.** 1998. Severity of respiratory syncytial virus disease related to type and genotype of virus and to cytokine values in nasopharyngeal secretions. Pediatr Infect Dis J **17:**1114-1121.
88. **Panayiotou C, Richter J, Koliou M, Kalogirou N, Georgiou E, Christodoulou C.** 2014. Epidemiology of respiratory syncytial virus in children in Cyprus during three consecutive winter seasons (2010-2013): age distribution, seasonality and association between prevalent genotypes and disease severity. Epidemiol Infect**:**1-6.
89. **Brandenburg AH, van Beek R, Moll HA, Osterhaus AD, Claas EC.** 2000. G protein variation in respiratory syncytial virus group A does not correlate with clinical severity. J Clin Microbiol **38:**3849-3852.
90. **Devincenzo JP.** 2004. Natural infection of infants with respiratory syncytial virus subgroups A and B: a study of frequency, disease severity, and viral load. Pediatr Res **56:**914-917.
91. **Fodha I, Vabret A, Ghedira L, Seboui H, Chouchane S, Dewar J, Gueddiche N, Trabelsi A, Boujaafar N, Freymuth F.** 2007. Respiratory syncytial virus infections in hospitalized infants: association between viral load, virus subgroup, and disease severity. J Med Virol **79:**1951-1958.

92. **Hendry RM, Talis AL, Godfrey E, Anderson LJ, Fernie BF, McIntosh K.** 1986. Concurrent circulation of antigenically distinct strains of respiratory syncytial virus during community outbreaks. J Infect Dis **153:**291-297.
93. **Kneyber MC, Brandenburg AH, Rothbarth PH, de Groot R, Ott A, van Steensel-Moll HA.** 1996. Relationship between clinical severity of respiratory syncytial virus infection and subtype. Arch Dis Child **75:**137-140.
94. **McIntosh ED, De Silva LM, Oates RK.** 1993. Clinical severity of respiratory syncytial virus group A and B infection in Sydney, Australia. Pediatr Infect Dis J **12:**815-819.
95. **Monto AS, Ohmit S.** 1990. Respiratory syncytial virus in a community population: circulation of subgroups A and B since 1965. J Infect Dis **161:**781-783.
96. **Russi JC, Chiparelli H, Montano A, Etorena P, Hortal M.** 1989. Respiratory syncytial virus subgroups and pneumonia in children. Lancet **2:**1039-1040.
97. **Wilson E, Orvell C, Morrison B, Thomas E.** 1990. Pediatric RSV infection during two winter seasons in British Columbia: A role for subgroup analysis in young children? Can J Infect Dis **1:**112-116.
98. **Collins PL, Crowe JE, Jr.** 2007. Respiratory Syncytial Virus and Metapneumovirus, p. 1601-1646. *In* Knipe DM, Howley PM (ed.), Fields Virology, vol. 2. Lippincott, Williams, and Wilkins, Philadelphia, PA.
99. **Collins PL, Hill MG, Camargo E, Grosfeld H, Chanock RM, Murphy BR.** 1995. Production of infectious human respiratory syncytial virus from cloned cDNA confirms an essential role for the transcription elongation factor from the 5' proximal open reading frame of the M2 mRNA in gene expression and provides a capability for vaccine development. Proc Natl Acad Sci U S A **92:**11563-11567.
100. **Karron RA, Wright PF, Belshe RB, Thumar B, Casey R, Newman F, Polack FP, Randolph VB, Deatly A, Hackell J, Gruber W, Murphy BR, Collins PL.** 2005. Identification of a recombinant live attenuated respiratory syncytial virus vaccine candidate that is highly attenuated in infants. J Infect Dis **191:**1093-1104.
101. **Biacchesi S, Murphy BR, Collins PL, Buchholz UJ.** 2007. Frequent frameshift and point mutations in the SH gene of human metapneumovirus passaged in vitro. J Virol **81:**6057-6067.
102. **Jin H, Clarke D, Zhou HZ, Cheng X, Coelingh K, Bryant M, Li S.** 1998. Recombinant human respiratory syncytial virus (RSV) from cDNA and construction of subgroup A and B chimeric RSV. Virology **251:**206-214.
103. **Yun SI, Kim SY, Rice CM, Lee YM.** 2003. Development and application of a reverse genetics system for Japanese encephalitis virus. J Virol **77:**6450-6465.
104. **Almazan F, Gonzalez JM, Penzes Z, Izeta A, Calvo E, Plana-Duran J, Enjuanes L.** 2000. Engineering the largest RNA virus genome as an infectious bacterial artificial chromosome. Proc Natl Acad Sci U S A **97:**5516-5521.
105. **Hall RN, Meers J, Fowler E, Mahony T.** 2012. Back to BAC: The Use of Infectious Clone Technologies for Viral Mutagenesis. Viruses **4:**211-235.
106. **Zhou B, Jerzak G, Scholes DT, Donnelly ME, Li Y, Wentworth DE.** 2011. Reverse genetics plasmid for cloning unstable influenza A virus gene segments. J Virol Methods **173:**378-383.

107. **Fan ZC, Bird RC.** 2008. An improved reverse genetics system for generation of bovine viral diarrhea virus as a BAC cDNA. J Virol Methods **149:**309-315.
108. **Buchholz UJ, Finke S, Conzelmann KK.** 1999. Generation of bovine respiratory syncytial virus (BRSV) from cDNA: BRSV NS2 is not essential for virus replication in tissue culture, and the human RSV leader region acts as a functional BRSV genome promoter. J Virol **73:**251-259.
109. **Huang K, Lawlor H, Tang R, MacGill RS, Ulbrandt ND, Wu H.** 2010. Recombinant respiratory syncytial virus F protein expression is hindered by inefficient nuclear export and mRNA processing. Virus Genes **40:**212-221.
110. **Grosfeld H, Hill MG, Collins PL.** 1995. RNA replication by respiratory syncytial virus (RSV) is directed by the N, P, and L proteins; transcription also occurs under these conditions but requires RSV superinfection for efficient synthesis of full-length mRNA. J Virol **69:**5677-5686.
111. **Dochow M, Krumm SA, Crowe JE, Jr., Moore ML, Plemper RK.** 2012. Independent structural domains in the paramyxovirus polymerase protein. J Biol Chem **287:**6878-6891.
112. **Shcherbo D, Murphy CS, Ermakova GV, Solovieva EA, Chepurnykh TV, Shcheglov AS, Verkhusha VV, Pletnev VZ, Hazelwood KL, Roche PM, Lukyanov S, Zaraisky AG, Davidson MW, Chudakov DM.** 2009. Far-red fluorescent tags for protein imaging in living tissues. Biochem J **418:**567-574.
113. **Bukreyev A, Camargo E, Collins PL.** 1996. Recovery of infectious respiratory syncytial virus expressing an additional, foreign gene. J Virol **70:**6634-6641.
114. **Warming S, Costantino N, Court DL, Jenkins NA, Copeland NG.** 2005. Simple and highly efficient BAC recombineering using galK selection. Nucleic Acids Res **33:**e36.
115. **Donofrio G, Sartori C, Ravanetti L, Cavirani S, Gillet L, Vanderplasschen A, Taddei S, Flammini CF.** 2007. Establishment of a bovine herpesvirus 4 based vector expressing a secreted form of the bovine viral diarrhoea virus structural glycoprotein E2 for immunization purposes. BMC Biotechnol **7:**e68.
116. **Moyer CL, Wiethoff CM, Maier O, Smith JG, Nemerow GR.** 2011. Functional genetic and biophysical analyses of membrane disruption by human adenovirus. J Virol **85:**2631-2641.
117. **Studier FW, Rosenberg AH, Dunn JJ, Dubendorff JW.** 1990. Use of T7 RNA polymerase to direct expression of cloned genes. Methods Enzymol **185:**60-89.
118. **Kwilas AR, Yednak MA, Zhang L, Liesman R, Collins PL, Pickles RJ, Peeples ME.** 2010. Respiratory syncytial virus engineered to express the cystic fibrosis transmembrane conductance regulator corrects the bioelectric phenotype of human cystic fibrosis airway epithelium in vitro. J Virol **84:**7770-7781.
119. **Walker SC, Avis JM, Conn GL.** 2003. General plasmids for producing RNA in vitro transcripts with homogeneous ends. Nucleic Acids Res **31:**e82.
120. **Mink MA, Stec DS, Collins PL.** 1991. Nucleotide sequences of the 3' leader and 5' trailer regions of human respiratory syncytial virus genomic RNA. Virology **185:**615-624.
121. **Collins PL, Wertz GW.** 1985. Nucleotide sequences of the 1B and 1C nonstructural protein mRNAs of human respiratory syncytial virus. Virology **143:**442-451.

122. **Stec DS, Hill MG, 3rd, Collins PL.** 1991. Sequence analysis of the polymerase L gene of human respiratory syncytial virus and predicted phylogeny of nonsegmented negative-strand viruses. Virology **183:**273-287.
123. **Collins PL, Olmsted RA, Spriggs MK, Johnson PR, Buckler-White AJ.** 1987. Gene overlap and site-specific attenuation of transcription of the viral polymerase L gene of human respiratory syncytial virus. Proc Natl Acad Sci U S A **84:**5134-5138.
124. **Moudy RM, Sullender WM, Wertz GW.** 2004. Variations in intergenic region sequences of Human respiratory syncytial virus clinical isolates: analysis of effects on transcriptional regulation. Virology **327:**121-133.
125. **Collins PL, Olmsted RA, Johnson PR.** 1990. The small hydrophobic protein of human respiratory syncytial virus: comparison between antigenic subgroups A and B. J Gen Virol **71 (Pt 7):**1571-1576.
126. **Johnson PR, Collins PL.** 1988. The fusion glycoproteins of human respiratory syncytial virus of subgroups A and B: sequence conservation provides a structural basis for antigenic relatedness. J Gen Virol **69 (Pt 10):**2623-2628.
127. **Perrotta AT, Been MD.** 1991. A pseudoknot-like structure required for efficient self-cleavage of hepatitis delta virus RNA. Nature **350:**434-436.
128. **Walsh EE, Hruska JF.** 1983. Identification of the virus-specific proteins of respiratory syncytial virus temperature-sensitive mutants by immunoprecipitation. Proc Soc Exp Biol Med **172:**202-206.
129. **Zhou H, Thompson WW, Viboud CG, Ringholz CM, Cheng PY, Steiner C, Abedi GR, Anderson LJ, Brammer L, Shay DK.** 2012. Hospitalizations associated with influenza and respiratory syncytial virus in the United States, 1993-2008. Clin Infect Dis **54:**1427-1436.
130. **Herlocher ML, Ewasyshyn M, Sambhara S, Gharaee-Kermani M, Cho D, Lai J, Klein M, Maassab HF.** 1999. Immunological properties of plaque purified strains of live attenuated respiratory syncytial virus (RSV) for human vaccine. Vaccine **17:**172-181.
131. **Boyoglu-Barnum S, Gaston KA, Todd SO, Boyoglu C, Chirkova T, Barnum TR, Jorquera P, Haynes LM, Tripp RA, Moore ML, Anderson LJ.** 2013. A respiratory syncytial virus (RSV) anti-G protein F(ab')2 monoclonal antibody suppresses mucous production and breathing effort in RSV rA2-line19F-infected BALB/c mice. J Virol **87:**10955-10967.
132. **Yin HS, Wen X, Paterson RG, Lamb RA, Jardetzky TS.** 2006. Structure of the parainfluenza virus 5 F protein in its metastable, prefusion conformation. Nature **439:**38-44.
133. **Steinhauer DA, Plemper RK.** 2012. Structure of the primed paramyxovirus fusion protein. Proc Natl Acad Sci U S A **109:**16404-16405.
134. **Lawlor HA, Schickli JH, Tang RS.** 2013. A single amino acid in the F2 subunit of respiratory syncytial virus fusion protein alters growth and fusogenicity. J Gen Virol **94 Pt 12:**2627-2635.
135. **Li P, Mc LRHW, Brown G, Sugrue RJ.** 2007. Functional analysis of the N-linked glycans within the fusion protein of respiratory syncytial virus. Methods Mol Biol **379:**69-83.

136. **Martin D, Calder LJ, Garcia-Barreno B, Skehel JJ, Melero JA.** 2006. Sequence elements of the fusion peptide of human respiratory syncytial virus fusion protein required for activity. J Gen Virol **87:**1649-1658.
137. **Zimmer G, Trotz I, Herrler G.** 2001. N-glycans of F protein differentially affect fusion activity of human respiratory syncytial virus. J Virol **75:**4744-4751.
138. **Luque LE, Bridges OA, Mason JN, Boyd KL, Portner A, Russell CJ.** 2010. Residues in the heptad repeat a region of the fusion protein modulate the virulence of Sendai virus in mice. J Virol **84:**810-821.
139. **Luque LE, Russell CJ.** 2007. Spring-loaded heptad repeat residues regulate the expression and activation of paramyxovirus fusion protein. J Virol **81:**3130-3141.
140. **Stokes KL, Currier MG, Sakamoto K, Lee S, Collins PL, Plemper RK, Moore ML.** 2013. The respiratory syncytial virus fusion protein and neutrophils mediate the airway mucin response to pathogenic respiratory syncytial virus infection. J Virol **87:**10070-10082.
141. **Hotard AL, Shaikh FY, Lee S, Yan D, Teng MN, Plemper RK, Crowe JE, Jr., Moore ML.** 2012. A stabilized respiratory syncytial virus reverse genetics system amenable to recombination-mediated mutagenesis. Virology **434:**129-136.
142. **Ishikawa H, Meng F, Kondo N, Iwamoto A, Matsuda Z.** 2012. Generation of a dual-functional split-reporter protein for monitoring membrane fusion using self-associating split GFP. Protein Eng Des Sel **25:**813-820.
143. **Pettersen EF, Goddard TD, Huang CC, Couch GS, Greenblatt DM, Meng EC, Ferrin TE.** 2004. UCSF Chimera--a visualization system for exploratory research and analysis. J Comput Chem **25:**1605-1612.
144. **Cianci C, Langley DR, Dischino DD, Sun Y, Yu KL, Stanley A, Roach J, Li Z, Dalterio R, Colonno R, Meanwell NA, Krystal M.** 2004. Targeting a binding pocket within the trimer-of-hairpins: small-molecule inhibition of viral fusion. Proc Natl Acad Sci U S A **101:**15046-15051.
145. **Abarca K, Jung E, Fernandez P, Zhao L, Harris B, Connor EM, Losonsky GA.** 2009. Safety, tolerability, pharmacokinetics, and immunogenicity of motavizumab, a humanized, enhanced-potency monoclonal antibody for the prevention of respiratory syncytial virus infection in at-risk children. Pediatr Infect Dis J **28:**267-272.
146. **Johnson S, Oliver C, Prince GA, Hemming VG, Pfarr DS, Wang SC, Dormitzer M, O'Grady J, Koenig S, Tamura JK, Woods R, Bansal G, Couchenour D, Tsao E, Hall WC, Young JF.** 1997. Development of a humanized monoclonal antibody (MEDI-493) with potent in vitro and in vivo activity against respiratory syncytial virus. J Infect Dis **176:**1215-1224.
147. **Kondo N, Miyauchi K, Meng F, Iwamoto A, Matsuda Z.** 2010. Conformational changes of the HIV-1 envelope protein during membrane fusion are inhibited by the replacement of its membrane-spanning domain. J Biol Chem **285:**14681-14688.
148. **Lotz MT, Peebles RS, Jr.** 2012. Mechanisms of respiratory syncytial virus modulation of airway immune responses. Current allergy and asthma reports **12:**380-387.

149. **Gardner AE, Dutch RE.** 2007. A conserved region in the F(2) subunit of paramyxovirus fusion proteins is involved in fusion regulation. J Virol **81:**8303-8314.
150. **Plemper RK, Compans RW.** 2003. Mutations in the putative HR-C region of the measles virus F2 glycoprotein modulate syncytium formation. J Virol **77:**4181-4190.
151. **DeVincenzo JP, El Saleeby CM, Bush AJ.** 2005. Respiratory syncytial virus load predicts disease severity in previously healthy infants. J Infect Dis **191:**1861-1868.
152. **DeVincenzo JP, Wilkinson T, Vaishnaw A, Cehelsky J, Meyers R, Nochur S, Harrison L, Meeking P, Mann A, Moane E, Oxford J, Pareek R, Moore R, Walsh E, Studholme R, Dorsett P, Alvarez R, Lambkin-Williams R.** 2010. Viral load drives disease in humans experimentally infected with respiratory syncytial virus. American journal of respiratory and critical care medicine **182:**1305-1314.
153. **El Saleeby CM, Bush AJ, Harrison LM, Aitken JA, Devincenzo JP.** 2011. Respiratory syncytial virus load, viral dynamics, and disease severity in previously healthy naturally infected children. J Infect Dis **204:**996-1002.
154. **Miller AL, Strieter RM, Gruber AD, Ho SB, Lukacs NW.** 2003. CXCR2 regulates respiratory syncytial virus-induced airway hyperreactivity and mucus overproduction. J Immunol **170:**3348-3356.
155. **Tekkanat KK, Maassab H, Berlin AA, Lincoln PM, Evanoff HL, Kaplan MH, Lukacs NW.** 2001. Role of interleukin-12 and stat-4 in the regulation of airway inflammation and hyperreactivity in respiratory syncytial virus infection. The American journal of pathology **159:**631-638.
156. **Rudd BD, Smit JJ, Flavell RA, Alexopoulou L, Schaller MA, Gruber A, Berlin AA, Lukacs NW.** 2006. Deletion of TLR3 alters the pulmonary immune environment and mucus production during respiratory syncytial virus infection. J Immunol **176:**1937-1942.
157. **Miller AL, Gerard C, Schaller M, Gruber AD, Humbles AA, Lukacs NW.** 2006. Deletion of CCR1 attenuates pathophysiologic responses during respiratory syncytial virus infection. J Immunol **176:**2562-2567.
158. **Rudd BD, Schaller MA, Smit JJ, Kunkel SL, Neupane R, Kelley L, Berlin AA, Lukacs NW.** 2007. MyD88-mediated instructive signals in dendritic cells regulate pulmonary immune responses during respiratory virus infection. J Immunol **178:**5820-5827.
159. **Petersen BC, Dolgachev V, Rasky A, Lukacs NW.** 2014. IL-17E (IL-25) and IL-17RB promote respiratory syncytial virus-induced pulmonary disease. Journal of leukocyte biology.
160. **Reed M, Morris SH, Jang S, Mukherjee S, Yue Z, Lukacs NW.** 2013. Autophagy-inducing protein beclin-1 in dendritic cells regulates CD4 T cell responses and disease severity during respiratory syncytial virus infection. J Immunol **191:**2526-2537.
161. **Johnson JB, Schmitt AP, Parks GD.** 2013. Point mutations in the paramyxovirus F protein that enhance fusion activity shift the mechanism of complement-mediated virus neutralization. J Virol **87:**9250-9259.

162. **Zhang Y, Xu W, Shen K, Xie Z, Sun L, Lu Q, Liu C, Liang G, Beeler JA, Anderson LJ.** 2007. Genetic variability of group A and B human respiratory syncytial viruses isolated from 3 provinces in China. Archives of virology **152:**1425-1434.
163. **Zlateva KT, Vijgen L, Dekeersmaeker N, Naranjo C, Van Ranst M.** 2007. Subgroup prevalence and genotype circulation patterns of human respiratory syncytial virus in Belgium during ten successive epidemic seasons. J Clin Microbiol **45:**3022-3030.
164. **Almajhdi FN, Farrag MA, Amer HM.** 2014. Group B strains of human respiratory syncytial virus in Saudi Arabia: molecular and phylogenetic analysis. Virus Genes **48:**252-259.
165. **Agoti CN, Mayieka LM, Otieno JR, Ahmed JA, Fields BS, Waiboci LW, Nyoka R, Eidex RB, Marano N, Burton W, Montgomery JM, Breiman RF, Nokes DJ.** 2014. Examining strain diversity and phylogeography in relation to an unusual epidemic pattern of respiratory syncytial virus (RSV) in a long-term refugee camp in Kenya. BMC infectious diseases **14:**178.
166. **Agoti CN, Otieno JR, Gitahi CW, Cane PA, Nokes DJ.** 2014. Rapid spread and diversification of respiratory syncytial virus genotype ON1, Kenya. Emerging infectious diseases **20:**950-959.
167. **Avadhanula V, Chemaly RF, Shah DP, Ghantoji SS, Azzi JM, Aideyan LO, Mei M, Piedra PA.** 2014. Infection with Novel Respiratory Syncytial Virus Genotype Ontario (ON1) in Adult Hematopoietic Cell Transplant Recipients, Texas, 2011-2013. J Infect Dis.
168. **Pierangeli A, Trotta D, Scagnolari C, Ferreri ML, Nicolai A, Midulla F, Marinelli K, Antonelli G, Bagnarelli P.** 2014. Rapid spread of the novel respiratory syncytial virus A ON1 genotype, central Italy, 2011 to 2013. Euro surveillance : bulletin Europeen sur les maladies transmissibles = European communicable disease bulletin **19**.
169. **Bukreyev A, Yang L, Fricke J, Cheng L, Ward JM, Murphy BR, Collins PL.** 2008. The secreted form of respiratory syncytial virus G glycoprotein helps the virus evade antibody-mediated restriction of replication by acting as an antigen decoy and through effects on Fc receptor-bearing leukocytes. J Virol **82:**12191-12204.
170. **Melendi GA, Bridget D, Monsalvo AC, Laham FF, Acosta P, Delgado MF, Polack FP, Irusta PM.** 2011. Conserved cysteine residues within the attachment G glycoprotein of respiratory syncytial virus play a critical role in the enhancement of cytotoxic T-lymphocyte responses. Virus Genes **42:**46-54.
171. **Cane PA, Matthews DA, Pringle CR.** 1991. Identification of variable domains of the attachment (G) protein of subgroup A respiratory syncytial viruses. J Gen Virol **72 (Pt 9):**2091-2096.
172. **Zlateva KT, Lemey P, Vandamme AM, Van Ranst M.** 2004. Molecular evolution and circulation patterns of human respiratory syncytial virus subgroup a: positively selected sites in the attachment g glycoprotein. J Virol **78:**4675-4683.
173. **Kwilas S, Liesman RM, Zhang L, Walsh E, Pickles RJ, Peeples ME.** 2009. Respiratory syncytial virus grown in Vero cells contains a truncated attachment

protein that alters its infectivity and dependence on glycosaminoglycans. J Virol **83:**10710-10718.

174. **Feldman SA, Hendry RM, Beeler JA.** 1999. Identification of a linear heparin binding domain for human respiratory syncytial virus attachment glycoprotein G. J Virol **73:**6610-6617.
175. **Bourgeois C, Bour JB, Lidholt K, Gauthray C, Pothier P.** 1998. Heparin-like structures on respiratory syncytial virus are involved in its infectivity in vitro. J Virol **72:**7221-7227.
176. **Messerle M, Crnkovic I, Hammerschmidt W, Ziegler H, Koszinowski UH.** 1997. Cloning and mutagenesis of a herpesvirus genome as an infectious bacterial artificial chromosome. Proc Natl Acad Sci U S A **94:**14759-14763.
177. **Haynes LM, Moore DD, Kurt-Jones EA, Finberg RW, Anderson LJ, Tripp RA.** 2001. Involvement of toll-like receptor 4 in innate immunity to respiratory syncytial virus. J Virol **75:**10730-10737.
178. **Behera AK, Matsuse H, Kumar M, Kong X, Lockey RF, Mohapatra SS.** 2001. Blocking intercellular adhesion molecule-1 on human epithelial cells decreases respiratory syncytial virus infection. Biochemical and biophysical research communications **280:**188-195.
179. **Corti D, Bianchi S, Vanzetta F, Minola A, Perez L, Agatic G, Guarino B, Silacci C, Marcandalli J, Marsland BJ, Piralla A, Percivalle E, Sallusto F, Baldanti F, Lanzavecchia A.** 2013. Cross-neutralization of four paramyxoviruses by a human monoclonal antibody. Nature **501:**439-443.
180. **Smith EC, Smith SE, Carter JR, Webb SR, Gibson KM, Hellman LM, Fried MG, Dutch RE.** 2013. Trimeric transmembrane domain interactions in paramyxovirus fusion proteins: roles in protein folding, stability and function. J Biol Chem.
181. **Hazenberg MD, Spits H.** 2014. Human innate lymphoid cells. Blood **124:**700-709.
182. **Taube C, Tertilt C, Gyulveszi G, Dehzad N, Kreymborg K, Schneeweiss K, Michel E, Reuter S, Renauld JC, Arnold-Schild D, Schild H, Buhl R, Becher B.** 2011. IL-22 is produced by innate lymphoid cells and limits inflammation in allergic airway disease. PLoS One **6:**e21799.
183. **Rawling J, Melero JA.** 2007. The use of monoclonal antibodies and lectins to identify changes in viral glycoproteins that are influenced by glycosylation: the case of human respiratory syncytial virus attachment (G) glycoprotein. Methods Mol Biol **379:**109-125.
184. **McLellan JS, Chen M, Joyce MG, Sastry M, Stewart-Jones GB, Yang Y, Zhang B, Chen L, Srivatsan S, Zheng A, Zhou T, Graepel KW, Kumar A, Moin S, Boyington JC, Chuang GY, Soto C, Baxa U, Bakker AQ, Spits H, Beaumont T, Zheng Z, Xia N, Ko SY, Todd JP, Rao S, Graham BS, Kwong PD.** 2013. Structure-based design of a fusion glycoprotein vaccine for respiratory syncytial virus. Science **342:**592-598.
185. 2013-2014, posting date. PATH's Work in Vaccine Development: Respiratory Syncytial Virus. [Online.]